

Dissertation

Decays of Charginos and Neutralinos in the MSSM

ausgeführt zum Zwecke der Erlangung des akademischen Grades eines
Doktors der technischen Wissenschaften unter der Leitung von

Univ. Prof. Walter Majerotto

E 136

Institut für Theoretische Physik

und

Institut für Hochenergiephysik der ÖAW

eingereicht an der Technischen Universität Wien
Technisch-naturwissenschaftliche Fakultät

von

Dipl. Ing. Bernhard Schraußer

9731027

Gaußgasse 4/39, 8010 Graz

donat@hephy.oeaw.ac.at

Wien, am 11. Jänner 2010

Acknowledgements

First of all I would like to thank my supervisor Prof. Walter Majerotto for not loosing his patience and for making it possible, that I could finally bring this thesis to an end. I also would like to thank Dr. Helmut Eberl for his help and advices.

Further thanks goes to Dr. Karol Kovařík for providing examples for the program structures and for teaching me how to use the "SelfEnergyDataBase" and the parameter conversion program $\overline{DR}2OS$.

Special thanks goes to Dr. Gerhard Walzel, not only for providing a fast and stable computer system, but also for several interesting discussions and for being a patriotic Styrian.

Finally, very special thanks finally goes to my former roommate and friend Dipl.-Ing. Georg Sulyok for countless invaluable discussions, for understanding not only the physical problems and for being such an idealistic physicist.

Kurzfassung

Das Minimale Supersymmetrische Standard Modell (MSSM) ist eine der anerkanntesten Erweiterungen des Standard Modells (SM) der Elementarteilchen. Es wird eine Symmetrie zwischen bosonischen und fermionischen Teilchen angenommen, und so zu jedem SM Teilchen ein so genannter "Superpartner" eingeführt. Außerdem werden vier zusätzliche Higgs Teilchen benötigt. Die fermionischen Partner der Higgs- und der Eichbosonen mischen, und bilden Masseneigenzustände, die sogenannten Charginos und Neutralinos.

Wenn Supersymmetrie in der Form des MSSM in der Natur realisiert ist, sollten Superpartner schon bald im Zuge zukünftiger Beschleunigerexperimente (wie des LHC am CERN) gefunden werden. Unter diesen neuen Teilchen würden sich auch Charginos und Neutralinos befinden. Da diese, bis auf das leichteste Neutralino, instabil wären, müssten auch deren Zerfälle zu beobachten sein. Deshalb ist es wichtig, die Zerfallseigenschaften von Charginos und Neutralinos zu untersuchen. Diese Arbeit beschäftigt sich somit mit der Berechnung von Zerfallsbreiten und besonders von Zerfallsbreitenverhältnissen für alle Zweikörperzerfälle von Charginos und Neutralinos.

Um die Ergebnisse in der benötigten Genauigkeit zu erhalten, wird die Rechnung nicht auf die niedrigste Ordnung Störungstheorie, den so genannten "Treelevel" beschränkt, sondern es werden die vollen Strahlungskorrekturen in Einschleifenapproximation berücksichtigt. Die dafür notwendige Berechnung von hunderten von Feynmandiagrammen erfolgt mit Hilfe spezieller algebraischer Software.

Die Einbeziehung von Schleifenkorrekturen führt zu bedeutenden Problemen: Die Integration der Feynmanamplituden führt zu so genannten Ultraviolett-(UV) und Infrarotdivergenzen (IR) für sehr große beziehungsweise verschwindende Teilchenimpulse. Die UV-Divergenzen werden durch grundsätzliche Unterschiede zwischen den in der Lagrangedichte der Theorie auftretenden, und den experimentell messbaren, realen Größen, verursacht. Um die UV-Divergenzen zu beseitigen, wird ein "Renormierung" genanntes Verfahren benötigt. Es werden so genannte "Counterterme" eingebracht, mit deren Hilfe sich die Divergenzen wegzkürzen lassen. Zu allen Kopplungen auf Treelevel-Ordnung werden die notwendigen Counterterme für Kopplungsparameter und Teilchenfelder berechnet und aufsummiert.

Zur Beseitigung der IR-Divergenzen ist es notwenig, die Abstrahlung von Photonen und Gluonen durch elektrisch oder quantenchromodynamisch geladene Teilchen zu berücksichtigen. Auf diese Weise heben sich die Divergenzen, die durch den Austausch virtueller, masseloser Teilchen (Photonen und Gluonen) entstehen, auf. Diese Abstrahlungsprozesse werden allgemein für Zerfälle von Fermionen in ein Fermion sowie ein skalares oder Vektor-Teilchen angegeben, und dann explizit für die Neutralino- und Charginozerfälle verwendet.

Nach dem Aufsummieren der Schleifenkorrekturen, Counterterme und Abstrahlungsprozesse können Ergebnisse wie Zerfallsbreiten und Zerfallsbreitenverhältnisse präsentiert werden. Die Wahl der dafür verwendeten Eingangsparameter orientiert sich am sogenannten SPS1a' Referenzpunkt, einem zum Zweck der besseren Vergleichbarkeit von Ergebnissen eingeführten speziellen MSSM Parameterpunkt.

Aus den Ergebnissen wird ersichtlich, dass die Schleifenkorrekturen mit bis über zehn Prozent signifikant zum Ergebnis der Zerfallsbreiten beitragen. Da allerdings die Korrekturen für verschiedene Zerfallskanäle oftmals gleiches Vorzeichen und Größenordnung aufweisen, fallen die relativen Korrekturen der Zerfallsbreitenverhältnisse geringer aus.

Abstract

The Minimal Supersymmetric Standard Model (MSSM) is one of the most accepted extensions of the Standard Model (SM) of elementary particle physics. Assuming a symmetry between bosonic and fermionic particles, it introduces so called "superpartners" to all SM particles and four additional Higgs states. The fermionic partners of Higgs bosons and gauge bosons mix to form mass eigenstates, called charginos and neutralinos.

If supersymmetry is realized in nature in the way the MSSM suggests, superpartners should be discovered in the near future at collider experiments like the Large Hadron Collider (LHC) at CERN. Among these new particles, there would be also charginos and neutralinos. Since despite the lightest neutralino all of them are assumed to be unstable, it should be possible to observe them decay. Therefore it is important to study the decay characteristics of charginos and neutralinos. So this thesis deals with calculation of decay widths and especially the branching ratios of all possible two-body decays of charginos and neutralinos.

To obtain the required precision we take into account the full radiative corrections on one-loop level. In addition to the so called "treelevel" the contributions of all one-loop graphs are calculated. The necessary computation of hundreds of Feynman diagrams is done by application of a special algebraic software.

Considering loop corrections leads to major problems: The integration of the Feynman-amplitudes leads to so called ultraviolet (UV) and infrared (IR) divergencies for very large and for vanishing particle momenta. The UV divergencies are caused by a fundamental difference between the parameters that occur in the Lagrange density that describes the theory and their physical counterparts, measured in experiment. A procedure called "renormalization" is needed to remove the UV divergencies. So called "counterterms" are introduced, that cancel away the divergencies. The necessary counterterms to all tree-level couplings are calculated and summed up with the the loop corrections to obtain a finite result.

Concerning the IR divergencies, it is necessary to take into account the radiation of photons or gluons by electrically or quantumcromodynamically charged particles. That way the divergencies, which origin from the exchange of virtual massless particles (photons or gluons) are canceled. The radiation processes are presented in a general form for the decays of one fermion into another fermion and a scalar or vector particle. Then the formulas are applied to the neutralino and chargino decays.

After summing up all treelevels, loop corrections, counterterms and photon or gluon radiation graphs, results like decay widths and branching ratios are presented. For the parameters input we choose the framework of the SPS1a' reference point. It is a certain MSSM parameter point that was introduced for better comparability.

The loop corrections contribute significantly to the results in the range of up to more than ten percent. Since the corrections to different decay channels often show the same sign and similar size, the corrections to the branching ratios are in general smaller.

Contents

1 Supersymmetry: Motivation and successes	1
2 The Minimal Supersymmetric Standard Model	5
2.1 MSSM Lagrangian	8
2.2 MSSM spectrum	9
2.2.1 Higgs sector	9
2.2.2 Sfermion sector	11
2.2.3 Neutralino sector	12
2.2.4 Chargino sector	14
3 Renormalization	15
3.1 Fermionic particles with mixing	17
3.2 Scalar particles with mixing	20
3.3 SM gauge sector	22
3.4 Electric charge	23
4 Decays of Neutralinos and Charginos	25
5 Bremsstrahlung	28
5.1 Bremsstrahlung processes for decays (fermion \rightarrow scalar, fermion)	28
5.2 Bremsstrahlung processes for decays (fermion \rightarrow vector, fermion)	31
5.3 Bremsstrahlung integrals for processes with an outgoing massless particle	32
6 Numerical Results	33
6.1 Input parameters, according the SPA convention	36
6.2 On-shell masses	37
6.3 Neutralino Decays	40
6.3.1 Variation of M_2	40
6.3.2 Variation of μ	46
6.3.3 Variation of $\tan\beta$	51
6.4 Chargino Decays	54
6.4.1 Variation of M_2	54
6.4.2 Variation of μ	58
6.4.3 Variation of $\tan\beta$	61
A Tree-level Couplings and Counterterms	64

B Calculations for Bremsstrahlung	81
B.1 Matrixelements	81
B.2 $a \times a$	82
B.3 $b \times b$	83
B.4 $c \times c$	84
B.5 $a \times b$	85
B.6 $a \times c$	86
B.7 $b \times c$	87
B.8 Bremsstrahlung integrals for processes with an outgoing neutrino	88
C Generic Vertex Structures	89
C.1 Generic structure I	90
C.2 Generic structure II	91
C.3 Generic structure III	92
C.4 Generic structure IV	93
C.5 Generic structure V	93
C.6 Generic structure VI	94
C.7 Generic structure VII	95
C.8 Generic structure VIII	96
C.9 Generic structure IX	96
C.10 Generic structure X	97
C.11 Generic structure XI	98
C.12 Generic structure XII	99
D Generic Selfenergies (SE)	100
D.1 Fermion SE: Fermion-Scalar-Loop	100
D.2 Fermion SE: Fermion-Vector-Loop	100
D.3 Vector SE: Fermion-Fermion-Loop	101
D.4 Vector SE: Scalar-Scalar-Loop	102
D.5 Vector SE: Vector-Vector-Loop	102
D.6 Vector SE: Vector-Scalar-Loop	103
D.7 Vector SE: Ghost-Ghost-Loop	103
D.8 Vector SE: Scalar-Loop	103
D.9 Vector SE: Vector-Loop	104
D.10 Scalar SE: Fermion-Fermion-Loop	104
D.11 Scalar SE: Fermion-Fermion-Loop	105
D.12 Scalar SE: Scalar-Loop	105
D.13 Scalar SE: Vector-Loop	105
D.14 Scalar SE: Vector-Scalar-Loop	106
D.15 Scalar/Vector SE: Fermion-Fermion-Loop	106
D.16 Scalar/Vector SE: Scalar-Scalar-Loop	107
D.17 Scalar/Vector SE: Vector-Scalar-Loop	107

E Vertex-Contributions	108
E.1 $\tilde{\chi}^+ \rightarrow \tilde{\chi}^0 W^+$	108
E.2 $\tilde{\chi}^+ \rightarrow \tilde{\chi}^+ Z^0$	109
E.3 $\tilde{\chi}^+ \rightarrow \tilde{\chi}^+ \gamma$	109
E.4 $\tilde{\chi}^+ \rightarrow \tilde{\chi}^0 \phi^+$	110
E.5 $\tilde{\chi}^+ \rightarrow \tilde{\chi}^+ \phi^0$	110
E.6 $\tilde{\chi}^+ \rightarrow f\tilde{f}'$	111
E.7 $\tilde{\chi}^+ \rightarrow \tilde{\chi}^0 W^+$	111
E.8 $\tilde{\chi}^0 \rightarrow \tilde{\chi}^0 Z^0$	112
E.9 $\tilde{\chi}^0 \rightarrow \tilde{\chi}^0 \gamma$	112
E.10 $\tilde{\chi}^0 \rightarrow \tilde{\chi}^+ \phi^+$	113
E.11 $\tilde{\chi}^0 \rightarrow \tilde{\chi}^0 \phi^0$	113
E.12 $\tilde{\chi}^0 \rightarrow f\tilde{f}$	114
E.13 $\tilde{\chi}^0 \rightarrow g\tilde{g}$	114
F Selfenergy-Contributions	115
F.1 Selfenergies for $\tilde{\chi}^+, \tilde{\chi}^0, f = (u_g, d_g, \nu_g, e_g)$	116
F.2 Selfenergies for $f = (\tilde{u}_g, \tilde{d}_g, \tilde{\nu}_g, \tilde{e}_g)$	117
F.3 Selfenergies for $\phi^0 = (h^0, H^0, A^0, G^0)$	118
F.4 Selfenergies for $\phi^+ = (H^+, G^+)$	119
F.5 Selfenergies for Z^0	120
F.6 Selfenergies for W^+	121
F.7 Mixed Selfenergies for $A^0, G^0, Z^0, H^+, G^+, W^+$	122

Chapter 1

Supersymmetry: Motivation and successes

The Standard Model (SM) of elementary particle physics is a remarkably successful description of presently known phenomena. Nevertheless, it is for sure not the most general way to describe nature. It has to be extended to describe physics at high energies properly, and there are a number of theoretical and phenomenological issues that the SM fails to address adequately. One of the most promising attempts to improve our understanding of elementary particle physics is supersymmetry.

The main idea of supersymmetry is the concept of an underlying symmetry between bosons and fermions that leads to superpartners for all SM particles. These superpartners have the same quantum numbers and mass but a different spin. Since no superpartners have been discovered yet, they seem to have a significant higher mass, which can be explained by spontaneous breaking of supersymmetry.

The mathematical concepts that describes supersymmetry are a symmetry transformation, that transforms a particle into its superpartner, and the corresponding algebra. Supersymmetry is a symmetry between bosons and fermions. Using the Minimal Supersymmetric Standard Model (MSSM), we only deal with a $N = 1$ supersymmetry, that means that there is only one generator, and only one superpartner per particle. This generator Q_α and its hermitian conjugate $\overline{Q}_{\dot{\alpha}} = (Q_\alpha)^*$ are fermionic operators with

$$\begin{aligned} Q|\text{Boson}\rangle &= |\text{Fermion}\rangle \\ Q|\text{Fermion}\rangle &= |\text{Boson}\rangle \end{aligned} \tag{1.1}$$

The indices $\alpha, \dot{\alpha} = 1, 2$ are always the left- and right-handed spinor indices.

Q_α and $Q_{\dot{\alpha}}$ satisfy an algebra of anticommutation and commutation relations:

$$\{Q_\alpha, Q_\beta\} = 0 \quad (1.2)$$

$$\{Q_\alpha, \overline{Q}_{\dot{\beta}}\} = 2\sigma^{\mu}_{\alpha\dot{\beta}} P_\mu \quad (1.3)$$

$$[Q_\alpha, P_\mu] = 0 \quad (1.4)$$

where σ stands for the Pauli matrices and P_μ means the momentum generator of spacetime translations. Since P_μ is the generator of the Poincaré transformation, the second relation shows a connection between supersymmetry and general relativity.

Applied to particle physics, supersymmetry has long been considered one of the best-motivated possibilities for new physics at the TeV scale. The main reasons that low energy supersymmetry is taken very seriously are not only its elegance or its theoretical motivation, but its successful explanations and predictions. Of course, these successes may just be remarkable coincidences because there is as yet no direct experimental evidence for supersymmetry. Either superpartners and a light Higgs boson must be discovered or demonstrated not to exist at the Large Hadron Collider (LHC) at CERN. In the latter case low energy supersymmetry would not describe nature. There are several open questions, that the SM fails to address adequately [1]. To some of them supersymmetry may provide answers:

- **Hierarchy problem:**

From the phenomenologic point of view, the mass of the Higgs boson associated with electroweak symmetry breaking must be in the range of $O(100\text{GeV})$. However, radiative corrections to the Higgs mass are quadratically dependent on the ultraviolet cutoff Λ , since the masses of fundamental scalar fields are not protected by chiral or gauge symmetries. The “natural” value of the Higgs mass is therefore of $O(\Lambda)$ rather than $O(100\text{ GeV})$. In other words, to achieve $m \sim O(100\text{ GeV})$ it is necessary to fine-tune the scalar mass-squared parameter $m^2 \sim \Lambda^2$ of the fundamental ultraviolet theory to a precision of m^2/Λ^2 . If, for example, $\Lambda = 10^{16}\text{ GeV}$ and $m = 100\text{ GeV}$, the precision of tuning must be 10^{-28} . This is considered to be unnatural.

Supersymmetry provides a solution to the hierarchy problem [2], as the Higgs mass parameter is not renormalized as long as supersymmetry is unbroken. Supersymmetry also mitigates the gauge hierarchy problem by breaking the electroweak symmetry radiatively through logarithmic running.

- **Electroweak symmetry breaking:**

In the SM, electroweak symmetry breaking is parameterized by the Higgs boson h and its potential $V(h)$. However, the parameters of the Higgs sector are not constrained by any symmetry principles, and therefore the energy scale of the electroweak symmetry breaking and the Higgs mass are not consequences of this potential.

With plausible boundary conditions at a high scale (certain couplings such as the top quark Yukawa of $O(1)$ and no bare Higgs mass parameter μ in the superpotential), low energy supersymmetry can provide the explanation of the origin of electroweak symmetry breaking [3, 4, 5, 6, 7]. The SM effective Higgs potential has the

form $V = m^2 h^2 + \lambda h^4$. First, supersymmetry requires that the quartic coupling λ is a function of the $U(1)_Y$ and $SU(2)$ gauge couplings $\lambda = (g'^2 + g^2)/2$. Second, the m^2 parameter runs to negative values at the electroweak scale, driven by the large top quark Yukawa coupling. Thus the “Mexican hat” potential with a minimum away from $h = 0$ is derived rather than assumed. As it is typical for progress in physics, this explanation is not from first principles, but it is an explanation in terms of the next level of the effective theory which depends on the crucial assumption that the complex SUSY-breaking mass parameters have values of order the electroweak scale. Once superpartners are discovered, the question of supersymmetry breaking must be answered in any case and it is a genuine success of the theory that whatever explains supersymmetry breaking is also capable of resolving the crucial issue of $SU(2) \times U(1)$ breaking.

- **Gauge coupling unification:**

The idea that the gauge couplings undergo renormalization group evolution in such a way that they meet at a point at a high scale lends credence to the picture of grand unified theories (GUTs) and certain string theories. However, precise measurements of the low energy values of the gauge couplings demonstrated that the SM cannot describe gauge coupling unification (see *e.g.* [8]) accurately enough.

In contrast to the SM, the MSSM allows for the unification of the gauge couplings, as first pointed out in the context of GUT models by [9, 10, 11]. The extrapolation of the low energy values of the gauge couplings using renormalization group equations and the MSSM particle content shows that the gauge couplings unify at the scale $M_G \simeq 3 \times 10^{16}$ GeV [12, 13, 14, 15]. Gauge coupling unification and electroweak symmetry breaking depend on essentially the same physics since each needs the soft masses and μ to be of order the electroweak scale.

Gauged supersymmetry additionally includes a coupling between gravity and matter, the invariance of the lagrangian density under a local supersymmetry transformation leads to a quantized form of Einstein’s general relativity. However, like all known theories that include general relativity, supergravity is nonrenormalizable as a quantum field theory.

- **Cosmological questions:**

Several difficulties are encountered when trying to build cosmological models based solely on the SM particle content. The SM does neither have a viable candidate for the cold dark matter of the universe nor a viable inflaton. In addition, the SM gives when trying to connect it with the gravitational sector, much too large a cosmological constant.

In supersymmetric theories, the lightest superpartner (LSP) can be stable. This stable superpartner provides a nice cold dark matter candidate [16, 17]. Simple estimates of its relic density are of the right order of magnitude to provide the observed amount. LSPs were noticed as good candidates before the need for nonbaryonic cold dark matter was established.

In addition to the theoretical benefits that come along with the introduction of supersymmetry, there are also some theoretical indications for the realisation of supersymmetry in nature. Although there is no direct experimental evidence, several correct predictions have been made [1]:

- Supersymmetry predicted in the early 1980s that the top quark would be heavy [18, 19], because this was a necessary condition for the validity of the electroweak symmetry breaking explanation.
- Supersymmetric grand unified theories with a high fundamental scale accurately predicted the present experimental value of $\sin^2 \theta_W$ before it was measured [10, 9, 20, 21].
- Supersymmetry requires a light Higgs boson to exist [22, 23], consistent with current precision measurements, which suggest $M_h < 200$ GeV [24].
- When LEP began to run in 1989 it was recognized that either LEP would discover superpartners if they were very light or, because all supersymmetry effects at LEP are loop effects and supersymmetry effects decouple as superpartners get heavier, there would be no significant deviations from the SM discovered at LEP. That is, it is only possible to have loop effects large enough to measure at LEP + SLC if superpartners are light enough to observe directly. In nonsupersymmetric approaches with strong interactions near the electroweak scale it was natural to expect significant deviations from the Standard Model at LEP.

Chapter 2

The Minimal Supersymmetric Standard Model

The *Minimal Supersymmetric Standard Model* (MSSM) is a simple and attractive extension of the Standard Model (SM) of particle physics. It extends the particle content of the Standard Model in two different ways. On the one hand, all particles get a superpartner, on the other hand there is a larger Higgs sector with two complex Higgs doublets. This extension is minimal since it only uses one set of SUSY-generators (so only the so called $N = 1$ supersymmetry is considered) and the additionally introduced particles and couplings are only those needed for consistency.

The superpartners get the same names as their corresponding SM-particles, just with the prefix 's' for spin = 0 superpartners and the suffix '-ino' for the spin = $\frac{1}{2}$ superpartners. That leads to names like sfermions on the one, and gauginos and higgsinos on the other hand. Particles and superpartners together form so called supermultiplets, as shown in Tables 2.2 and 2.1.

The particle content of the SM, and so also the MSSM can be expressed in 3 sectors:

- **Gauge fields**

The spin-1 gauge bosons of the SM are responsible for the conservation of the local $SU(3)_C \otimes SU(2)_L \otimes U(1)_Y$ gauge symmetry, and introduce interactions between the matter particles. Now in the MSSM, they are extended by spin- $\frac{1}{2}$ superpartners. In particular, the eight gluons of QCD, g_μ^a , get eight spin- $\frac{1}{2}$ partners \tilde{g}^a called *gluinos*, the $SU(2)$ gauge bosons W_μ^i get three *winos* \tilde{W}^i as partners and the $U(1)$ gauge boson B_μ gets a *bino* \tilde{B} . Since $SU(2)_L \times U(1)_Y$ is broken in the SM, the winos and the bino do not form mass eigenstates but mix with fields with the same charge but different $SU(2)_L \otimes U(1)_Y$ quantum numbers.

SM gauge bosons and their superpartners form the so called gauge supermultiplet of the MSSM, shown in Tab.2.1.

Names	spin 0	spin 1/2	$SU(3)_C \otimes SU(2)_L \otimes U(1)_Y$
gluino, gluon	\tilde{g}	g	(8, 1, 0)
winos, W bosons	$\lambda^\pm \ \lambda^3$	$W^\pm \ W^0$	(1, 3, 0)
bino, B boson	λ'	B^0	(1, 1, 0)

Table 2.1: Gauge supermultiplets in the Minimal Supersymmetric Standard Model.

Names	spin 0	spin 1/2	$SU(3)_C \otimes SU(2)_L \otimes U(1)_Y$
squarks, quarks (×3 families)	$(\tilde{u}_L \ \tilde{d}_L)$ \tilde{u}_R^* \tilde{d}_R^*	$(u_L \ d_L)$ \bar{u}_R \bar{d}_R	(3, 2, $\frac{1}{3}$) ($\bar{3}$, 1, $-\frac{4}{3}$) ($\bar{3}$, 1, $\frac{2}{3}$)
sleptons, leptons (×3 families)	$(\tilde{\nu} \ \tilde{e}_L)$ \tilde{e}_R^*	$(\nu \ e_L)$ \bar{e}_R	(1, 2, -1) (1, 1, 2)
Higgs, higgsinos	$(H_2^+ \ H_2^0)$ $(H_1^0 \ H_1^-)$	$(\tilde{H}_2^+ \ \tilde{H}_2^0)$ $(\tilde{H}_1^0 \ \tilde{H}_1^-)$	(1, 2, -1) (1, 2, 1)

Table 2.2: Chiral supermultiplets in the Minimal Supersymmetric Standard Model.

- **Matter fields**

The matter fermions of the SM contain three generations of leptons and quarks, i.e. for each generation two $SU(2)_L$ fermion doublets and three singlets for the right-handed fermions,

$$L = \begin{pmatrix} \nu_L \\ e_L \end{pmatrix}, \quad E = \bar{e}_R, \quad Q = \begin{pmatrix} u_L \\ d_L \end{pmatrix}, \quad D = \bar{d}_R, \quad U = \bar{u}_R. \quad (2.1)$$

The MSSM introduces a spin-0 bosonic superpartner to each SM matter particle, called *sleptons* and *squarks*:

$$\tilde{L} = \begin{pmatrix} \tilde{\nu}_L \\ \tilde{e}_L \end{pmatrix}, \quad \tilde{E} = \tilde{e}_R^*, \quad \tilde{Q} = \begin{pmatrix} \tilde{u}_L \\ \tilde{d}_L \end{pmatrix}, \quad \tilde{D} = \tilde{d}_R^*, \quad \tilde{U} = \tilde{u}_R^*. \quad (2.2)$$

- **Higgs sector**

Different to the SM, the MSSM needs two complex Higgs doublets, which couple at tree level to up and down type chiral fermions separately. This is required by supersymmetry itself as well as by the attempt to keep the theory anomaly free. Those anomaly constraints require the the two Higgs doublets to have opposite Hypercharges. Like all other particles, the spin-0 Higgs particles also obtain superpartners , the spin- $\frac{1}{2}$ higgsinos \tilde{H}_i^j :

$$\begin{aligned} H_1 &= \begin{pmatrix} H_1^1 \\ H_1^2 \end{pmatrix}, & H_2 &= \begin{pmatrix} H_2^1 \\ H_2^2 \end{pmatrix}, \\ \tilde{H}_1 &= \begin{pmatrix} \tilde{H}_1^1 \\ \tilde{H}_1^2 \end{pmatrix}, & \tilde{H}_2 &= \begin{pmatrix} \tilde{H}_2^1 \\ \tilde{H}_2^2 \end{pmatrix}. \end{aligned} \quad (2.3)$$

Together with the matter particles and their superpartners, the Higgs and higgsino particles form the Chiral supermultiplets in the MSSM, as shown in Tab.2.2.

2.1 MSSM Lagrangian

The complete Lagrangian of the MSSM can be written as

$$\begin{aligned}\mathcal{L}_{\text{SUSY}} = & -i\bar{\psi}\bar{\sigma}^\mu D_\mu\psi - D^\mu\phi^*D_\mu\phi - \frac{1}{2}(W^{ij}\psi_i\psi_j + W^{*ij}\bar{\psi}_i\bar{\psi}_j) \\ & -W^iW_i^* + \frac{1}{2}g_a^2(\phi^*T^a\phi)^2 - \frac{1}{4}F_{\mu\nu}^aF^{\mu\nu a} - i\bar{\lambda}^a\bar{\sigma}^\mu D_\mu\lambda^a \\ & -\sqrt{2}g((\phi^*T^a\psi)\lambda^a + \bar{\lambda}^a(\bar{\psi}T^a\phi)) + \mathcal{L}_{\text{soft}}\end{aligned}\quad (2.4)$$

The first line shows the kinetic terms of fermions and scalars; the last term comes from the superpotential W :

$$W = \frac{1}{2}M^{ij}\phi_i\phi_j + \frac{1}{6}y^{ijk}\phi_i\phi_j\phi_k \quad (2.5)$$

$$W^i = \frac{\delta W}{\delta\phi_i}, \quad W^{ij} = \frac{\delta^2 W}{\delta\phi_i\delta\phi_j} \quad (2.6)$$

M^{ij} is a symmetric mass matrix for the fermion fields, and y^{ijk} is a Yukawa coupling of a scalar ϕ_k with two fermions $\psi_i\psi_j$, which is totally symmetric under interchange of i, j, k .

In the second line of Eqn.2.4, the first two terms come from the scalar-potential, the third term describes the self interaction of gauge-fields (T^a denoting the generators of the gauge group), the last is the kinetic term of gauginos.

The last row finally consists of additional couplings (between a scalar, fermion and a gaugino) and the soft supersymmetry breaking lagrangian.

To understand the necessity for a SUSY-breaking term, one has to remember, that no supersymmetric particles have been discovered yet. So they must have significantly higher masses than the standard model particles. Like electroweak symmetry breaking, supersymmetry may be broken spontaneously. Although this mechanism of producing the symmetry breaking at high energies is not totally understood yet, its possible to use theoretical conditions like renormalizability to find a general representation of the possible supersymmetry breaking terms in the lagrangian at low energies, given in Eqn.2.7:

$$\begin{aligned}\mathcal{L}_{\text{soft}} = & -\frac{1}{2}(M_\lambda\lambda^a\lambda^a + \text{c.c.}) - (m^2)_j^i\phi^{j*}\phi_i \\ & - \left(\frac{1}{2}b^{ij}\phi_i\phi_j + \frac{1}{6}a^{ijk}\phi_i\phi_j\phi_k + \text{c.c.} \right)\end{aligned}\quad (2.7)$$

M_λ are the gaugino masses for each gauge group, $(m^2)_i^j$ and b^{ij} scalar (mass)² terms, and a^{ijk} (scalar)³ couplings.

A more detailed derivation of the lagrangian of the MSSM may be found in [28] and [29]. The problem of soft SUSY-breaking is discussed in [1].

2.2 MSSM spectrum

2.2.1 Higgs sector

In the MSSM, two complex Higgs doublets (H_1, H_2) with eight real scalar degrees of freedom are needed for electroweak symmetry breaking.

$$H_1 = \begin{pmatrix} H_1^1 \\ H_1^2 \end{pmatrix} = \begin{pmatrix} H_1^0 \\ H_1^- \end{pmatrix}, \quad H_2 = \begin{pmatrix} H_2^1 \\ H_2^2 \end{pmatrix} = \begin{pmatrix} H_2^+ \\ H_2^0 \end{pmatrix}$$

Three of these eight real scalar degrees of freedom become the longitudinal modes of the massive vector bosons Z^0 and W^\pm . By expanding the Higgs potential around its minimum, one obtains five Higgs bosons, corresponding to the five degrees of freedom not required for the gauge boson masses. The five Higgs bosons of the MSSM consist of three neutral Higgs bosons h^0, H^0, A^0 and the two charged ones, H^\pm .

The scalar Higgs potential in the MSSM is given by

$$\begin{aligned} V = & (m_{H_1}^2 + |\mu|^2)|H_1|^2 + (m_{H_2}^2 + |\mu|^2)|H_2|^2 - m_{12}^2(H_1 H_2 + H_1^\dagger H_2^\dagger) \\ & + \frac{1}{8}(g^2 + g'^2)(|H_1|^2 - |H_2|^2)^2 + \frac{g^2}{2}|H_1^\dagger H_2|^2. \end{aligned} \quad (2.8)$$

$m_{H_i}^2$ and m_{12}^2 are soft SUSY-breaking parameters, μ is the analogue to the SM Higgs mass parameter. In contrast to the SM, where the Higgs self interaction is introduced by hand, in the MSSM it is determined by the gauge couplings g' and g .

To obtain electroweak symmetry breaking, it is assumed that both Higgs doublets have non-vanishing vacuum expectation values (VEV). Without loss of generality one can choose $\langle H_2^+ \rangle = 0$ at the minimum of the potential, implying that also the VEV of the negatively charged component of H_1 is vanishing, $\langle H_1^- \rangle = 0$. So the VEVs of H_1 and H_2 can be written as

$$\langle H_1 \rangle = \begin{pmatrix} v_1 \\ 0 \end{pmatrix}, \quad \langle H_2 \rangle = \begin{pmatrix} 0 \\ v_2 \end{pmatrix}. \quad (2.9)$$

This leads to nonvanishing VEVs for the neutral Higgs boson fields, both charged Higgs scalars remain unaffected. So only weak interaction, but not electromagnetism is broken, which agrees with experiment.

A common parameterization for the two Higgs doublets is:

$$H_1 \equiv \begin{pmatrix} H_1^0 \\ H_1^- \end{pmatrix} = \begin{pmatrix} v_1 + (\phi_1^0 + i\chi_1^0)/\sqrt{2} \\ \phi_1^- \end{pmatrix}, \quad Y_{H_1} = -1 \quad (2.10)$$

$$H_2 \equiv \begin{pmatrix} H_2^+ \\ H_2^0 \end{pmatrix} = \begin{pmatrix} \phi_2^+ \\ v_2 + (\phi_2^0 + i\chi_2^0)/\sqrt{2} \end{pmatrix}, \quad Y_{H_2} = +1 \quad (2.11)$$

The minimum of the Higgs potential is obtained by solving the equations

$$\frac{\partial V}{\partial H_1^0} \Big|_{\langle H_n^0 \rangle = v_n} = \frac{\partial V}{\partial H_2^0} \Big|_{\langle H_n^0 \rangle = v_n} = 0. \quad (2.12)$$

This leads to the two minimization conditions

$$(m_{H_1}^2 + |\mu|^2)v_1 = -m_{12}^2v_2 - \frac{1}{4}(g^2 + g'^2)(v_1^2 - v_2^2), \quad (2.13)$$

$$(m_{H_2}^2 + |\mu|^2)v_2 = -m_{12}^2v_1 + \frac{1}{4}(g^2 + g'^2)(v_1^2 - v_2^2). \quad (2.14)$$

From experiment, the following relations are well known:

$$m_Z^2 = \frac{g^2 + g'^2}{2}(v_1^2 + v_2^2), \quad m_W^2 = \frac{g^2}{2}(v_1^2 + v_2^2), \quad (2.15)$$

$$v^2 \equiv (v_1^2 + v_2^2) = \frac{2m_Z^2}{g^2 + g'^2} \approx (174 \text{ GeV})^2. \quad (2.16)$$

Now we can express both VEVs in terms of one single parameter

$$\tan \beta \equiv \frac{v_2}{v_1} \geq 0, \quad 0 \leq \beta \leq \frac{\pi}{2}. \quad (2.17)$$

Eqs. (2.13) and (2.14) may now be written as

$$(m_{H_1}^2 + |\mu|^2) = -m_{12}^2 \tan \beta - \frac{1}{2}m_Z^2 \cos 2\beta, \quad (2.18)$$

$$(m_{H_2}^2 + |\mu|^2) = -m_{12}^2 \cot \beta + \frac{1}{2}m_Z^2 \cos 2\beta. \quad (2.19)$$

Evaluating the second derivatives of the Higgs potential taken at its minimum leads to the Higgs mass spectrum

$$M_{ij}^{2,\text{Higgs}} = \frac{1}{2} \left. \frac{\partial^2 V}{\partial H_i \partial H_j} \right|_{\langle H_n^0 \rangle = v_n}. \quad (2.20)$$

At tree level, $M_{ij}^{2,\text{Higgs}}$ can be split into independent 2×2 mass matrices. As a result of separate diagonalization, we obtain finally the mass eigenstates, in terms of the original gauge eigenstate fields, given by

$$\begin{pmatrix} H^0 \\ h^0 \end{pmatrix} = \begin{pmatrix} \cos \alpha & \sin \alpha \\ -\sin \alpha & \cos \alpha \end{pmatrix} \begin{pmatrix} \phi_1^0 \\ \phi_2^0 \end{pmatrix}, \quad (2.21)$$

$$\begin{pmatrix} G^0 \\ A^0 \end{pmatrix} = \begin{pmatrix} -\cos \beta & \sin \beta \\ \sin \beta & \cos \beta \end{pmatrix} \begin{pmatrix} \chi_1^0 \\ \chi_2^0 \end{pmatrix}, \quad (2.22)$$

$$\begin{pmatrix} G^\pm \\ H^\pm \end{pmatrix} = \begin{pmatrix} -\cos \beta & \sin \beta \\ \sin \beta & \cos \beta \end{pmatrix} \begin{pmatrix} \phi_1^\pm \\ \phi_2^\pm \end{pmatrix}. \quad (2.23)$$

The Goldstone bosons G^0 and G^\pm are absorbed by the longitudinal components of the vector bosons Z^0 and W^\pm and so are responsible for the creation of their masses. The remaining physical Higgs bosons spectrum consists of two neutral CP-even states (h^0, H^0), one neutral CP-odd state A^0 and the two charged Higgs bosons H^\pm .

The masses Higgs sector, as well as the mixing angle α , may be described at tree level by two independent parameters. Usually, one chooses m_{A^0} and $\tan \beta$:

$$m_{h^0, H^0}^2 = \frac{1}{2} \left[m_{A^0}^2 + m_Z^2 \mp \sqrt{(m_{A^0}^2 + m_Z^2)^2 - 4m_{A^0}^2 m_Z^2 \cos^2 \beta} \right], \quad (2.24)$$

$$m_{H^\pm}^2 = m_{A^0}^2 + m_W^2, \quad (2.25)$$

$$\tan 2\alpha = \tan 2\beta \frac{m_{A^0}^2 + m_Z^2}{m_{A^0}^2 - m_Z^2}, \quad -\frac{\pi}{2} \leq \alpha \leq 0 \quad (2.26)$$

Loop corrections have a great influence on Higgs masses and other parameters of the Higgs sector. As an example, the mass of the lightest Higgs boson h_0 is even below m_Z on tree-level, what would be already ruled out by the experiment. After taking into account higher order corrections, m_{h_0} is increased to a value still compatible with the experiment (e.g. $m_{h_0} > m_Z$).

2.2.2 Sfermion sector

The sfermion mixing can be described by the sfermion mass matrix in the left-right interaction basis (f_L, f_R) , transformed in the mass basis $(\tilde{f}_1, \tilde{f}_2)$, $f = \tilde{t}, \tilde{b}$ or $\tilde{\tau}$ by a rotation matrix $R^{\tilde{f}}$,

$$\mathcal{M}_{\tilde{f}}^2 = \begin{pmatrix} m_{\tilde{f}_L}^2 & a_f m_f \\ a_f m_f & m_{\tilde{f}_R}^2 \end{pmatrix} = (R^{\tilde{f}})^\dagger \begin{pmatrix} m_{\tilde{f}_1}^2 & 0 \\ 0 & m_{\tilde{f}_2}^2 \end{pmatrix} R^{\tilde{f}}, \quad (2.27)$$

with

$$m_{\tilde{f}_L}^2 = M_{\{\tilde{Q}; \tilde{L}\}}^2 + m_f^2 + m_Z^2 \cos 2\beta (I_f^{3L} - e_f \sin^2 \theta_W), \quad (2.28)$$

$$m_{\tilde{f}_R}^2 = M_{\{\tilde{U}; \tilde{D}\}}^2 + m_f^2 + m_Z^2 \cos 2\beta e_f \sin^2 \theta_W, \quad (2.29)$$

$$a_f m_f = \begin{cases} m_u (A_u^* - \mu \cot \beta) & \dots \text{for up-type sfermions} \\ m_d (A_d^* - \mu \tan \beta) & \dots \text{for down-type sfermions} \end{cases}. \quad (2.30)$$

$M_{\tilde{Q}}, M_{\tilde{L}}, M_{\tilde{U}}, M_{\tilde{D}}$ and $M_{\tilde{E}}$ are soft SUSY-breaking masses, A_f is the trilinear scalar coupling parameter, μ the higgsino mass parameter, β is the ratio of the VEVs of the two neutral Higgs states (introduced in Subsection 2.2.1).

I_f^{3L} denotes the third component of the weak isospin of the fermion f , e_f the electric charge in terms of the elementary charge e_0 , and θ_W is the Weinberg angle.

The 2×2 rotation matrix to that diagonalizes the mass matrix by the rotation angle $\theta_{\tilde{f}}$ to obtain the mass eigenstates is given by

$$R_{ij}^{\tilde{f}} = \begin{pmatrix} \cos \theta_{\tilde{f}} & \sin \theta_{\tilde{f}} \\ -\sin \theta_{\tilde{f}} & \cos \theta_{\tilde{f}} \end{pmatrix}, \quad (2.31)$$

Applying the rotation matrix $R_{i\alpha}^{\tilde{f}}$ to the interaction eigenstates \tilde{f}_α ($\alpha = L, R$), one receives the mass eigenstates \tilde{f}_i ($i = 1, 2$) and vice versa:

$$\tilde{f}_i = \begin{pmatrix} \tilde{f}_1 \\ \tilde{f}_2 \end{pmatrix} = R^{\tilde{f}} \cdot \begin{pmatrix} \tilde{f}_L \\ \tilde{f}_R \end{pmatrix} = R_{i\alpha}^{\tilde{f}} \tilde{f}_\alpha \quad (2.32)$$

$$\tilde{f}_\alpha = \begin{pmatrix} \tilde{f}_L \\ \tilde{f}_R \end{pmatrix} = (R^{\tilde{f}})^\dagger \cdot \begin{pmatrix} \tilde{f}_1 \\ \tilde{f}_2 \end{pmatrix} = R_{i\alpha}^{\tilde{f}*} \tilde{f}_i \quad (2.33)$$

For the sfermion masses we use the convention

$$m_{\tilde{f}_2} > m_{\tilde{f}_1}. \quad (2.34)$$

The mass eigenvalues and the mixing angle in terms of primary parameters are

$$m_{\tilde{f}_{1,2}}^2 = \frac{1}{2} \left(m_{\tilde{f}_L}^2 + m_{\tilde{f}_R}^2 \mp \sqrt{(m_{\tilde{f}_L}^2 - m_{\tilde{f}_R}^2)^2 + 4a_f^2 m_f^2} \right), \quad (2.35)$$

$$\cos \theta_{\tilde{f}} = \frac{-a_f m_f}{\sqrt{(m_{\tilde{f}_L}^2 - m_{\tilde{f}_1}^2)^2 + a_f^2 m_f^2}} \quad (0 \leq \theta_{\tilde{f}} < \pi), \quad (2.36)$$

Since we assume massles neutrinos to be sufficient good approximation, there is no mixing among the sneutrinos, and the mass of the sneutrino $\tilde{\nu}_\tau$ is given by

$$m_{\tilde{\nu}_\tau}^2 = M_L^2 + \frac{1}{2} m_Z^2 \cos 2\beta. \quad (2.37)$$

2.2.3 Neutralino sector

Due to electroweak symmetry breaking, higgsinos and gauginos mix with each other. The mass eigenstates formed by the superpartners of the neutral gauge bosons (\tilde{B}_μ and \tilde{W}_μ^3), and of the neutral Higgs bosons (\tilde{H}_1^0 and \tilde{H}_2^0) are called *neutralinos*.

Using the gauge-eigenstate (interaction-eigenstate) basis

$$\psi_j^0 = (-i\tilde{B}, -i\tilde{W}^3, \tilde{H}_1^0, \tilde{H}_2^0), \quad (2.38)$$

the neutralino mass terms occurring in the lagrangian are

$$\mathcal{L} = -\frac{1}{2} (\psi^0)^T Y \psi^0 + h.c.. \quad (2.39)$$

The neutralino mass matrix used in Eqn.2.39 is defined as

$$Y = \begin{pmatrix} M_1 & 0 & -m_Z s_W \cos \beta & m_Z s_W \sin \beta \\ 0 & M_2 & m_Z c_W \cos \beta & -m_Z c_W \sin \beta \\ -m_Z s_W \cos \beta & m_Z c_W \cos \beta & 0 & -\mu \\ m_Z s_W \sin \beta & -m_Z c_W \sin \beta & -\mu & 0 \end{pmatrix}. \quad (2.40)$$

The abbreviations s_W and c_W are the short forms for the sine and the cosine of the Weinberg angle. M_1 and M_2 originate from the soft SUSY-breaking parts of the lagrangian, $-\mu$ are the supersymmetric higgsino mass terms. The remaining offdiagonal terms proportional to m_Z evolve from the Higgs-higgsino-gaugino couplings.

Since neutralinos are Majorana particles the mass matrix Y can be diagonalized using only one single rotation matrix Z :

$$ZYZ^{-1} = \text{diag}(m_{\tilde{\chi}_1^0}, m_{\tilde{\chi}_2^0}, m_{\tilde{\chi}_3^0}, m_{\tilde{\chi}_4^0}) \quad |m_{\tilde{\chi}_1^0}| \leq |m_{\tilde{\chi}_2^0}| \leq |m_{\tilde{\chi}_3^0}| \leq |m_{\tilde{\chi}_4^0}| \quad (2.41)$$

For the labeling, we use the conventional ascending order:

$$|m_{\tilde{\chi}_1^0}| \leq |m_{\tilde{\chi}_2^0}| \leq |m_{\tilde{\chi}_3^0}| \leq |m_{\tilde{\chi}_4^0}| \quad (2.42)$$

The physical neutralino mass states $\tilde{\chi}_i^0$ can be calculated by applying a unitary mixing matrix Z , which diagonalizes the mass matrix Y , on the interaction states:

$$\tilde{\chi}_i^0 \equiv Z_{ij} \tilde{\psi}_j^0 \quad (2.43)$$

Finally, the mass term Lagrangian gets can be written as

$$\mathcal{L} = -\frac{1}{2} \sum_{i=1}^4 m_{\tilde{\chi}_i^0} \bar{\tilde{\chi}}_i^0 \tilde{\chi}_i^0. \quad (2.44)$$

Since the mass eigenstates $\tilde{\chi}_i^0$ are mixtures of gauginos and higgsinos, they combine "gaugino-like" and "higgsino-like" parts. In this context, an interesting limit can be found in the case of

$$m_Z \ll |\mu \pm M_1|, \quad m_Z \ll |\mu \pm M_2|. \quad (2.45)$$

In this limit, the electroweak symmetry breaking only causes a small perturbation on the neutralino mass matrix. So the mass eigenstates can be assumed approximately as

$$\begin{aligned} \tilde{\chi}_1^0 &\approx \tilde{B} \\ \tilde{\chi}_2^0 &\approx \tilde{W}^0 \\ \tilde{\chi}_3^0 &\approx (\tilde{H}_u^0 + \tilde{H}_d^0)/\sqrt{2} \\ \tilde{\chi}_4^0 &\approx (\tilde{H}_u^0 - \tilde{H}_d^0)/\sqrt{2}. \end{aligned} \quad (2.46)$$

So we have a "bino-like" $\tilde{\chi}_1^0$ and a "wino-like" $\tilde{\chi}_2^0$, and "higgsino-like" heavier neutralinos $\tilde{\chi}_3^0$ and $\tilde{\chi}_4^0$. This case seems to be not so unlikely, since the "bino-like" $\tilde{\chi}_1^0$ would be a adequate candidate to describe dark matter. In addition, this particular limit fulfills minimal supergravity boundaries.

2.2.4 Chargino sector

Similar to the neutral gauginos and higgsinos, also the electrically charged superpartners of gauge bosons (W^\pm) and Higgs (H^\pm) particles mix to form mass eigenstates. The resulting physical particles are called *charginos*.

In Weyl representation, the chargino fields [30] can be written as

$$\psi^+ = (-i\tilde{W}^+, \tilde{H}_2^+) \quad \psi^- = (-i\tilde{W}^-, \tilde{H}_1^-). \quad (2.47)$$

The corresponding mass term of the Lagrangian has the form

$$\mathcal{L} = -\frac{1}{2} (\psi^+, \psi^-) \cdot \begin{pmatrix} 0 & X^T \\ X & 0 \end{pmatrix} \cdot \begin{pmatrix} \psi^+ \\ \psi^- \end{pmatrix} + \text{h.c.}, \quad (2.48)$$

with the mass matrix

$$X = \begin{pmatrix} M_2 & \sqrt{2}m_W \sin \beta \\ \sqrt{2}m_W \cos \beta & \mu \end{pmatrix}. \quad (2.49)$$

The mass matrix X can be diagonalized by two 2×2 matrices U and V :

$$UXV^{-1} = \begin{pmatrix} m_{\tilde{\chi}_1^\pm} & 0 \\ 0 & m_{\tilde{\chi}_2^\pm} \end{pmatrix}, \quad |m_{\tilde{\chi}_1^\pm}| \leq |m_{\tilde{\chi}_2^\pm}|. \quad (2.50)$$

In Dirac representation, the relation between the mass eigenstates and the gauge eigenstates is given by

$$\tilde{\chi}_i^\pm \equiv \begin{pmatrix} V_{ij} \psi_j^+ \\ U_{ij} \bar{\psi}_j^- \end{pmatrix}. \quad (2.51)$$

The mass eigenvalues can be computed analytically:

$$m_{\tilde{\chi}_{1,2}^\pm}^2 = \frac{1}{2} \left[M^2 + \mu^2 + 2m_W^2 \mp \sqrt{(M^2 + \mu^2 + 2m_W^2)^2 - 4(m_W^2 \sin 2\beta - \mu M)^2} \right] \quad (2.52)$$

Like the neutralinos, the charginos decompose into one "wino-like" and one "higgsino-like" state in the limit of large $|\mu|$ and/or large M_1, M_2 :

$$\begin{aligned} \tilde{\chi}_1^\pm &\approx \widetilde{W}^\pm \\ \tilde{\chi}_2^\pm &\approx \widetilde{H}^\pm \end{aligned} \quad (2.53)$$

Chapter 3

Renormalization

The progress of accelerators and detectors lead to a considerable improvement of the accuracy of high energy physics experiments. Therefor, it is not longer sufficient to consider only the lowest level of perturbation theory, the so called Born approximation or tree-level. To reach an accuracy in calculation, that allows to compare the results with the precision experiments, it is necessary to include higher orders. In the picture of *Feynman diagrams* that means to add loop graphs to the tree-levels graphs. Unfortunately, this can not be done easily in a naive, straight forward way. The loop diagrams, that represent the next to leading order of perturbation theory introduce integrals of the form

$$\int \frac{d^4 q}{q^2 - m^2 + i\epsilon}. \quad (3.1)$$

These integrals are divergent for large momenta. The divergencies are caused by fundamental theoretical reasons. Integrating over the whole range from $q = 0$ to $q = \infty$ means to assume implicitly, that our models work for all energy and length scales. That is of course rather implausible. The problem can also be viewed from another side. Just adding the loop diagrams simply straight forward neglects the fact, that there is a difference between the parameters in a calculation of certain order, and the realistic, physical parameters, that result of all possible processes in nature, up to infinite order.

The way out of this dilemma is called *renormalization*. The divergencies are absorbed into the relations between the physical parameters and the "bare" parameters or the not renormalized theory. Using the redefined Lagrangian, the results become finite again and our lack of knowledge is shifted to the now diverging bare parameters.

In particular, we will use the so-called *multiplicative renormalization*. All bare parameters and fields of the original Lagrangian are replaced by the corresponding *renormalized* ones, which are obtained by the multiplication with renormalization constants:

$$g_0 \rightarrow Z_g g = \left(1 + \frac{\delta g}{g}\right) g, \quad (3.2)$$

$$\phi_0 \rightarrow Z_\phi^{1/2} \phi = \left(1 + \frac{1}{2} \delta Z_\phi\right) \phi. \quad (3.3)$$

By expanding the renormalization constants Z_g and $Z_\phi^{1/2}$ around the value 1, the original Lagrangian can be split into a renormalized Lagrangian and a part containing the *counter terms* δg and δZ_ϕ , i.e.

$$\mathcal{L}(g_0, \phi_0) = \mathcal{L}(g, \phi) + \delta\mathcal{L}(g, \phi, \delta g, \delta Z_\phi). \quad (3.4)$$

In order to absorb the divergences mentioned above and to give the parameters a well-defined meaning, these counter terms have to fulfill several requirements (renormalization conditions) depending on the chosen renormalization scheme. For our calculations, we use the *on-shell renormalization scheme* [31], that identifies the renormalized parameters with observables.

Before the renormalization process itself can be done, it is necessary to find a way to remove the infinities from the divergent integrals. This procedure is called *regularization*. Regularization is of course not a physically motivated treatment like the following renormalization. It just means to parameterize the divergent parts, so that it becomes possible to "switch the divergencies on and off" by changing one parameter. After the renormalization process is done, the result should be a sum of several terms, which are together independent of this parameter, and so finite, even if the single parts alone were not. For supersymmetric models, appropriate regularization schemes are dimensional reduction (DRED), introduced by W. Siegel [34], or constrained differential renormalization (CDR) [35], used by Thomas Hahn in his FormCalc package [36].

Although all our calculations are done using the on-shell scheme, the input parameters for the plots shown in Chapter 6 will be given in the *SPA-convention* [32], that uses the so called $\overline{\text{DR}}$ -scheme [33]. In other renormalization schemes than the on-shell scheme, the renormalized quantities are not defined by observables, but by just subtracting divergent terms. One may define a divergence parameter

$$\Delta = \frac{2}{\epsilon} - \gamma_E + \log 4\pi, \quad (3.5)$$

whereas γ_E is the Euler constant ($0.57721\dots$). One may define a renormalization scheme by the "mininal subtraction" of only the divergent terms including ϵ or by subtracting the whole divergence parameter, also including the constants $-\gamma_E$ and $\log 4\pi$. In the $\overline{\text{DR}}$ -scheme the whole divergence parameter is subtracted and dimensional reduction (DRED) is used for regularization.

In the following we introduce the renormalization constants necessary to renormalize neutralino and chargino decays at one-loop level. That includes as well renormalization of wave functions, masses and mixing matrices and coupling constants. The generic forms of the used selfenergies are listed in Appendix D, a listing of all contributions to the selfenergies can be found in Appendix F.

3.1 Fermionic particles with mixing

The renormalized Lagrangian \mathcal{L} can be obtained by inserting renormalized fields ψ_j and mass parameters m_i into the bare Lagrangian \mathcal{L}_0 :

$$\mathcal{L} = \bar{\psi}_j \delta_{ij} (i \not{\partial} - m_i) \psi_i, \quad (3.6)$$

$$\mathcal{L}_0 = \bar{\psi}_{0,j} \delta_{ij} (i \not{\partial} - m_{0,i}) \psi_{0,i} \quad (3.7)$$

The unrenormalized quantities in terms of the renormalized are given by

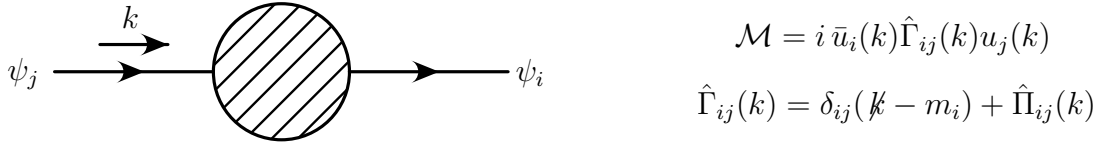
$$\psi_{0,j} = (\delta_{jk} + \frac{1}{2} \delta Z_{jk}^L P_L + \frac{1}{2} \delta Z_{jk}^R P_R) \psi_k, \quad (3.8)$$

$$\bar{\psi}_{0,i} = \bar{\psi}_l (\delta_{il} + \frac{1}{2} \delta Z_{il}^{R\dagger} P_L + \frac{1}{2} \delta Z_{il}^{L\dagger} P_R), \quad (3.9)$$

$$m_{0,i} = m_i + \delta m_i, \quad (3.10)$$

with $\delta Z_{il}^{L,R\dagger}$ meaning hermitian conjugated of $\delta Z_{il}^{L,R}$ with regard to the spinor indices.

To "pin down" and find the well defined form of the renormalization constants in the on-shell scheme, we use the renormalized one particle irreducible (1PI) two-point-function



The renormalized self-energy, that represents the contributions of loops and counterterms can be decomposed as

$$\hat{\Pi}_{ij}(k) = \not{k} P_L \hat{\Pi}_{ij}^L(k) + \not{k} P_R \hat{\Pi}_{ij}^R(k) + \hat{\Pi}_{ij}^{S,L}(k) P_L + \hat{\Pi}_{ij}^{S,R}(k) P_R. \quad (3.11)$$

If we insert the counter-term Lagrangian

$$\delta\mathcal{L} = \bar{\psi}_i (\not{k} P_L C_{ij}^L + \not{k} P_R C_{ij}^R - C_{ij}^{S,L} P_L - C_{ij}^{S,R} P_R) \psi_j, \quad (3.12)$$

into the bare Lagrangian $\mathcal{L}_0 = \mathcal{L} + \delta\mathcal{L}$, the coefficients $C_{ij}^{...}$ become

$$C_{ij}^L = \frac{1}{2} (\delta Z_{ij}^L + \delta Z_{ji}^{L\dagger}), \quad (3.13)$$

$$C_{ij}^R = \frac{1}{2} (\delta Z_{ij}^R + \delta Z_{ji}^{R\dagger}), \quad (3.14)$$

$$C_{ij}^{S,L} = \frac{1}{2} (m_i \delta Z_{ij}^L + m_j \delta Z_{ji}^{L\dagger}) + \delta_{ij} \delta m_i, \quad (3.15)$$

$$C_{ij}^{S,R} = \frac{1}{2} (m_i \delta Z_{ij}^R + m_j \delta Z_{ji}^{R\dagger}) + \delta_{ij} \delta m_i. \quad (3.16)$$

Thus the renormalized self-energies can be written as

$$\hat{\Pi}_{ij}^L = \Pi_{ij}^L + \frac{1}{2}(\delta Z_{ij}^L + \delta Z_{ji}^{L\dagger}), \quad (3.17)$$

$$\hat{\Pi}_{ij}^R = \Pi_{ij}^R + \frac{1}{2}(\delta Z_{ij}^R + \delta Z_{ji}^{R\dagger}), \quad (3.18)$$

$$\hat{\Pi}_{ij}^{S,L} = \Pi_{ij}^{S,L} - \frac{1}{2}(m_i \delta Z_{ij}^L + m_j \delta Z_{ji}^{L\dagger}) - \delta_{ij} \delta m_i, \quad (3.19)$$

$$\hat{\Pi}_{ij}^{S,R} = \Pi_{ij}^{S,R} - \frac{1}{2}(m_i \delta Z_{ij}^R + m_j \delta Z_{ji}^{R\dagger}) - \delta_{ij} \delta m_i. \quad (3.20)$$

The on-shell renormalization scheme requires that the renormalized mass parameter is the real part of the propagator's pole, and so is equal to the physical mass. It is further required that the propagator's residue has the value 1. These assumptions lead to the on-shell renormalization conditions

$$\begin{aligned} \text{Re } \hat{\Gamma}_{ij}(k) u_j(k) \Big|_{k^2=m_j^2} &= 0, \\ \lim_{k^2 \rightarrow m_i^2} \frac{1}{k - m_i} \text{Re } \hat{\Gamma}_{ii}(k) u_i(k) &= u_i(k). \end{aligned} \quad (3.21)$$

If we now apply the renormalization conditions in eq. (3.21), we get the counter terms for the mass parameter and the wave-function corrections

$$\delta m_i = \frac{1}{2} \text{Re} \left[m_i \left(\Pi_{ii}^L(m_i) + \Pi_{ii}^R(m_i) \right) + \Pi_{ii}^{S,L}(m_i) + \Pi_{ii}^{S,R}(m_i) \right]. \quad (3.22)$$

$$\delta Z_{ij}^L = \frac{2}{m_i^2 - m_j^2} \text{Re} \left[m_j^2 \Pi_{ij}^L(m_j) + m_i m_j \Pi_{ij}^R(m_j) + m_i \Pi_{ij}^{S,L} + m_j \Pi_{ij}^{S,R} \right], \quad (3.23)$$

$$\begin{aligned} \delta Z_{ii}^L &= -\Pi_{ii}^L(m_i) + \frac{1}{2m_i} \left[\Pi_{ii}^{S,L}(m_i) - \Pi_{ii}^{S,R}(m_i) \right] \\ &\quad - m_i \frac{\partial}{\partial k^2} \left[m_i (\Pi_{ii}^L(k) + \Pi_{ii}^R(k)) + \Pi_{ii}^{S,L}(k) + \Pi_{ii}^{S,R}(k) \right] \Big|_{k^2=m_i^2}. \end{aligned} \quad (3.24)$$

The right-handed terms are obtained by interchanging $\Pi^{(S),R} \leftrightarrow \Pi^{(S),L}$.

When dealing with mixing fermions, one faces couplings containing mixing matrices. These mixing matrices need to be renormalized too. In our case we need counterterms to the chargino mixing matrices U_{ij} and V_{ij} , and to the neutralino mixing matrix N_{ij} . With no experimental data available, a process and scale independent fixing is chosen.

$$\delta U_{ij} = \frac{1}{4} \sum_{k=1}^2 \left(\delta Z_{ik}^R(\tilde{\chi}^+)^C - \delta Z_{ki}^R(\tilde{\chi}^+) \right) U_{kj}$$

$$\delta V_{ij} = \frac{1}{4} \sum_{k=1}^2 \left(\delta Z_{ik}^L(\tilde{\chi}^+) - \delta Z_{ki}^R(\tilde{\chi}^+)^C \right) U_{kj} \quad (3.25)$$

$$\delta N_{ij} = \frac{1}{4} \sum_{k=1}^4 \left(\delta Z_{ik}^L(\tilde{\chi}^0) - \delta Z_{ki}^R(\tilde{\chi}^0) \right) N_{kj} \quad (3.26)$$

The anti-hermitian parts of the off-diagonal wave function corrections cancel the rotation. That the counter-terms comply with the requirements concerning the cancelation of the UV-divergences is shown in [37]. Their gauge-independence within the Feynman-tHooft gauge is shown in [38]. For more detailed information about the renormalization of the chargino and neutralino mass matrices refer to [39] and [40].

3.2 Scalar particles with mixing

Again, we change from the bare Lagrangian \mathcal{L}_0 to the renormalized Lagrangian \mathcal{L}

$$\mathcal{L}_0 = -\phi_{0,i}^* \delta_{ij} (\partial_\mu \partial^\mu + m_{0,i}^2) \phi_{0,j}, \quad (3.27)$$

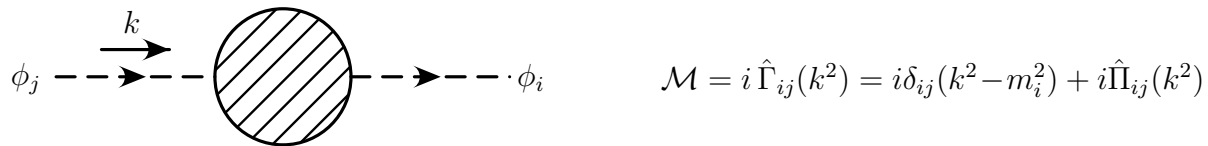
$$\mathcal{L} = -\phi_i^* \delta_{ij} (\partial_\mu \partial^\mu + m_i^2) \phi_j. \quad (3.28)$$

The unrenormalized fields $\phi_{0,i}$ and mass parameters $m_{0,i}$ in the bare Lagrangian are replaced by the corresponding renormalized ones:

$$\phi_{0,j} = \sqrt{Z_{jk}} \phi_k = (\delta_{jk} + \frac{1}{2} \delta Z_{jk}) \phi_k + \mathcal{O}(\delta Z^2), \quad (3.29)$$

$$(m_{0,i})^2 = m_i^2 + \delta m_i^2. \quad (3.30)$$

Like for the fermions before, we use a renormalized two-point-function to fix the renormalization constants.



The renormalized self-energy $\hat{\Pi}_{ij}(k^2)$ consists of the bare self-energy $\Pi_{ij}(k^2)$ and counter-terms:

$$\hat{\Pi}_{ij}(k^2) = \Pi_{ij}(k^2) - \delta_{ij} \delta m_i^2 + \frac{1}{2} (k^2 - m_i^2) \delta Z_{ij} + \frac{1}{2} (k^2 - m_j^2) \delta Z_{ji}^*. \quad (3.31)$$

The on-shell renormalization conditions

$$\text{Re } \hat{\Gamma}_{ij}(k^2) \Big|_{k^2=m_j^2} = 0, \quad \lim_{k^2 \rightarrow m_i^2} \frac{1}{k^2 - m_i^2} \text{Re } \hat{\Gamma}_{ii}(k^2) = 1, \quad (3.32)$$

lead then to

$$\delta m_i^2 = \text{Re } \Pi_{ii}(m_i^2), \quad (3.33)$$

$$\delta Z_{ij} = \frac{2}{m_i^2 - m_j^2} \text{Re } \Pi_{ij}(m_j^2) \quad i \neq j, \quad (3.34)$$

$$\delta Z_{ii} = \delta Z_{ii}^* = -\text{Re } \dot{\Pi}_{ii}(m_i^2). \quad (3.35)$$

For the renormalization of couplings containing sfermions, we need to define the renormalization constant of the rotation matrix $R_{ij}^{\tilde{f}}$. It is determined similar to the chargino and neutralino rotation matrizes such as to cancel the anti-hermitian part of the sfermion wavefunction corrections,

$$\delta R_{ij}^{\tilde{f}} = \frac{1}{4} \sum_{k=1}^2 \left(\delta Z_{ik}(\tilde{f}) - \delta Z_{ki}(\tilde{f}) \right) R_{kj}^{\tilde{f}}. \quad (3.36)$$

Concerning the Higgs-sector, it is also necessary to renormalize the parameters α and β which occur in several couplings. Similar to the sfermion mixing, there exists a rotation matrix

$$R_{ij}^{H^0} \equiv R_{ij}(\alpha) = \begin{pmatrix} \cos \alpha & \sin \alpha \\ -\sin \alpha & \cos \alpha \end{pmatrix}_{ij}, \quad (3.37)$$

that diagonalizes the Higgs mass matrix:

$$M^2(H^0, h^0) = (R^{H^0})^T \cdot \begin{pmatrix} m_{H^0}^2 & 0 \\ 0 & m_{h^0}^2 \end{pmatrix} \cdot R^{H^0}, \quad m_{h^0} < m_{H^0}$$

If we define the renormalization constant of the rotation matrix $R_{ij}^{H^0}$ such as to cancel the anti-hermitian part of the Higgs wave-function corrections,

$$\delta R_{ij}^{H^0} = \sum_{k=1}^2 \frac{1}{4} (\delta Z_{ki}^{H^0} - \delta Z_{ik}^{H^0}) R_{kj}^{H^0}, \quad (3.38)$$

we get for the counter term of α

$$\delta \sin \alpha = \frac{1}{4} (\delta Z_{21}^H - \delta Z_{12}^H) = \frac{1}{2(m_{H^0}^2 - m_{h^0}^2)} \text{Re} \left(\Pi_{12}^H(m_{H^0}^2) + \Pi_{21}^H(m_{h^0}^2) \right). \quad (3.39)$$

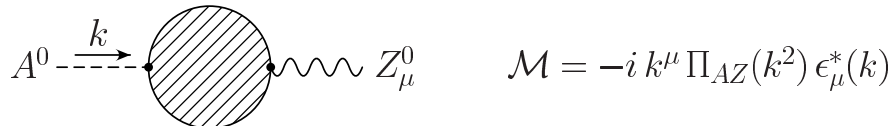
For the other parameter, the mixing angle β we use the renormalization concept introduced in [41] and [42]. It is fixed in that way, that the renormalized transition from A^0 to Z^0 vanishes when $p^2 = m_{A^0}$:

$$\text{Im} \hat{\Pi}_{A^0 Z^0}(m_{A^0}^2) = 0 \quad (3.40)$$

That leads to the counter term

$$\frac{\delta \tan \beta}{\tan \beta} = \frac{1}{m_Z \sin 2\beta} \text{Im} \Pi_{A^0 Z^0}(m_{A^0}^2). \quad (3.41)$$

The mixing self-energy $\Pi_{A^0 Z^0}(m_{A^0}^2)$ can be visualized by the following diagram:



3.3 SM gauge sector

The MSSM does not introduce any further interactions between SM particles, and so no new gauge bosons either. That means, that the renormalization procedure of the electroweak gauge sector is the same for the MSSM as for the SM. More details may be found in [43] and [44].

Once again, the free fields are expressed in terms of the renormalized ones and the renormalization constants δZ :

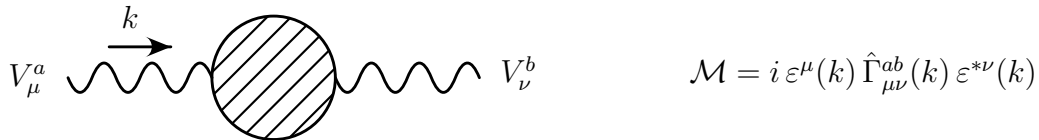
$$W_\mu^\pm \rightarrow (1 + \frac{1}{2}\delta Z_W) W_\mu^\pm, \quad (3.42)$$

$$\begin{pmatrix} A_\mu \\ Z_\mu \end{pmatrix} \rightarrow \begin{pmatrix} 1 + \frac{1}{2}\delta Z_{AA} & \frac{1}{2}\delta Z_{AZ} \\ \frac{1}{2}\delta Z_{ZA} & 1 + \frac{1}{2}\delta Z_{ZZ} \end{pmatrix} \begin{pmatrix} A_\mu \\ Z_\mu \end{pmatrix}. \quad (3.43)$$

For the mass corrections of the massive gauge bosons Z^0 and W^\pm we get

$$\begin{aligned} m_W^2 &\rightarrow m_W^2 + \delta m_W^2 \\ m_Z^2 &\rightarrow m_Z^2 + \delta m_Z^2. \end{aligned} \quad (3.44)$$

The vector two-point-functions



can be decomposed into transverse and longitudinal parts

$$\hat{\Gamma}_{\mu\nu}^W(k) = -ig_{\mu\nu}(k^2 - m_W^2) - i\left(g_{\mu\nu} - \frac{k_\mu k_\nu}{k^2}\right)\hat{\Pi}_T^W(k^2) - i\frac{k_\mu k_\nu}{k^2}\hat{\Pi}_L^W(k^2), \quad (3.45)$$

$$\hat{\Gamma}_{\mu\nu}^{ab}(k) = -ig_{\mu\nu}(k^2 - m_a^2)\delta_{ab} - i\left(g_{\mu\nu} - \frac{k_\mu k_\nu}{k^2}\right)\hat{\Pi}_T^{ab}(k^2) - i\frac{k_\mu k_\nu}{k^2}\hat{\Pi}_L^{ab}(k^2), \quad (3.46)$$

containing the renormalized self-energies

$$\hat{\Pi}_{T,L}^W(k^2) = \Pi_{T,L}^W(k^2) + (k^2 - m_W^2)\delta Z^W - \delta m_W^2, \quad (3.47)$$

$$\hat{\Pi}_{T,L}^{AA}(k^2) = \Pi_{T,L}^{AA}(k^2) + k^2\delta Z^{AA}, \quad (3.48)$$

$$\hat{\Pi}_{T,L}^{ZZ}(k^2) = \Pi_{T,L}^{ZZ}(k^2) + (k^2 - m_Z^2)\delta Z^{ZZ} - \delta_{ab}\delta m_Z^2, \quad (3.49)$$

$$\hat{\Pi}_{T,L}^{AZ}(k^2) = \Pi_{T,L}^{AZ}(k^2) + \frac{1}{2}k^2\delta Z^{AZ} + \frac{1}{2}(k^2 - m_Z^2)\delta Z^{ZA}, \quad (3.50)$$

$$\hat{\Pi}_{T,L}^{ZA}(k^2) = \Pi_{T,L}^{ZA}(k^2) + \frac{1}{2}k^2\delta Z^{AZ} + \frac{1}{2}(k^2 - m_Z^2)\delta Z^{ZA}. \quad (3.51)$$

The renormalization conditions

$$\text{Re } \hat{\Gamma}_{\mu\nu}^{ab}(k) \varepsilon^\nu(k) \Big|_{k^2=m_a^2} = 0, \quad \lim_{k^2 \rightarrow m_a^2} \frac{1}{k^2 - m_a^2} \text{Re } \hat{\Gamma}_{\mu\nu}^{ab}(k) \varepsilon^\nu(k) = -\varepsilon^\mu(k), \quad (3.52)$$

set the poles by using the physical pole masses and set the residua to on shell ($k^2 = m_a^2$). This determines to the renormalization constants ($a, b = A, Z$) as

$$\begin{aligned} \delta Z^{aa} &= -\text{Re } \dot{\Pi}_T^{aa}(m_a^2), & \delta Z^W &= -\text{Re } \dot{\Pi}_T^W(m_W^2), \\ \dot{\Pi}(m^2) &= \frac{\partial}{\partial k^2} \Pi(k^2) \Big|_{k^2=m^2} \\ \delta Z^{ab} &= \frac{2}{m_a^2 - m_b^2} \text{Re } \Pi_T^{ab}(m_b^2), & a \neq b, \end{aligned} \quad (3.53)$$

$$\delta m_Z^2 = \text{Re } \Pi_T^{ZZ}(m_Z^2), \quad \delta m_W^2 = \text{Re } \Pi_T^{WW}(m_W^2), \quad (3.54)$$

The mixing angle can be written in terms of the gauge boson masses $\cos \theta_W \equiv c_W = \frac{m_W}{m_Z}$ [31], and so the corresponding counterterm also may be expressed by using the gauge bosonss mass counterterms:

$$\frac{\delta c_W^2}{c_W^2} = \frac{\delta m_W^2}{m_W^2} - \frac{\delta m_Z^2}{m_Z^2}, \quad \frac{\delta s_W^2}{s_W^2} = -\frac{c_W^2}{s_W^2} \frac{\delta c_W^2}{c_W^2}. \quad (3.55)$$

3.4 Electric charge

For the renormalization of the electric charge one needs a well know process to pin down the value of the charge. Usually the electron–positron–photon vertex is used for that purpose. The momentum of the photon is set to zero, all external particles are on-shell. This configuration is also known as Thomson limit. In experiments, the value for the fine structure constant in the Thomson limit $\alpha = e^2/4\pi = 1/137.036$ can be measured. The renormalization condition in the Thomson limit is

$$\bar{u}(p) \hat{\Gamma}_\mu^{ee\gamma}(p, p) u(p) \Big|_{p^2=m_e^2} = ie \bar{u}(p) \gamma_\mu u(p), \quad (3.56)$$

with the renormalized three-point function

$$\hat{\Gamma}_\mu^{ee\gamma} = e \gamma_\mu \left(1 + \frac{\delta e}{e} + \frac{1}{2} \delta Z^{\gamma\gamma} - \frac{s_W}{2c_W} \delta Z^{Z\gamma} + \delta Z^e \right) + e \Lambda_\mu^{\gamma e\bar{e}} = e \gamma_\mu. \quad (3.57)$$

The term $\Lambda_\mu^{\gamma e\bar{e}}$ represents the vertex-loop-diagrams, the contributions of the fermion self-energies δZ^e cancel due to a Ward identity. The counter term for the electric charge in $e_0 = e + \delta e$ is then given by

$$\frac{\delta e}{e} = -\frac{1}{2}\delta Z^{\gamma\gamma} + \frac{s_W}{c_W}\frac{1}{2}\delta Z^{Z\gamma} = \frac{1}{2}\dot{\Pi}_T^{\gamma\gamma}(0) + \frac{s_W}{c_W}\frac{\Pi_T^{\gamma Z}(0)}{m_Z^2}. \quad (3.58)$$

As mentioned above, the presented renormalization procedure defines the electric charge in the Thomson limit, which is a low energy limit. Recent Particle Physics experiments use much higher energies in the range of hundreds of GeV. Taking into account loop effects, the vacuum behaves similar to a polarizable dielectric medium. That means, that the value of the electric charge is not longer independent of distance, and so the energy scale. Especially the contribution of light hadrons in $\dot{\Pi}_T^{\gamma\gamma}(0)$ lead to large theoretical uncertainties [44, 45]. This problem can be avoided by using as input an effective $\overline{\text{MS}}$ running coupling $\alpha_{\overline{\text{MS}}}^{\text{eff}}(m_Z^2)$ at the energy scale $Q = m_Z$,

$$\alpha_{\overline{\text{MS}}}^{\text{eff}}(m_Z^2) = \frac{\alpha}{1 - \Delta\alpha_{\overline{\text{MS}}}^{\text{eff}}(m_Z^2)} \simeq \frac{1}{127.7}, \quad (3.59)$$

where the contributions from light fermions are already absorbed [39, 40].

α still denotes the fine structure constant in the Thomson limit ($\alpha = 1/137.036$) and $\Delta\alpha_{\overline{\text{MS}}}^{\text{eff}}(m_Z^2)$ is an abbreviation for

$$\Delta\alpha_{\overline{\text{MS}}}^{\text{eff}}(m_Z^2) = \frac{\alpha}{\pi} \left(\frac{5}{3} + \frac{55}{27} \left(1 + \frac{\alpha}{\pi} \right) \right) + \Delta\alpha_{\text{lep}}(m_Z^2) + \Delta\alpha_{\text{had}}^{(5)}(m_Z^2), \quad (3.60)$$

with the leptonic contributions $\Delta\alpha_{\text{lep}}(m_Z^2) \simeq 0.031497687$ and the hadronic contributions $\Delta\alpha_{\text{had}}^{(5)}(m_Z^2) = 0.02769 \pm 0.00035$ [46].

Finally, the counter term for the electric charge δe is then given by

$$\begin{aligned} \frac{\delta e}{e} = & \frac{1}{(4\pi)^2} \frac{e^2}{6} \left[4 \sum_f N_C^f e_f^2 \left(\Delta + \log \frac{Q^2}{x_f^2} \right) + \sum_{\tilde{f}} \sum_{m=1}^2 N_C^f e_f^2 \left(\Delta + \log \frac{Q^2}{m_{\tilde{f}_m}^2} \right) \right. \\ & \left. + 4 \sum_{k=1}^2 \left(\Delta + \log \frac{Q^2}{m_{\tilde{\chi}_k^+}^2} \right) + \sum_{k=1}^2 \left(\Delta + \log \frac{Q^2}{m_{H_k^+}^2} \right) - 22 \left(\Delta + \log \frac{Q^2}{m_W^2} \right) \right], \end{aligned} \quad (3.61)$$

with $x_f = m_Z \forall m_f < m_Z$ and $x_t = m_t$. N_C^f is the colour factor, $N_C^f = 1, 3$ for (s)leptons and (s)quarks, respectively. Δ denotes the UV divergence factor, $\Delta = 2/\epsilon - \gamma + \log 4\pi$, with the Euler–Mascheroni constant $\gamma = \lim_{m \rightarrow \infty} (\sum_{k=1}^m \frac{1}{k} - \log m) \sim 0.577216$.

Chapter 4

Decays of Neutralinos and Charginos

One of the main goals of the new Large Hadron Collider (LHC) at CERN is to look for supersymmetric particles. Assuming that supersymmetry is realized in the way the MSSM suggests, it is most likely observed at LHC by gluino or squark production. Lighter squarks and gluinos would decay into quark pairs and finally hadron jets, and the lightest neutralino, which is assumed to be the stable lightest supersymmetric particle (LSP). The heavier squarks and gluinos could decay again into quark pairs, but together with a chargino or a heavier neutralino. At an electron-positron collider, like the projected Linear Collider, charginos and neutralinos could occur as decay products of squark and slepton pairs, additionally there could be directly produced chargino or neutralino pairs.

Both charginos as well as the heavier neutralinos are unstable and decay further into lighter MSSM and SM model particles. So it is necessary to study chargino and neutralino decays in order to understand the various decay signatures. In this context, the branching ratio Γ/Γ_{total} (ratio between the width of a single decay channel and the total decay width) is a relevant parameter.

To obtain a finite result for the decay widths on one-loop level, it is necessary not only to add the loop corrections to the tree-level result, but also counterterms and Bremsstrahlung contributions, in order to cope with UV and IR divergencies. So the total, finite decay width is given by Eqn.4.1:

$$\Gamma = \Gamma_{tree} + \Gamma_{loop} + \Gamma_{CT} + \Gamma_{IR} \quad (4.1)$$

Generic forms for Γ_{tree} , Γ_{loop} and Γ_{CT} are listed in the following in Eqn.4.2, 4.3, 4.5, 4.6, 4.7 and 4.8, Γ_{IR} is derived Section 5 and Appendix B. The generic structures for the formfactors Λ and Π are listed in Appendix C. The tree-level couplings for all decay channels are listed in Tab.4.1, and defined in Appendix A. All vertex correction contributing graphs are listed in Appendix E. All needed couplings, that are not yet listed in Tab.4.1 can be found in [47]. Using the same conventions for the generic structures as given in [48], index "2" stands for the incoming neutralino or chargino, "1" for the outgoing fermion and "0" for the outgoing vector or scalar particle.

$\tilde{\chi}_i^+ \rightarrow t\tilde{b}_k^*$	$g_R = A_{ik}^R$	$g_L = A_{ik}^L$	$\tilde{\chi}_l^0 \rightarrow t\tilde{t}_j^*$	$g_R = C_{lj}^R$	$g_L = C_{lj}^L$
$\tilde{\chi}_i^+ \rightarrow \bar{b}t_j$	$g_R = B_{ij}^{L*}$	$g_L = B_{ij}^{R*}$	$\tilde{\chi}_l^0 \rightarrow \bar{b}\tilde{b}_k$	$g_R = D_{lk}^{L*}$	$g_L = D_{lk}^{R*}$
$\tilde{\chi}_i^+ \rightarrow \tilde{\tau}_s^*\nu$	$g_R = A_{is}^R$	$g_L = A_{is}^L$	$\tilde{\chi}_l^0 \rightarrow \nu\tilde{\nu}^*$	$g_R = C_l'^R$	$g_L = C_l'^L$
$\tilde{\chi}_i^+ \rightarrow \bar{\tau}\tilde{\nu}$	$g_R = B_i'^L$	$g_L = B_i'^R$	$\tilde{\chi}_l^0 \rightarrow \bar{\tau}\tilde{\tau}_s$	$g_R = D_{ls}^{L*}$	$g_L = D_{ls}^{R*}$
$\tilde{\chi}_k^+ \rightarrow \tilde{\chi}_l^0 W^+$	$g_R = E_{kl}^R$	$g_L = E_{kl}^L$	$\tilde{\chi}_l^0 \rightarrow \tilde{\chi}_k^+ W^-$	$g_R = E_{kl}^{L*}$	$g_L = E_{kl}^{R*}$
$\tilde{\chi}_i^+ \rightarrow \tilde{\chi}_j^+ Z^0$	$g_R = E_{ji}^{+R}$	$g_L = E_{ji}^{+L}$	$\tilde{\chi}_k^0 \rightarrow \tilde{\chi}_l^0 Z^0$	$g_R = E_{lk}^{0R}$	$g_L = E_{lk}^{0L}$
$\tilde{\chi}_i^+ \rightarrow \tilde{\chi}_j^+ H_n^0$	$g_R = K_{jin}^+$	$g_L = K_{jin}^{+*}$	$\tilde{\chi}_k^0 \rightarrow \tilde{\chi}_l^0 H_n^0$	$g_R = K_{lkn}^0$	$g_L = K_{lkn}^{0*}$
$\tilde{\chi}_j^+ \rightarrow \tilde{\chi}_l^0 H^+$	$g_R = K_{jl}^{1L*}$	$g_L = K_{jl}^{1R*}$	$\tilde{\chi}_l^0 \rightarrow \tilde{\chi}_j^+ H^-$	$g_R = K_{jl}^{1R}$	$g_L = K_{jl}^{1L}$

Table 4.1: Decay channels for chargino and neutralino decays and the corresponding treelevel couplings. Note that b , \tilde{b} , t , \tilde{t} , τ , $\tilde{\tau}$, ν and $\tilde{\nu}$ stand for all three generations of (s)quark and (s)leptons.

Neutralinos and charginos may either decay into another fermion and scalar, or into a fermion and a vector particle. The tree-level decay width for a decay of a fermion into a fermion and a scalar is given in Eqn.4.2, for a decay of a fermion into a fermion and a vector particle in Eqn.4.3. The form factors Λ and Π in Eqs. 4.5 – 4.8 are listed in Appendix A.

$$\Gamma_{tree}(f \rightarrow fs) = \frac{\sqrt{\lambda}}{32\pi m_2^3} [(m_1^2 + m_2^2 - m_0^2)(g_R g_R^* + g_L g_L^*) + 2m_1 m_2 (g_R g_L^* + g_L g_R^*)] \quad (4.2)$$

$$\Gamma_{tree}(f \rightarrow fv) = \frac{\sqrt{\lambda}}{32\pi m_2^3} [\rho(g_R g_R^* + g_L g_L^*) + 6m_1 m_2 (g_R g_L^* + g_L g_R^*)] \quad (4.3)$$

$$\begin{aligned} \lambda &= m_2^4 + m_1^4 + m_0^4 - 2m_2^2 m_1^2 - 2m_2^2 m_0^2 - 2m_1^2 m_0^2, \\ \rho &= \frac{\lambda}{m_0^2} + 3(m_2^2 + m_1^2 - m_0^2) \end{aligned} \quad (4.4)$$

Eqn.4.5 and Eqn.4.6 show the one-loop corrections to the decay width of a fermion into a fermion and a scalar, and for a decay of a fermion into a fermion and a vector:

$$\begin{aligned} \Gamma_{loop}(f \rightarrow fs) &= \frac{\sqrt{\lambda}}{128\pi^3 m_2^3} [(m_1^2 + m_2^2 - m_0^2)(\Lambda_L g_L^* + \Lambda_R g_R^* + g_L \Lambda_L^* + g_R \Lambda_R^*) \\ &\quad + 2m_1 m_2 (\Lambda_R g_L^* + \Lambda_L g_R^* + g_R \Lambda_L^* + g_L \Lambda_R^*)] \end{aligned} \quad (4.5)$$

$$\begin{aligned}
\Gamma_{loop}(f \rightarrow fv) = & \frac{\sqrt{\lambda}}{128\pi^3 m_2^3} [\rho (\Lambda_L g_L^* + \Lambda_R g_R^* + g_L \Lambda_L^* + g_R \Lambda_R^*) \\
& - 6m_1 m_2 (\Lambda_R g_L^* + \Lambda_L g_R^* + g_R \Lambda_L^* + g_L \Lambda_R^*) \\
& - \frac{\lambda m_1}{2m_0^2} (\Pi_L g_L^* + \Pi_R g_R^* + g_L \Pi_L^* + g_R \Pi_R^*) \\
& - \frac{\lambda m_2}{2m_0^2} (\Pi_R g_L^* + \Pi_L g_R^* + g_R \Pi_L^* + g_L \Pi_R^*)]
\end{aligned} \tag{4.6}$$

The terms Γ_{CT} in Eqn.4.7 and Eqn.4.8 include the counterterms that are necessary for cancellation of the UV divergent parts of the one-loop corrections. δg_R and δg_L therefore include both coupling counterterms and wave function counterterms. Like the different tree-level couplings g_R and g_L , they are listed in Appendix A.

$$\begin{aligned}
\Gamma_{CT}(f \rightarrow fs) = & \frac{\sqrt{\lambda}}{128\pi^3 m_2^3} [(m_1^2 + m_2^2 - m_0^2)(\delta g_L g_L^* + \delta g_R g_R^* + g_L \Lambda_L^* + g_R \delta g_R^*) \\
& + 2m_1 m_2 (\delta g_R g_L^* + \delta g_L g_R^* + g_R \delta g_L^* + g_L \delta g_R^*)]
\end{aligned} \tag{4.7}$$

$$\begin{aligned}
\Gamma_{CT}(f \rightarrow fv) = & \frac{\sqrt{\lambda}}{128\pi^3 m_2^3} [\rho (\delta g_L g_L^* + \delta g_R g_R^* + g_L \Lambda_L^* + g_R \delta g_R^*) \\
& - 6m_1 m_2 (\delta g_R g_L^* + \delta g_L g_R^* + g_R \delta g_L^* + g_L \delta g_R^*)]
\end{aligned} \tag{4.8}$$

For the calculations of Feynman amplitudes the algebraic software FeynArts [49] by T. Hahn was used.

Chapter 5

Bremsstrahlung

Vertex functions and wave-function corrections with one single massless vector particle like photon or gluon in the loop show divergent amplitudes. These so called infrared (IR) divergencies originate from the zero mass or the photons or gluons, which leads for small momenta to divergent integrals. To regularize them, one introduces a small photon (or gluon) mass m_γ , leading to the expression

$$\frac{\partial}{\partial p^2} \frac{1}{i\pi^2} \int d^d q \frac{1}{(q^2 - m_\gamma^2)[(q + p)^2 - m^2]} \Big|_{p^2 = m^2} = -\frac{1}{2m^2} \left(2 - \log \frac{m^2}{m_\gamma^2} \right), \quad (5.1)$$

which diverges for $m_\gamma \rightarrow 0$.

The IR-divergencies can be cancelled by adding real Bremsstrahlungs processes, which contain an additional radiated photon per charged particle. In the following we present the expressions for the real Bremsstrahlungs diagrams for decays of one fermion into another fermion and a scalar particle as well as into another fermion and a vector particle. More detailed calculations for the processes (fermion \rightarrow scalar, fermion) are done in appendix B.

5.1 Bremsstrahlung processes for decays (fermion \rightarrow scalar, fermion)

The decay width of the Bremsstrahlung processes is given by:

$$\Gamma^{\text{brems}} = \frac{1}{2m_0} \int \frac{d^3 p_1}{(2\pi)^3 2E_1} \int \frac{d^3 p_2}{(2\pi)^3 2E_2} \int \frac{d^3 q}{(2\pi)^3 2E_q} (2\pi)^4 \delta^4(p_0 - p_1 - p_2 - q) |\mathcal{M}^{\text{brems}}|^2 \quad (5.2)$$

$$\begin{aligned} |\mathcal{M}^{\text{brems}}|^2 &= \mathcal{M}_a^\dagger \mathcal{M}_a + \mathcal{M}_b^\dagger \mathcal{M}_b + \mathcal{M}_c^\dagger \mathcal{M}_c + (\mathcal{M}_a^\dagger \mathcal{M}_b + \mathcal{M}_b^\dagger \mathcal{M}_a) \\ &\quad + (\mathcal{M}_a^\dagger \mathcal{M}_c + \mathcal{M}_c^\dagger \mathcal{M}_a) + (\mathcal{M}_b^\dagger \mathcal{M}_c + \mathcal{M}_c^\dagger \mathcal{M}_b) \end{aligned} \quad (5.3)$$

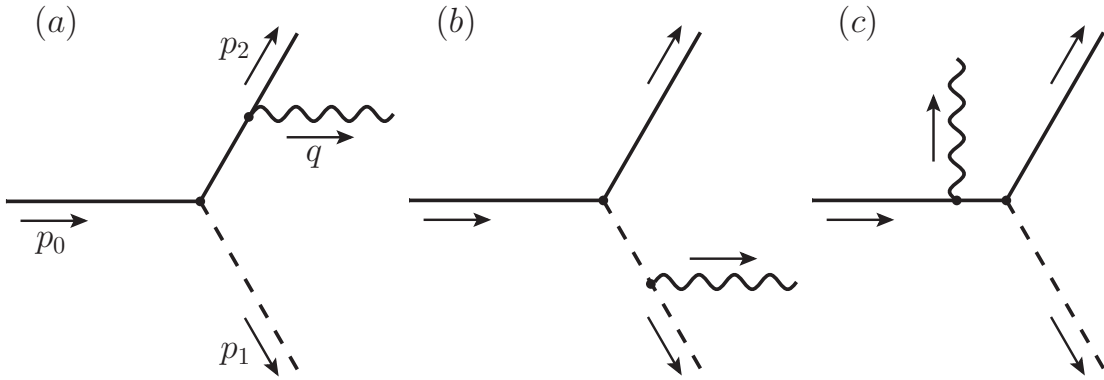


Figure 5.1: Real Bremsstrahlung diagrams needed to cancel the IR-divergences in decays of a fermion into another fermion and a scalar.

Performing the integrations leads to integrals of the following form, which are listed in [44]:

$$I_{i_1 \dots i_n}^{j_1 \dots j_m}(m_0, m_1, m_2) = \frac{1}{\pi^2} \int \frac{d^3 p_1}{2E_1} \frac{d^3 p_2}{2E_2} \frac{d^3 q}{2E_q} \delta^4(p_0 - p_1 - p_2 - q) \frac{(\pm 2p_{j_1} \cdot q) \dots (\pm 2p_{j_m} \cdot q)}{(\pm 2p_{i_1} \cdot q) \dots (\pm 2p_{i_n} \cdot q)} \quad (5.4)$$

The final result for the decay width of the Bremsstrahlungsprocesses for the (fermion → scalar, fermion) decays is

$$\begin{aligned} \Gamma_{f \rightarrow sf}^{\text{brems}} = & \frac{e^2}{128\pi^3 m_0} \left[Q_2^2 \left(8(g^{R*}g^R + g^{L*}g^L) \left(-\frac{m_2^2 Y}{2} I_{22} - \frac{m_2^2}{2} I_2 - \frac{1}{4} I_2^0 \right) \right. \right. \\ & + 8(g^{R*}g^L + g^{L*}g^R)m_0m_2 \left(-\frac{1}{2} I_2 - m_2^2 I_{22} \right) \left. \right) \\ & + Q_1^2 \left(2(g^{R*}g^R + g^{L*}g^L) \left(-2m_1^2 Y I_{11} - Y I_1 + 2m_1^2 I_1 + I \right) \right. \\ & + 8(g^{R*}g^L + g^{L*}g^R)m_0m_2 \left(-\frac{1}{2} I_1 - m_1^2 I_{11} \right) \left. \right) \\ & + Q_0^2 \left(8(g^{R*}g^R + g^{L*}g^L) \left(-\frac{m_0^2 Y}{2} I_{00} - \frac{m_0^2}{2} I_0 - \frac{1}{4} I_0^2 \right) \right. \\ & + 8(g^{R*}g^L + g^{L*}g^R)m_0m_2 \left(-\frac{1}{2} I_0 - m_0^2 I_{00} \right) \left. \right) \\ & + Q_1 Q_2 \left(2(g^{R*}g^R + g^{L*}g^L) \left(-2XY I_{12} + Y(I_2 + I_1) + X(I_2 - I_1) + WI_1 + I \right) \right. \\ & + 4(g^{R*}g^L + g^{L*}g^R)m_0m_2 \left(-2XI_{12} + I_2 + I_1 \right) \left. \right) \end{aligned}$$

$$\begin{aligned}
& + Q_0 Q_2 \left(4(g^{R*} g^R + g^{L*} g^L) \left(m_0^2 I_0 - Y^2 I_{02} + m_2^2 I_2 - Y I_2 - Y I_0 - \frac{1}{2} I \right) \right. \\
& + 4(g^{R*} g^L + g^{L*} g^R) m_0 m_2 \left(-I_2 - I_0 - 2Y I_{02} \right) \Big) \\
& + Q_0 Q_1 \left(2(g^{R*} g^R + g^{L*} g^L) \left(-I + W(I_0 - I_1) + X I_1 - Y(I_0 + Y I_1) - 2W Y I_{01} \right) \right. \\
& \left. \left. + 4(g^{R*} g^L + g^{L*} g^R) m_0 m_2 \left(-I_0 - I_1 - 2W I_{01} \right) \right) \right], \tag{5.5}
\end{aligned}$$

with the abbreviations

$$\begin{aligned}
X &= (m_0^2 - m_1^2 - m_2^2) \\
Y &= (m_0^2 - m_1^2 + m_2^2) \\
W &= (m_0^2 + m_1^2 - m_2^2). \tag{5.6}
\end{aligned}$$

In the case of photon emission, Q_0 , Q_1 , Q_2 mean the electric charge of the particles with the index 0, 1 or 2.

For the calculation of the gluon emission in processes with outgoing quarks or squarks, the decay width has to be changed to

$$\Gamma_{f \rightarrow sf}^{\text{brems}} \rightarrow \frac{4}{3} \frac{\alpha_s}{\alpha} \Gamma_{f \rightarrow sf}^{\text{brems}}, \tag{5.7}$$

with

$$Q_0 \rightarrow 0, \quad Q_1 \rightarrow 1, \quad Q_2 \rightarrow 1. \tag{5.8}$$

5.2 Bremsstrahlung processes for decays (fermion \rightarrow vector, fermion)

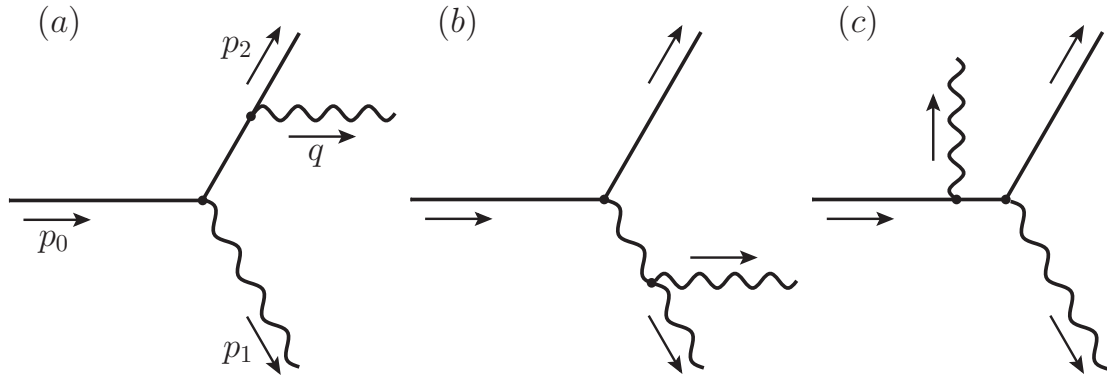


Figure 5.2: Real Bremsstrahlung diagrams needed to cancel the IR-divergences in decays of a fermion into another fermion and a vector particle.

$$\begin{aligned}
 \Gamma_{f \rightarrow vf}^{\text{brems}} = & \Gamma_{f \rightarrow vf}^{\text{tree}} \left(-\frac{\alpha}{\pi} \right) \frac{4m_0^2}{\kappa(m_0^2, m_1^2, m_2^2)} \left[-Q_0 Q_2 \left((m_1^2 - m_0^2 - m_2^2) I_0^2 \right) \right. \\
 & + Q_0^2 \left((m_0^2 I_{00} + I_0) - \left(1 + \frac{m_0^2 + m_2^2}{2m_1^2} \right) \frac{I_0^1}{G_1^-} - \frac{I}{G_1^-} \right) \\
 & + Q_2^2 \left((m_2^2 I_{22} + I_2) - \left(1 + \frac{m_0^2 + m_2^2}{2m_1^2} \right) \frac{I_2^1}{G_1^-} - \frac{I}{G_1^-} \right) \\
 & + Q_1^2 \left((m_1^2 I_{11} + I_1) - \frac{m_0^2 + m_2^2}{2m_1^2} \frac{I}{G_1^-} + 2 \frac{I_{11}^{02}}{G_1^-} \right) \\
 & + Q_0 Q_2 \left((m_1^2 + m_0^2 - m_2^2) I_{01} + 2 \frac{I_1^2}{G_1^-} \right) \\
 & \left. - Q_1 Q_2 \left((m_1^2 - m_0^2 + m_2^2) I_{12} + 2 \frac{I_1^0}{G_1^-} \right) \right] \quad (5.9)
 \end{aligned}$$

with

$$G_1^- = - \left(2m_1^2 - m_0^2 - m_2^2 - \frac{(m_0^2 - m_2^2)^2}{m_1^2} \right) \quad (5.10)$$

5.3 Bremsstrahlung integrals for processes with an outgoing massless particle

For processes with an outgoing massless particle, some of the Bremsstrahlungs integrals listed in [44] are not defined when $m_2 = 0$, and need to be modified. In our case, this is necessary for the process $\tilde{\chi}^\pm \rightarrow l\nu$, where the $m_2 = m_\mu = 0$. We show the treatment of I_{00} , for I_{11} and I_{01} it works in the same manner. The results for all needed integrals are listed in B.8.

As one can easily see, the original version of I_{00} (Eqn. 5.11) is not defined when $m_2 = 0$.

$$I_{00} = \frac{1}{4m_0^4} \left[\kappa \ln \left(\frac{\kappa}{m_\gamma m_0 m_1 m_2} \right) - \kappa - (m_1^2 - m_2^2) \ln \left(\frac{\beta_1}{\beta_2} \right) - m_0^2 \ln(\beta_0) \right], \quad (5.11)$$

$$\begin{aligned} \beta_0 &= \frac{m_0^2 - m_1^2 - m_2^2 - \kappa}{2m_1 m_2}, & \beta_1 &= \frac{m_0^2 - m_1^2 + m_2^2 - \kappa}{2m_0 m_2}, \\ \beta_2 &= \frac{m_0^2 + m_1^2 - m_2^2 - \kappa}{2m_0 m_1}, \\ \kappa &= \sqrt{(m_0^2 - m_1^2 - m_2^2)^2 - 4m_1^2 m_2^2}. \end{aligned} \quad (5.12)$$

The first step is now to expand β_0 , β_1 and β_2 into power series in m_2 around $m_2 = 0$. That leads to the results shown in Eqn. 5.13.

$$\begin{aligned} \beta_0 &\rightarrow \frac{2m_0^2 + 2m_1^2}{2m_1 m_2} + O(m_2) \\ \beta_1 &\rightarrow \frac{m_0 m_2}{m_0^2 - m_1^2} + O(m_2^2) \\ \beta_2 &\rightarrow \frac{m_1}{m_0} + O(m_2) \end{aligned} \quad (5.13)$$

Inserting these versions of β_0 , β_1 and β_2 , and doing some simplifications, one gets for I_{00} :

$$\begin{aligned} I_{00} &= -\frac{1}{4m_0^4} \left[m_0^2 \ln \left(\frac{m_0}{m_1} - \frac{m_1}{m_0} \right) - (m_0 - m_1)(m_0 + m_1) \left(-1 + \ln^2 \left(\frac{m_0^2 - m_1^2}{m_\gamma m_0^2 m_1} \right) \right) \right. \\ &\quad \left. + m_1^2 \ln \left(\frac{m_0^3}{m_0^2 m_1 - m_1^3} \right) \right] \end{aligned} \quad (5.14)$$

The form of I_{00} in Eqn. 5.14 is independent of m_2 , and so well defined at $m_2 = 0$.

Chapter 6

Numerical Results

Beyond tree-level, the parameters of the MSSM Lagrangian are not defined uniquely, but dependent on the chosen renormalization scheme. Several benchmark scenarios were introduced [50], taking in account constraints from collider experiments and from cosmology. To establish a common standard for MSSM input parameters, the SPA project [51] was founded. In order to make results comparable, the CP and R-parity conserving reference point SPS1a' was introduced [52]. It is based on the supersymmetry parameter convention SPA [32]:

- The masses of the SUSY particles and the Higgs bosons are defined as pole masses.
- All SUSY Lagrangian parameters, mass parameters and couplings, including $\tan \beta$, are given in the $\overline{\text{DR}}$ -scheme at the scale $Q = 1\text{TeV}$.
- Gaugino/higgsino and scalar mass matrices, rotation matrices and the corresponding angles are defined in the $\overline{\text{DR}}$ -scheme at Q , except for the Higgs system in which the mixing matrix is defined in the on-shell scheme, the momentum scale chosen as the light Higgs mass.
- The Standard Model input parameters of the gauge sector are chosen as G_F , α , M_Z and $\alpha^{\overline{\text{MS}}}(M_Z)$. All lepton masses are defined on-shell. The t quark mass is defined on-shell; the b, c quark masses are introduced in $\overline{\text{MS}}$ at the scale of the masses themselves while taken at a renormalization scale of 2 GeV for the light u, d, s quarks.

Our numerical analysis concentrates on the SPS1a' scenario. For that reason, the input is stated in terms of the SPA-convention [32]. The SPS1a' reference point was originally defined using the following mSUGRA parameters:

$M_{1/2}$	=	250 GeV	$\text{sign}(\mu)$	=	+1	(6.1)
M_0	=	70 GeV	$\tan \beta(\tilde{M})$	=	10	
A_0	=	-300 GeV				

Parameter	SM input	Parameter	SM input
m_e	$5.110 \cdot 10^{-4}$	m_t^{pole} $m_b(m_b)$	172.7
m_μ	0.1057		4.2
m_τ	1.777		91.1876
$m_u(Q)$	$3 \cdot 10^{-3}$	G_F	$1.1664 \cdot 10^{-5}$
$m_d(Q)$	$7 \cdot 10^{-3}$	$1/\alpha$	137.036
$m_s(Q)$	0.12	$\Delta\alpha_{had}^{(5)}$	0.02769
$m_c(m_c)$	1.2	$\alpha_s^{\overline{MS}}(m_Z)$	0.119

Table 6.1: Numerical values of the SM input to SPS1a'. Masses are given in GeV, for the leptons and the t quark the pole masses, for the lighter quarks the \overline{MS} masses either at the mass scale itself, for c, b , or, for u, d, s , at the scale $Q = 2$ GeV.

In Eqn. 6.1, $M_{1/2}$ stands for the universal gaugino mass, M_0 is the scalar mass and A_0 is the trilinear coupling (Yukawa couplings are factored out.). All these parameters are defined at the GUT scale M_{GUT} . The values of the SM input parameters are listed in Table 6.1. The MSSM Lagrangian parameters are generated by extrapolating the above mSUGRA parameters down to the $\tilde{M} = 1$ TeV scale, using W. Porod's SPheno[53].

In the original SPS1a' scenario the values for M_1 , M_2 and $m_{\tilde{g}}$ are $M_1 = 103.3$ GeV, $M_2 = 193.2$ GeV and $m_{\tilde{g}} = 571.7$ GeV. Since we also study the dependence of the decay widths on the variation of M_2 , we do not use the fixed SPS1a' values for M_1 and $m_{\tilde{g}}$, but the GUT-relations stated in Tab. 6.3.

Our calculations are done in the on-shell renormalization scheme, so a conversion of the \overline{DR} input parameters has to be done before they can be used in the calculations themselves. First, the \overline{DR} -scheme [33] input parameters are transformed to the on-shell renormalization scheme. This is done by subtracting finite shifts:

$$\mathcal{P}^{OS} = \mathcal{P} - \delta_1 \mathcal{P}^{OS}. \quad (6.2)$$

Thereafter, the thus obtained on-shell parameters are used to calculate the SUSY pole-masses. The procedure is described in detail in [54], [55] and [56].

In our case the MSSM spectrum first is generated by SPheno by W. Porod [53]. SPheno stands for S(upersymmetric) Pheno(menology) and is a program that accurately calculates the supersymmetric particle spectrum within a high scale theory. The program solves the renormalization group equations numerically to two-loop order. The complete one-loop formulas for the masses are used which are supplemented by two-loop contributions in case of the neutral Higgs bosons and the μ parameter. The spectrum can be used to calculate decay modes of supersymmetric particles.

After receiving the spectrum from SPheno, UV-finite shifts are subtracted from the parameters to obtain them in the on-shell scheme. The parameter in- and output is done in the SUSY Les Houches Accord [57] convention, using the program package of the SLHA library [58]. It

provides a universal interface for exchanging input SUSY parameters, spectrum output and decay information. The data is exchanged by using ASCII files and that way independent of the program structure or even the programming language.

The Higgs masses h^0 and H^0 need higher order corrections and are taken directly from the SPheno output, since SPheno already provides appropriate higher order corrections to them. We use the SPS1a' reference point as starting point for the variation of the parameters M_2 , μ and $\tan\beta$. For M_1 and $m_{\tilde{g}}$ GUT relations are applied.

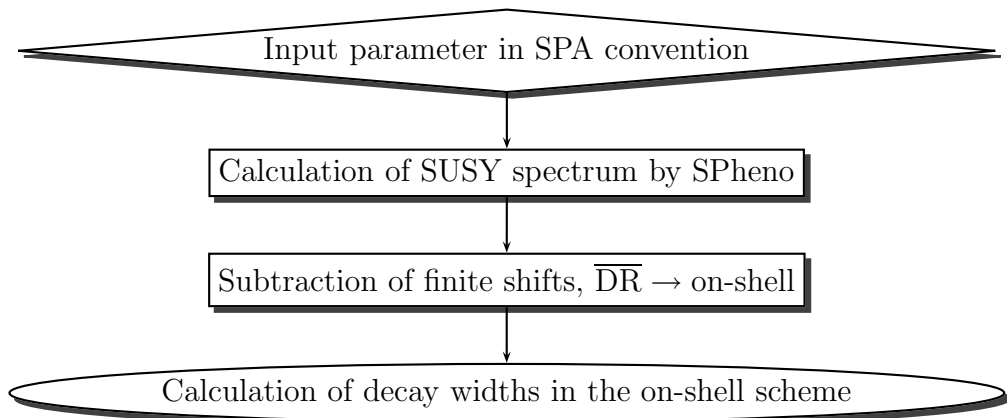


Figure 6.1: Flow diagram of the parameter preparation.

For several parameter points the results of our calculations have been compared with the Fortran code SDecay [59] and the results for the decay modes provided by SPheno. Since neither SDecay nor SPheno include all one loop corrections, we do not obtain exactly the same results, but all differences are within a small range.

The complete set of input parameter is stated in Section 6.1 in Tab.6.2, Tab.6.3, Tab.6.4.

6.1 Input parameters, according the SPA convention

In Tab.6.2, Tab.6.3 and Tab.6.4 we list the input parameters in SPA convention. They were calculated with SPheno [53] at the SPS1a' reference point. All quantities that have the dimension of a mass are given in terms of GeV.

α_e^{-1}	1.27931406×10^2	m_b	4.2
g_f	1.166390×10^{-5}	m_t	1.721×10^2
α_s	1.19×10^{-1}	m_τ	1.777
Q	1000	m_Z	91.1876

Table 6.2: SM paramters.

The electromagnetic and QCD coupling constants are given at the scale of m_Z , the bottom mass at the scale of m_b : $\alpha_e = \alpha_e(m_Z)$, $\alpha_s = \alpha_s(m_Z)$, $m_b = m_b(m_b)$.

μ	3.94765922×10^2
$M_{A_0}^2$	1.35309038×10^5
$\tan \beta$	10
M_1	$\frac{5}{3} \tan^2 \theta_W M_2$
M_2	1.93200073×10^2
$m_{\tilde{g}}$	$(\alpha_s(m_{\tilde{g}})/\alpha) \sin^2 \theta_W M_2$

Table 6.3: μ , M_{A_0} , $\tan \beta$, M_2 , GUT relations for M_1 and $m_{\tilde{g}}$ at $Q = 1000\text{GeV}$.

For M_1 and $m_{\tilde{g}}$ we do not define a fixed value but apply the GUT relations stated in Tab.6.3.

$M_{\tilde{L}_1}$	1.81018376×10^2	$M_{\tilde{L}_2}$	1.81011681×10^2	$M_{\tilde{L}_3}$	1.79129071×10^2
$M_{\tilde{E}_1}$	1.15664489×10^2	$M_{\tilde{E}_2}$	1.15643250×10^2	$M_{\tilde{E}_3}$	1.09539440×10^2
$M_{\tilde{Q}_1}$	5.25703063×10^2	$M_{\tilde{Q}_2}$	5.25700791×10^2	$M_{\tilde{Q}_3}$	4.71323565×10^2
$M_{\tilde{U}_1}$	5.07130306×10^2	$M_{\tilde{U}_2}$	5.07128154×10^2	$M_{\tilde{U}_3}$	3.87951664×10^2
$M_{\tilde{D}_1}$	5.04946104×10^2	$M_{\tilde{D}_2}$	5.04943480×10^2	$M_{\tilde{D}_3}$	5.00520898×10^2
A_e	-4.48231728×10^2	A_μ	-4.48218095×10^2	A_τ	-4.44376264×10^2
A_u	-7.99645520×10^2	A_c	-7.99640894×10^2	A_t	-5.70310180×10^2
A_d	-1.02419650×10^2	A_s	-1.02419194×10^2	A_b	-9.43132676×10^2

Table 6.4: Soft SUSY-breaking masses and Trilinear scalar coupling parameters at $Q = 1000\text{GeV}$.

6.2 On-shell masses

In Tables 6.5, 6.6, 6.7, 6.5, 6.6 and 6.7 we list the on-shell masses of SUSY particles used for the calculations at different values of M_2 and μ at $Q = 1$ TeV. All masses are given in GeV. The other parameters are as in Table 6.3.

	$M_2 = 100$	$M_2 = 300$	$M_2 = 600$
h^0	111.17	110.80	110.27
H^0	431.79	414.50	416.08
A^0	430.29	414.52	405.66
H^\pm	437.92	422.380	413.63

Table 6.5: On-shell masses of h^0 , H^0 , A^0 and H^\pm at $M_2 = 100$ GeV, $M_2 = 300$ GeV and $M_2 = 600$ GeV.

	$M_2 = 100$		$M_2 = 300$		$M_2 = 600$	
$\tilde{\nu}_e$	169.34		176.13		186.09	
$\tilde{\nu}_\mu$	169.33		176.12		186.08	
$\tilde{\nu}_\tau$	167.12		173.94		184.01	
$\tilde{e}_{1,2}$	124.61	187.15	125.92	193.32	128.54	202.43
$\tilde{\mu}_{1,2}$	124.534	187.18	125.85	193.34	128.48	202.45
$\tilde{\tau}_{1,2}$	105.71	192.70	107.96	198.24	112.08	206.53
$\tilde{u}_{1,2}$	523.73	540.59	560.06	578.38	464.63	492.20
$\tilde{c}_{1,2}$	523.76	540.55	560.09	578.34	464.65	492.18
$\tilde{t}_{1,2}$	346.88	566.53	385.78	602.38	240.76	508.68
$\tilde{d}_{1,2}$	523.56	546.39	559.85	583.80	464.14	498.58
$\tilde{s}_{1,2}$	523.56	546.39	559.85	583.80	464.14	498.58
$\tilde{b}_{1,2}$	483.02	521.09	522.16	557.77	421.00	462.21

Table 6.6: On-shell masses of sleptons and squarks at $M_2 = 100$ GeV, $M_2 = 300$ GeV and $M_2 = 600$ GeV.

	$M_2 = 100$	$M_2 = 300$	$M_2 = 600$
$\tilde{\chi}_1^\pm$	95.92	274.40	378.46
$\tilde{\chi}_2^\pm$	410.49	427.75	611.09
$\tilde{\chi}_1^0$	44.95	136.08	269.71
$\tilde{\chi}_2^0$	96.13	275.03	385.29
$\tilde{\chi}_3^0$	399.55	397.77	397.44
$\tilde{\chi}_4^0$	408.36	427.84	611.18
$m_{\tilde{g}}$	397.14	1015.00	1989.52

Table 6.7: On-shell masses of neutralinos, charginos and gluinos at $M_2 = 100$ GeV, $M_2 = 300$ GeV and $M_2 = 600$ GeV.

	$\mu = 100$	$\mu = 500$	$\mu = 1000$
h^0	111.06	111.09	111.41
H^0	380.72	439.01	516.33
A^0	380.22	437.67	514.07
H^\pm	388.71	445.11	519.78

Table 6.8: On-shell masses of h^0 , H^0 , A^0 and H^\pm at $\mu = 100$ GeV, $\mu = 500$ GeV and $\mu = 1000$ GeV.

	$\mu = 100$		$\mu = 500$		$\mu = 1000$	
$\tilde{\nu}_e$	172.57		172.23		172.03	
$\tilde{\nu}_\mu$	172.57		172.22		172.02	
$\tilde{\nu}_\tau$	170.34		169.93		169.10	
$\tilde{e}_{1,2}$	125.13	190.09	125.08	189.76	125.08	189.56
$\tilde{\mu}_{1,2}$	125.10	190.09	124.99	189.80	124.80	189.72
$\tilde{\tau}_{1,2}$	117.44	188.96	100.50	198.15	52.61	214.38
$\tilde{u}_{1,2}$	548.90	566.06	548.89	566.07	548.86	565.95
$\tilde{c}_{1,2}$	548.93	566.03	548.92	566.03	548.89	565.90
$\tilde{t}_{1,2}$	369.64	585.49	371.70	594.74	357.07	597.50
$\tilde{d}_{1,2}$	548.71	571.61	548.71	571.61	548.70	571.47
$\tilde{s}_{1,2}$	548.71	571.61	548.71	571.61	548.70	571.47
$\tilde{b}_{1,2}$	508.49	544.14	509.61	547.47	503.32	550.33

Table 6.9: On-shell masses of sleptons and squarks at $\mu = 100$ GeV, $\mu = 500$ GeV and $\mu = 1000$ GeV.

	$\mu = 100$	$\mu = 500$	$\mu = 1000$
$\tilde{\chi}_1^\pm$	79.00	188.49	194.83
$\tilde{\chi}_2^\pm$	234.74	511.63	994.15
$\tilde{\chi}_1^0$	54.56	88.34	89.16
$\tilde{\chi}_2^0$	110.07	188.61	194.85
$\tilde{\chi}_3^0$	114.27	500.60	990.01
$\tilde{\chi}_4^0$	234.79	510.52	993.18
$m_{\tilde{g}}$	683.59	683.72	683.88

Table 6.10: On-shell masses of neutralinos, charginos and gluinos at $\mu = 100$ GeV, $\mu = 500$ GeV and $\mu = 1000$ GeV.

6.3 Neutralino Decays

In the following subsections we show the dependence of the decay widths and the branching ratios of the neutralinos $\tilde{\chi}_4^0$, $\tilde{\chi}_3^0$ and $\tilde{\chi}_2^0$ on the variation of the mass parameters M_2 , μ and the mixing angle $\tan \beta$. Besides M_2 , μ and $\tan \beta$ the other input parameters are defined at the SPS1a' point, explicitly given in Tab.6.2, Tab.6.3 and Tab.6.4. For several parameter configurations, the SUSY on-shell masses are given in Tables 6.5, 6.6, 6.7, 6.5, 6.6 and 6.7.

6.3.1 Variation of M_2

Fig. 6.2 shows the total tree-level decay width of the neutralinos $\tilde{\chi}_4^0$, $\tilde{\chi}_3^0$ and $\tilde{\chi}_2^0$, depending on M_2 . The rapid change of the slope of the $\tilde{\chi}_3^0$ and $\tilde{\chi}_2^0$ lines between $M_2 = 615$ GeV and $M_2 = 620$ GeV is caused by the appearance of decays into quarks and squarks, mainly the channels $\tilde{\chi}_{3,2}^0 \rightarrow t\bar{t}$.

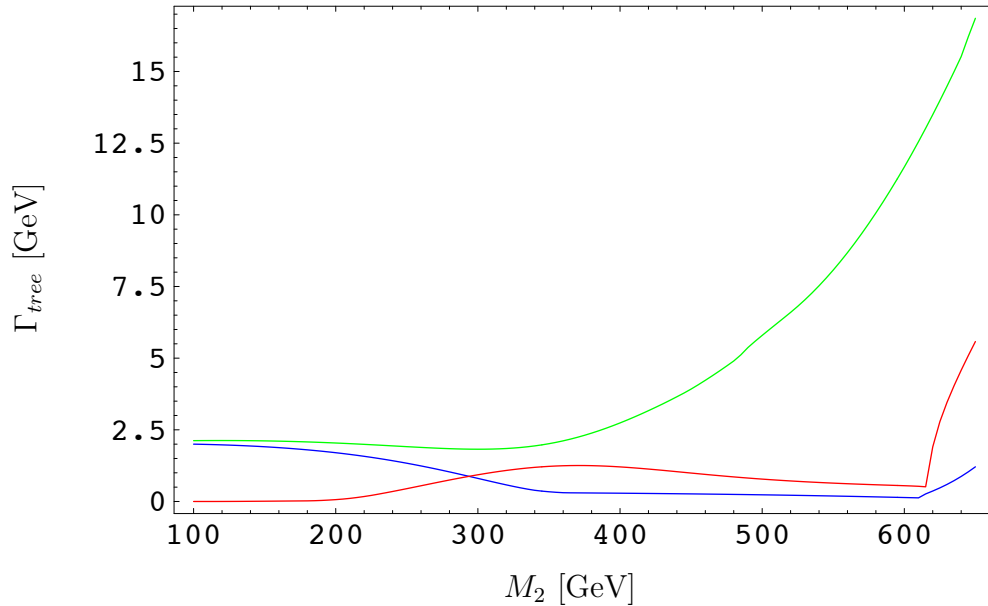


Figure 6.2: The dependence of the total tree-level decay width of $\tilde{\chi}_4^0$, $\tilde{\chi}_3^0$ and $\tilde{\chi}_2^0$ on M_2 .

Fig. 6.3 shows the relative one-loop level corrections to the total decay widths of $\tilde{\chi}_4^0$, $\tilde{\chi}_3^0$ and $\tilde{\chi}_2^0$, dependent on M_2 . The peak of the $\tilde{\chi}_4^0$ -line at $M_2 = 475$ GeV is caused by the appearance of several $\tilde{\chi}_4^0 \rightarrow q\bar{q}$ channels (see also Fig. 6.7).

The peak of the $\tilde{\chi}_3^0$ corrections at $M_2 = 360$ GeV is due to the closing of the channel $\tilde{\chi}_3^0 \rightarrow \tilde{\chi}^\pm W^\pm$ (see also Fig. 6.8).

The strong peaks of the $\tilde{\chi}_4^0$ and $\tilde{\chi}_3^0$ corrections between $M_2 = 615$ GeV and $M_2 = 620$ GeV are due to the appearance of the channels $\tilde{\chi}_{3,2}^0 \rightarrow t\bar{t}$, that already caused the dents in Figure 6.2.

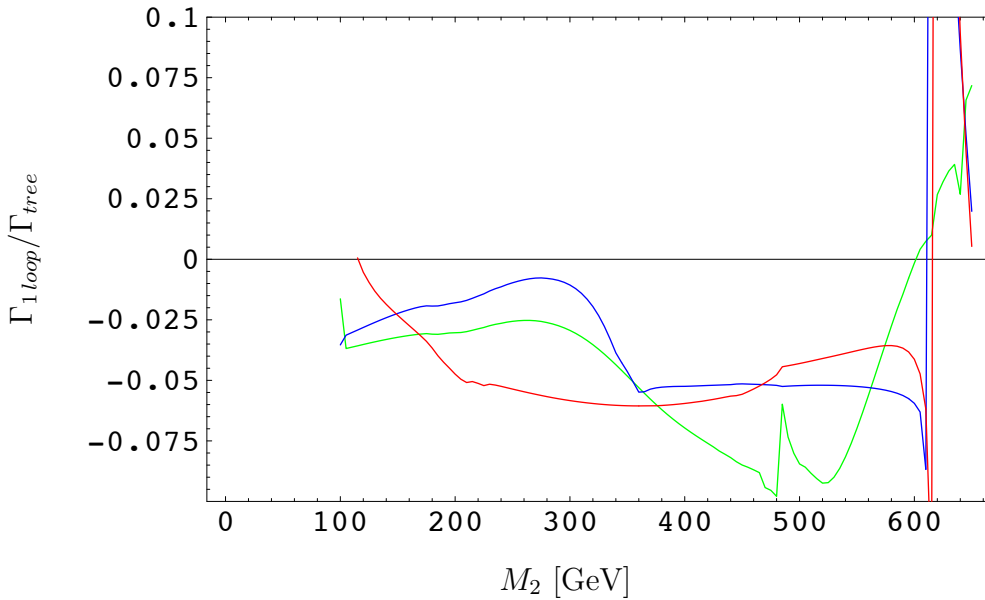


Figure 6.3: The dependence of the relative one-loop level corrections to the total decay width of $\tilde{\chi}_4^0$, $\tilde{\chi}_3^0$ and $\tilde{\chi}_2^0$ on M_2 .

Fig. 6.4 compares the parts of relative electroweak and QCD corrections to the total decay width of $\tilde{\chi}_4^0$, $\tilde{\chi}_3^0$ and $\tilde{\chi}_2^0$.

The cause of the peak at $M_2 = 475$ GeV are again the channels $\tilde{\chi}_4^0 \rightarrow q\bar{q}$. In Fig. 6.5 again occurs a kink at $M_2 = 360$ GeV, corresponding to the channel $\tilde{\chi}_3^0 \rightarrow \tilde{\chi}^\pm W^\pm$. In Fig. 6.5 and Fig. 6.6 one can clearly see that the corrections are mostly electroweak, since the channel $\tilde{\chi}_3^0 \rightarrow q\bar{q}$ and $\tilde{\chi}_2^0 \rightarrow q\bar{q}$ are kinematically not allowed for the major part of the plotted region. The strong peaks of the QCD corrections in Fig. 6.5 and Fig. 6.6 correspond to the opening of the quark-squark channels.

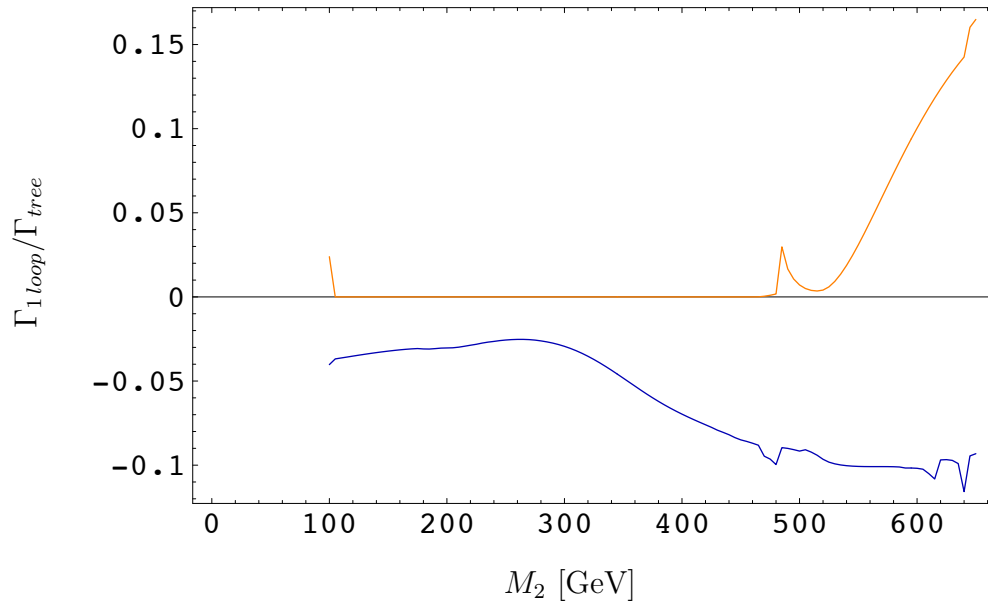


Figure 6.4: The dependence of the [electroweak](#) and the [QCD](#) corrections to the total decay width of the $\tilde{\chi}_4^0$ on M_2 .

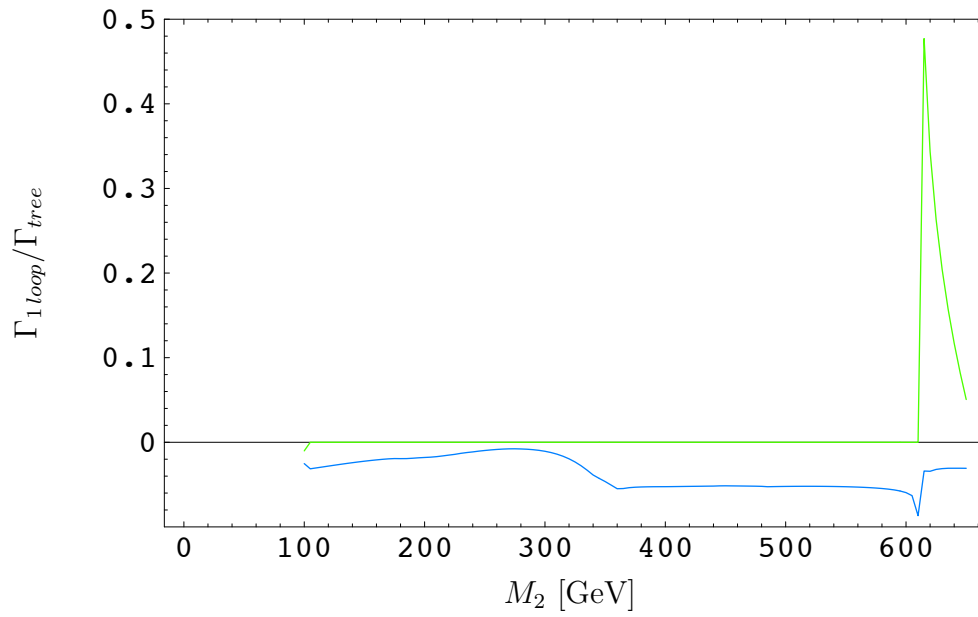


Figure 6.5: The dependence of the [electroweak](#) and the [QCD](#) corrections to the total decay width of the $\tilde{\chi}_3^0$ on M_2 .

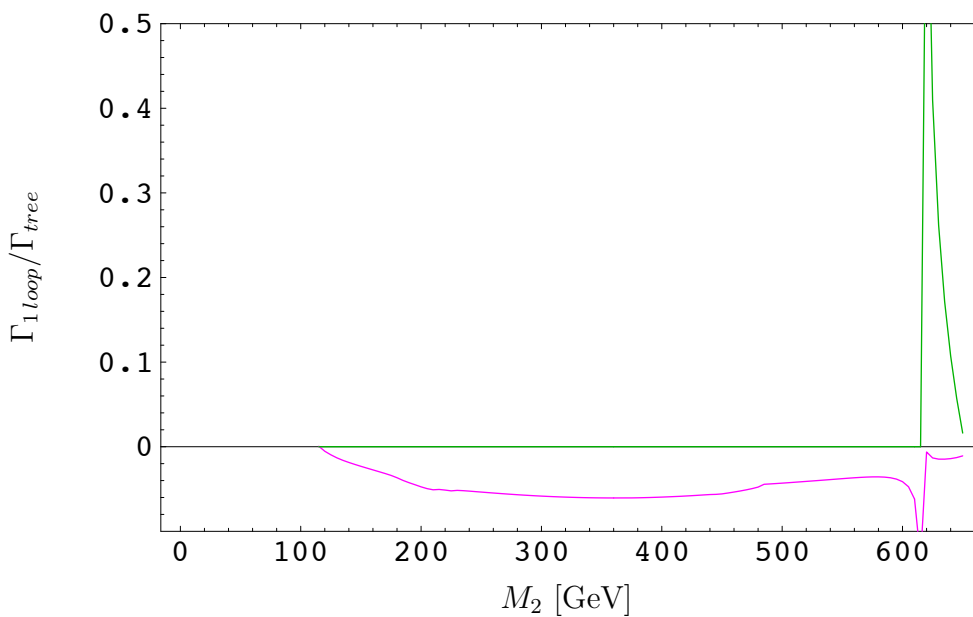


Figure 6.6: The dependence of the **electroweak** and the **QCD** corrections to the total decay width of the $\tilde{\chi}_2^0$ on M_2 .

Fig. 6.7, Fig. 6.8 and Fig. 6.9 show the branching ratios of the several decay channels of $\tilde{\chi}_4^0$, $\tilde{\chi}_3^0$ and $\tilde{\chi}_2^0$. The legend explaining the used colors is stated in Tab. 6.11. Solid lines represent the one-loop corrected, dashed lines the tree level branching ratios.

In Fig. 6.7 at $M_2 = 475$ GeV one can clearly observe the reasons for peaks in Fig. 6.3 and Fig. 6.4. At $M_2 = 450$ GeV the channels $\tilde{\chi}_4^0 \rightarrow \tilde{\chi}_1^0 Z^0$ and $\tilde{\chi}_2^0 \rightarrow \tilde{\chi}_2^0 Z^0$ almost vanish, while the channel $\tilde{\chi}_4^0 \rightarrow \tilde{\chi}_3^0 Z^0$ is emerging.

In Fig. 6.8, the vanishing of the channel $\tilde{\chi}_3^0 \rightarrow \tilde{\chi}^\pm W^\pm$ at $M_2 = 360$ GeV corresponds to the peak of the electroweak correction in Fig. 6.5.

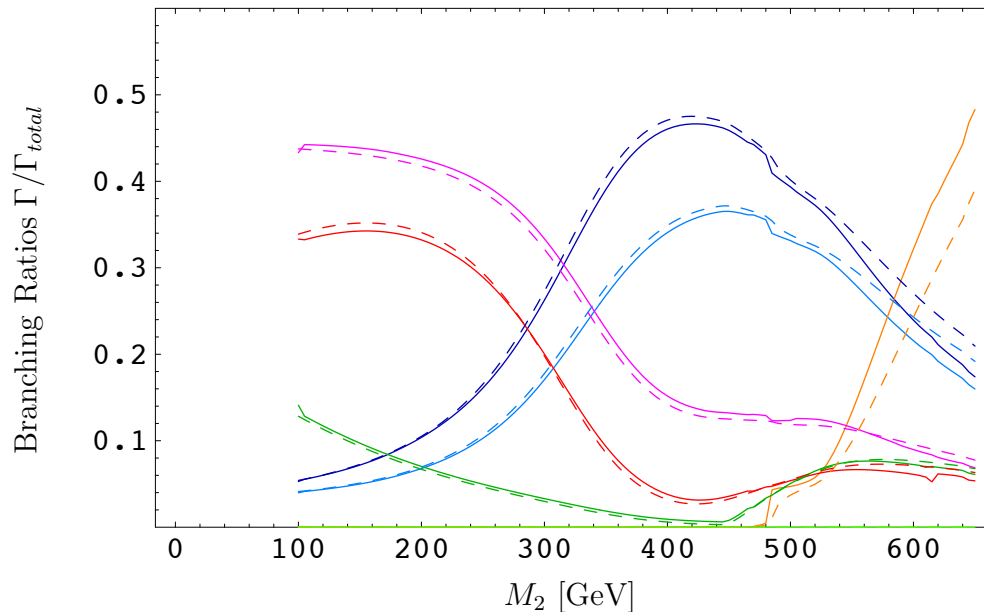


Figure 6.7: The dependence of the branching ratios of $\tilde{\chi}_4^0$ on M_2 .

dark blue	$\tilde{\chi}^0 \rightarrow \nu\bar{\nu}$	light green	$\tilde{\chi}^0 \rightarrow \tilde{\chi}^\pm H^\pm$
light blue	$\tilde{\chi}^0 \rightarrow l\bar{l}$	dark green	$\tilde{\chi}^0 \rightarrow \tilde{\chi}^0 Z^0$
orange	$\tilde{\chi}^0 \rightarrow q\bar{q}$	violet	$\tilde{\chi}^0 \rightarrow \tilde{\chi}^\pm W^\pm$
red	$\tilde{\chi}^0 \rightarrow \tilde{\chi}^0 H^0$	yellow	$\tilde{\chi}^0 \rightarrow g\bar{g}$

Table 6.11: Colors used in Figures 6.7, 6.8, 6.9, 6.14, 6.15, 6.16, 6.19, 6.20, 6.21.

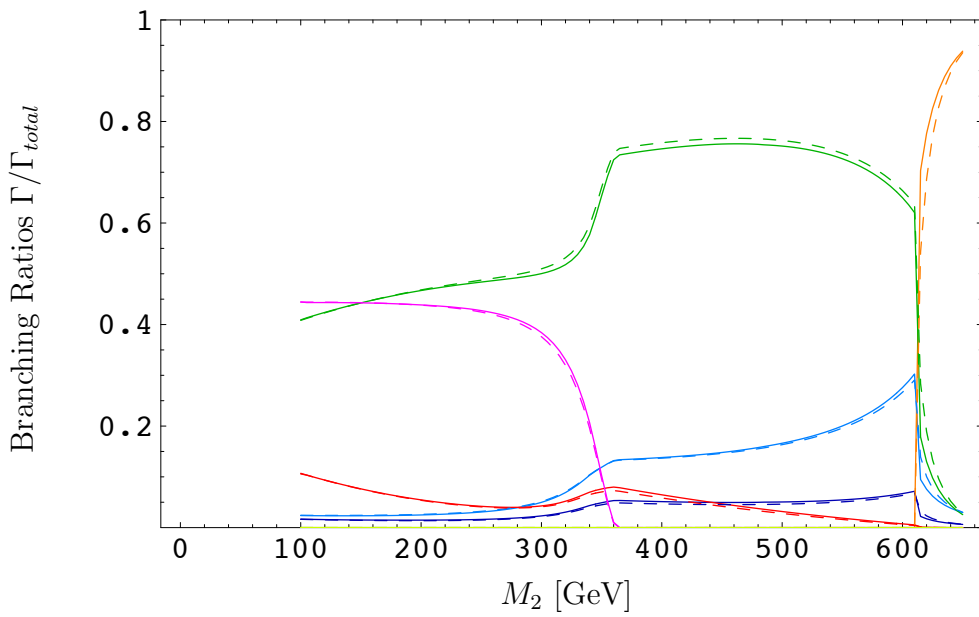


Figure 6.8: The dependence of the branching ratios of $\tilde{\chi}_3^0$ on M_2 .

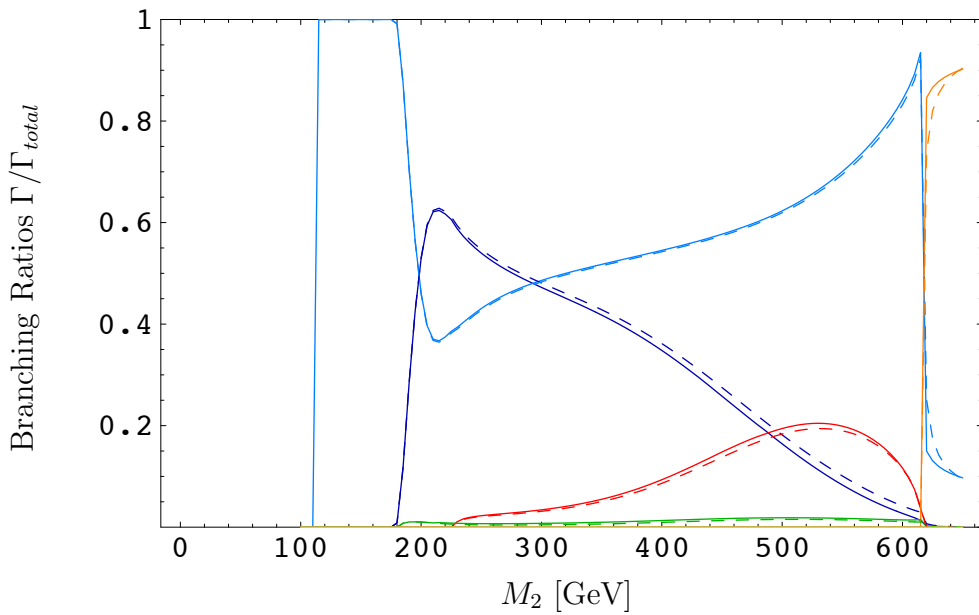


Figure 6.9: The dependence of the branching ratios of $\tilde{\chi}_2^0$ on M_2 .

6.3.2 Variation of μ

Fig. 6.10 shows the total tree-level decay width and Fig. 6.11 the relative one-loop level corrections to the total decay widths of $\tilde{\chi}_4^0$, $\tilde{\chi}_3^0$ and $\tilde{\chi}_2^0$, dependent on μ .

Fig. 6.12 and Fig. 6.13 again compare the parts of relative electroweak and QCD corrections to the total decay width of $\tilde{\chi}_4^0$, $\tilde{\chi}_3^0$ and $\tilde{\chi}_2^0$.

Like for the plots showing the M_2 dependence, the kinks and peaks may be explained by the appearing of new decay channels. Fig. 6.11 shows relative corrections. Therefor, and since the corrections of the new evolving channels are first oft the same magnitude as the tree-level, the peaks in Fig. 6.11 are especially prominent. The evolution of the several groups of channels can be observed in Fig. 6.14, Fig. 6.15 and Fig. 6.16, which show the branching ratios of the decay channels of $\tilde{\chi}_4^0$, $\tilde{\chi}_3^0$ and $\tilde{\chi}_2^0$. The legend explaining the colors used again is stated in Tab. 6.11, solid lines represent the one-loop corrected, dashed lines the tree level branching ratios.

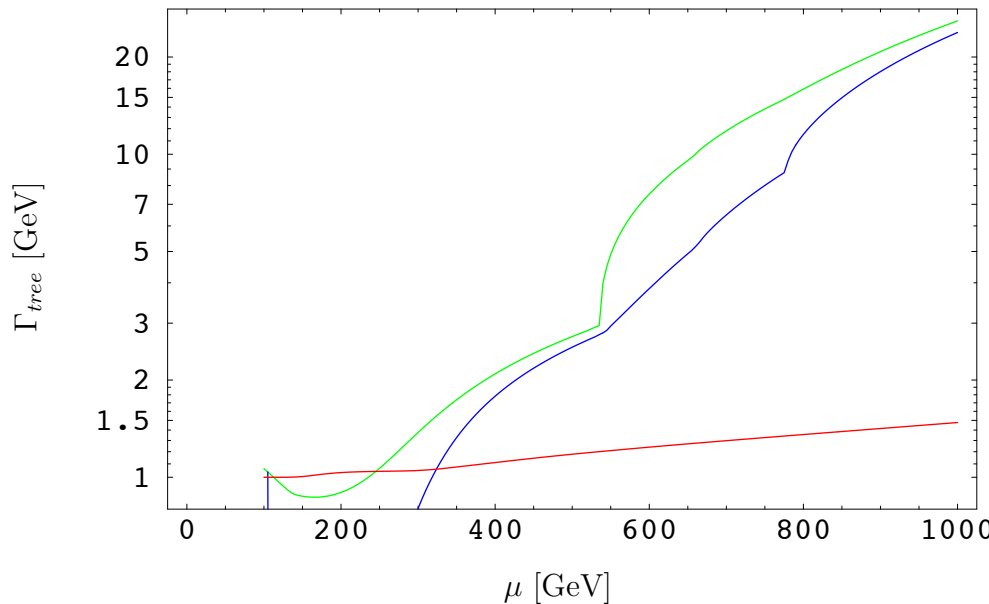


Figure 6.10: The dependence of the total tree-level decay width of $\tilde{\chi}_4^0$, $\tilde{\chi}_3^0$ and $\tilde{\chi}_2^0$ on μ .

In Fig. 6.10, Fig. 6.11 and Fig. 6.12, the kinks and peaks of the $\tilde{\chi}_4^0$ -line at $\mu = 530$ GeV correspond to the appearance of the $\tilde{\chi}_4^0 \rightarrow q\bar{q}$ channels. The peak of the $\tilde{\chi}_4^0$ in Fig. 6.11 and the peak of the electroweak correction in Fig. 6.12 at $\mu = 665$ GeV are caused by the opening of the channel $\tilde{\chi}^0 \rightarrow \tilde{\chi}^\pm H^\mp$.

For the $\tilde{\chi}_3^0$ -decays, the kinks in Fig. 6.10, Fig. 6.11 and Fig. 6.13 at $\mu = 550$ GeV are due to the appearance of the majority of the $\tilde{\chi}_3^0 \rightarrow q\bar{q}$ channels, at $\mu = 780$ GeV additionally the channel $\tilde{\chi}_3^0 \rightarrow t\bar{t}_2$ appears. The peaks in Fig. 6.11 and Fig. 6.13 between $\mu = 110$ GeV and $\mu = 220$ GeV are due to the channels $\tilde{\chi}_3^0 \rightarrow l\bar{l}$, $\tilde{\chi}_3^0 \rightarrow \tilde{\chi}^0 Z^0$, $\tilde{\chi}_3^0 \rightarrow \nu\bar{\nu}$, $\tilde{\chi}_3^0 \rightarrow \tilde{\chi}^0 H^0$ and $\tilde{\chi}_3^0 \rightarrow \tilde{\chi}^\pm W^\pm$. The peaks at $\mu = 670$ GeV are caused by the channel $\tilde{\chi}_3^0 \rightarrow \tilde{\chi}^\pm H^\pm$.

In Fig. 6.13 and Fig. 6.14 one can observe the correlation between the QCD corrections on the one hand and the channels $\tilde{\chi}^0 \rightarrow q\bar{q}$ on the other hand. Concerning the $\tilde{\chi}_2^0$ decays, there are no $\tilde{\chi}^0 \rightarrow q\bar{q}$ channels kinematically allowed. Therefor all corrections are electroweak.

Since $\tilde{\chi}_4^0$ and $\tilde{\chi}_3^0$ are dominated by their Higgs components at large μ , the $\tilde{\chi}^0 \rightarrow q\bar{q}$ -channels are dominated by the channels including a \tilde{t} . The other squark and lepton channels are negligible. As shown in [60], if all channels are kinematically allowed, 50% of the $\tilde{\chi}_4^0$ and $\tilde{\chi}_3^0$ decays will be into a t and \tilde{t} .

Beginning at $\mu = 820$ GeV the loop induced channel $\tilde{\chi}^0 \rightarrow g\tilde{g}$ gives a small but observable contribution.

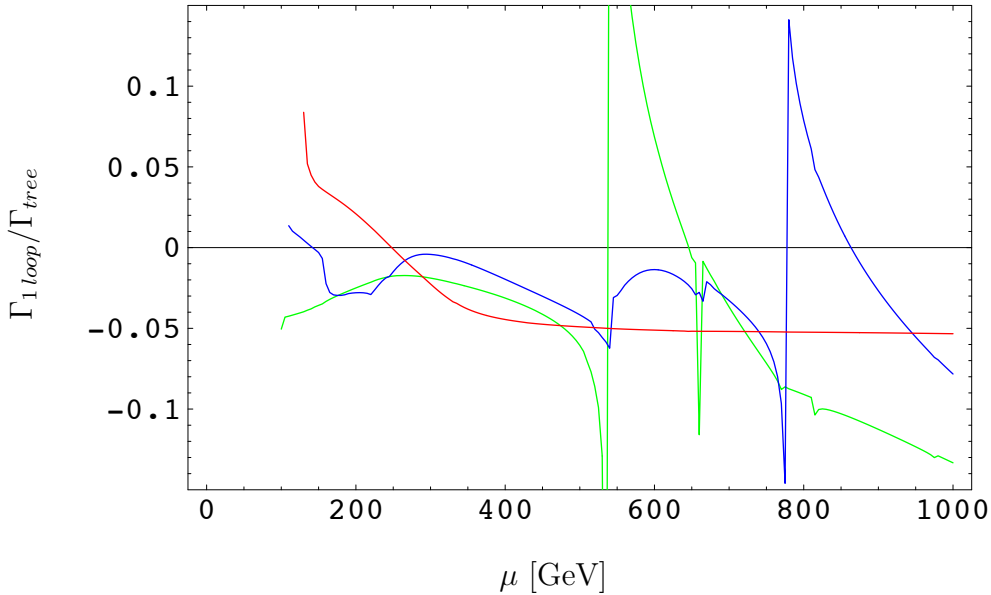


Figure 6.11: The dependence of the one-loop level corrections to the total decay width of $\tilde{\chi}_4^0$, $\tilde{\chi}_3^0$ and $\tilde{\chi}_2^0$ on μ .

In Fig. 6.16, there is almost no difference visible between the branching ratios on tree-level, and the One-Loop corrected branching ratios. This is due to the fact, that the corrections to all channels are of very similar size and the same sign.

The same effect may be seen also in Fig. 6.20, Fig. 6.21, Fig. 6.32 and Fig. 6.37.

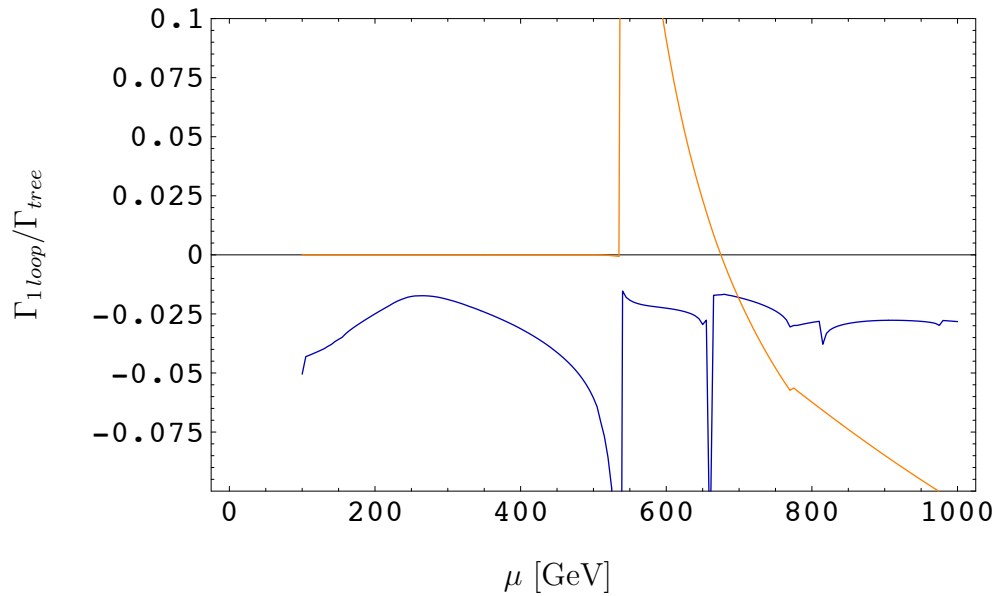


Figure 6.12: The dependence of the [electroweak](#) and the [QCD](#) corrections to the total decay width of the $\tilde{\chi}_4^0$ on μ .

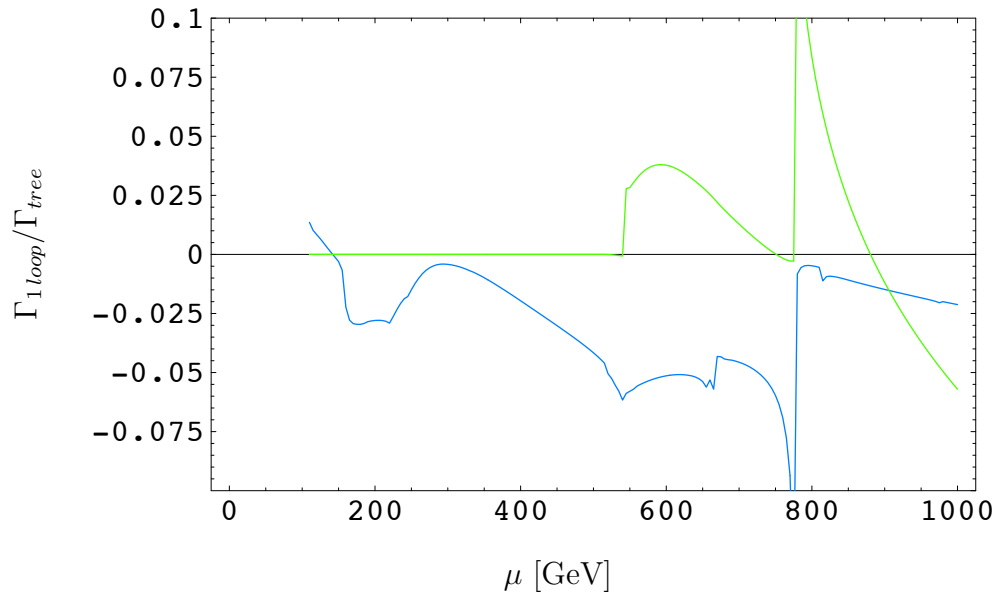


Figure 6.13: The dependence of the [electroweak](#) and the [QCD](#) corrections to the total decay width of the $\tilde{\chi}_3^0$ on μ .

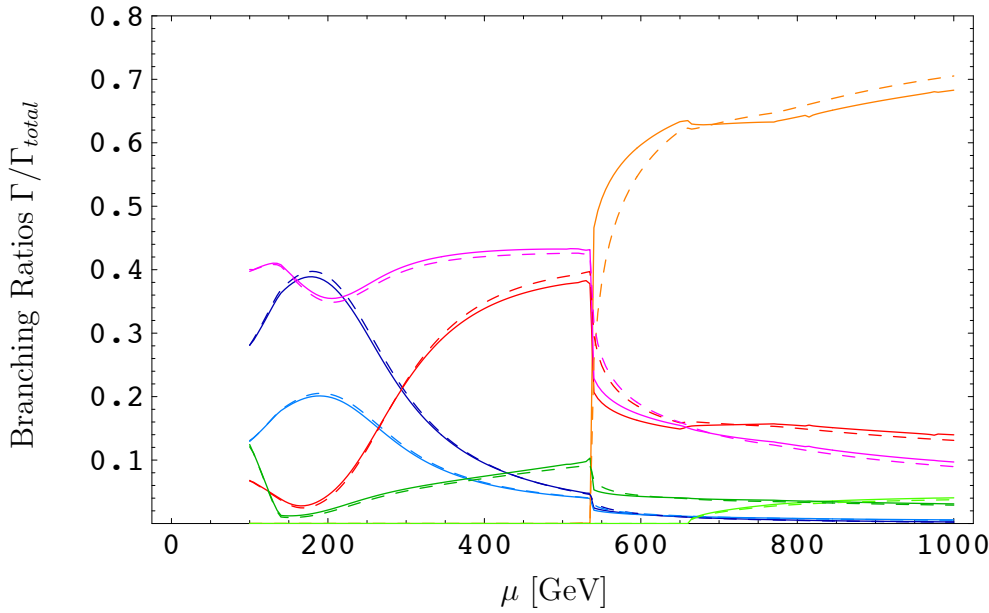


Figure 6.14: The dependence of the branching ratios of $\tilde{\chi}_4^0$ on μ .

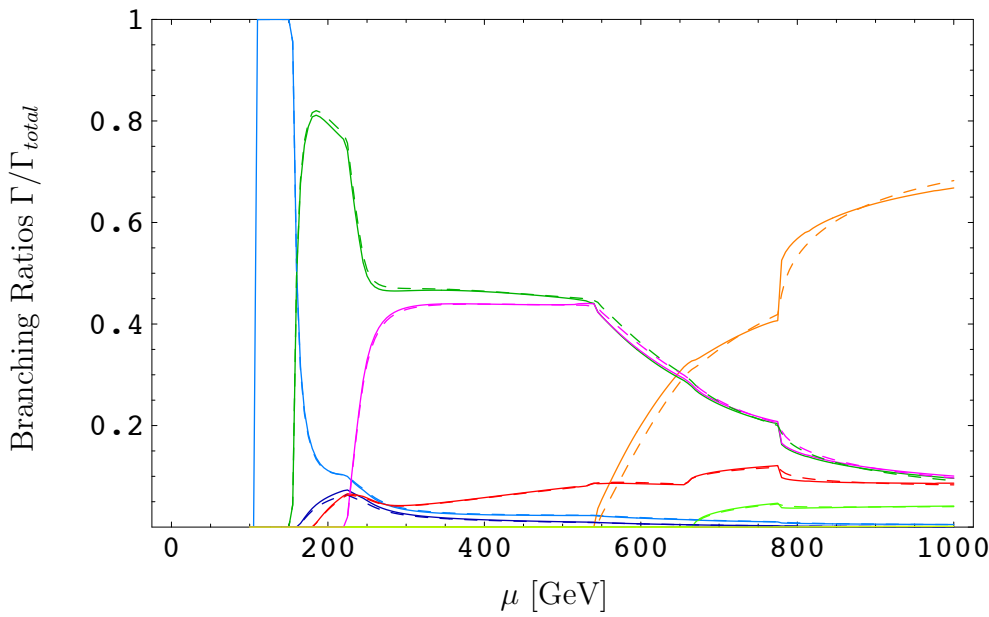


Figure 6.15: The dependence of the branching ratios of $\tilde{\chi}_3^0$ on μ .

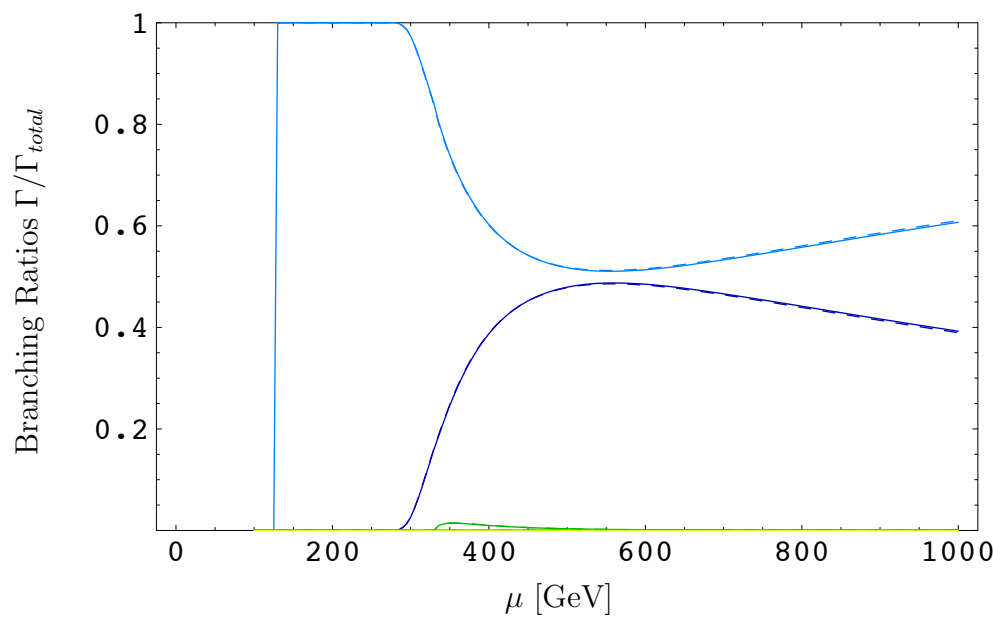


Figure 6.16: The dependence of the branching ratios of $\tilde{\chi}_2^0$ on μ .

6.3.3 Variation of $\tan \beta$

As visible in Fig. 6.17, Fig. 6.19 and Fig. 6.20, the decay widths of $\tilde{\chi}_4^0$ and $\tilde{\chi}_3^0$ seem to be rather independent of a variation of $\tan \beta$. Since there are no decays into quarks and squarks, all loop corrections are electroweak. Among the decays of the $\tilde{\chi}_2^0$ particle, the channels $\tilde{\chi}^0 \rightarrow \nu\bar{\nu}$, $\tilde{\chi}^0 \rightarrow l\bar{l}$, and up to $\tan \beta = 2.1$ the channel $\tilde{\chi}^0 \rightarrow \tilde{\chi}^\pm H^\mp$ are dominating.

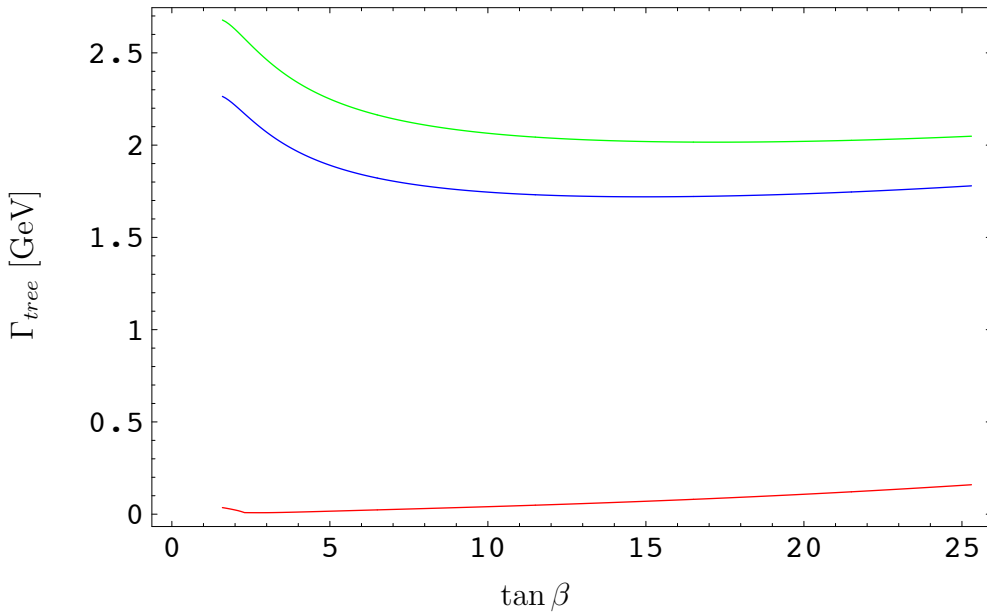


Figure 6.17: The dependence of the total tree-level decay width of $\tilde{\chi}_4^0$, $\tilde{\chi}_3^0$ and $\tilde{\chi}_2^0$ on $\tan \beta$.

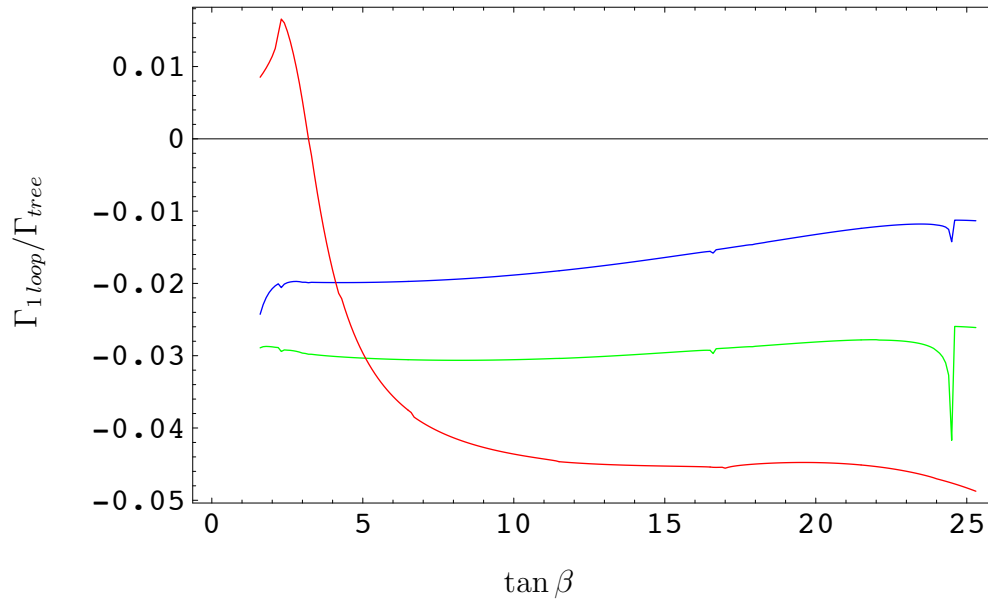


Figure 6.18: The dependence of the one-loop level corrections to the total decay width of $\tilde{\chi}_4^0$, $\tilde{\chi}_3^0$ and $\tilde{\chi}_2^0$ on $\tan \beta$.

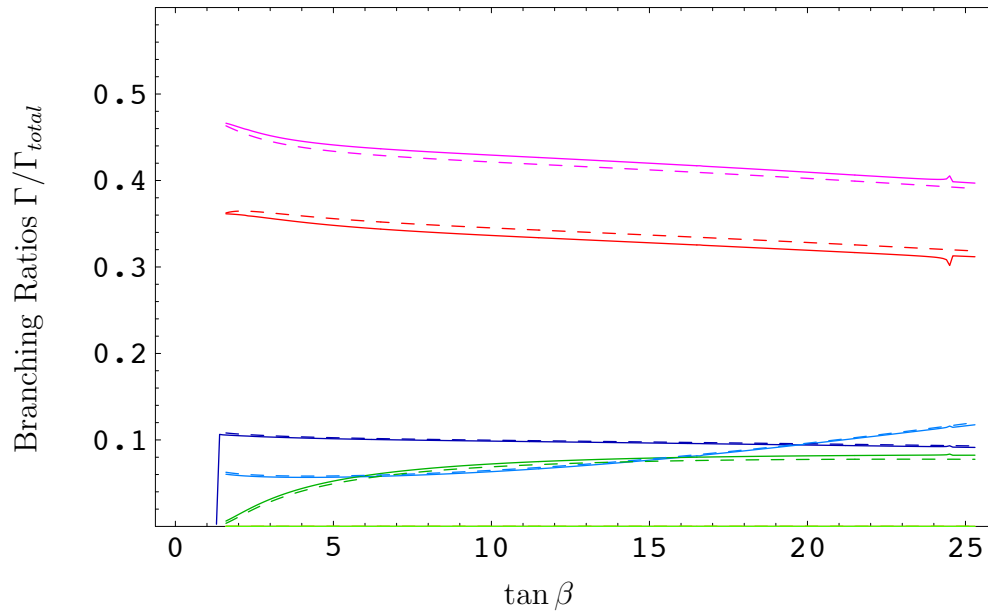


Figure 6.19: The dependence of the branching ratios of $\tilde{\chi}_4^0$ on $\tan \beta$.

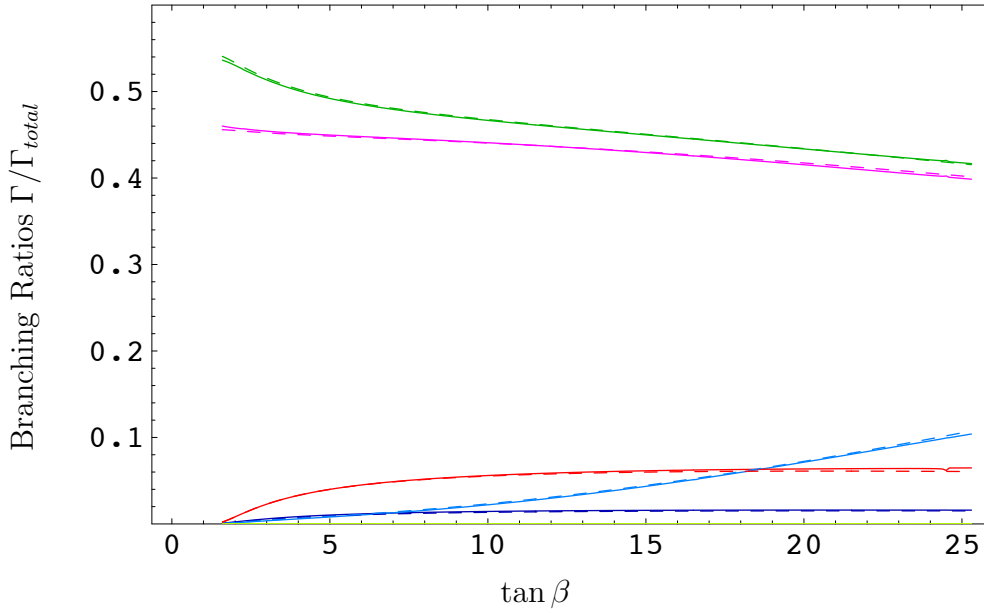


Figure 6.20: The dependence of the branching ratios of $\tilde{\chi}_3^0$ on $\tan \beta$.

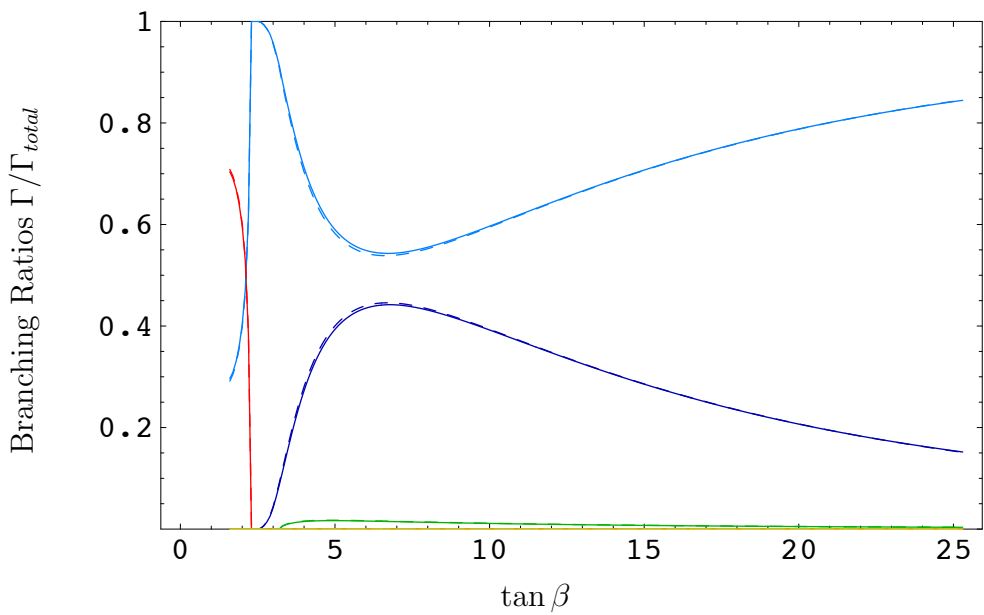


Figure 6.21: The dependence of the branching ratios of $\tilde{\chi}_2^0$ on $\tan \beta$.

6.4 Chargino Decays

In the following subsections we discuss the dependence of the decay widths and the branching ratios of the charginos $\tilde{\chi}_2^\pm$ and $\tilde{\chi}_1^\pm$ on the variation of the mass parameters M_2 , μ and the mixing angle $\tan \beta$. Like in the previous section dealing with the neutralino decays, the input parameters are defined at the SPS1a' point, explicitly given in Tab.6.2, Tab.6.3 and Tab.6.4.

6.4.1 Variation of M_2

Fig. 6.22 shows the total tree-level decay width of the charginos $\tilde{\chi}_2^\pm$ and $\tilde{\chi}_1^\pm$, dependent on the variation of M_2 . Fig. 6.23 shows the relative one-loop level corrections to the total decay widths. In Fig. 6.24 and Fig. 6.26 we compare the relative electroweak and QCD corrections to the total decay width of $\tilde{\chi}_2^\pm$ and $\tilde{\chi}_1^\pm$. Fig. 6.25 and Fig. 6.27 finally show the branching ratios of $\tilde{\chi}_2^\pm$ and $\tilde{\chi}_1^\pm$.

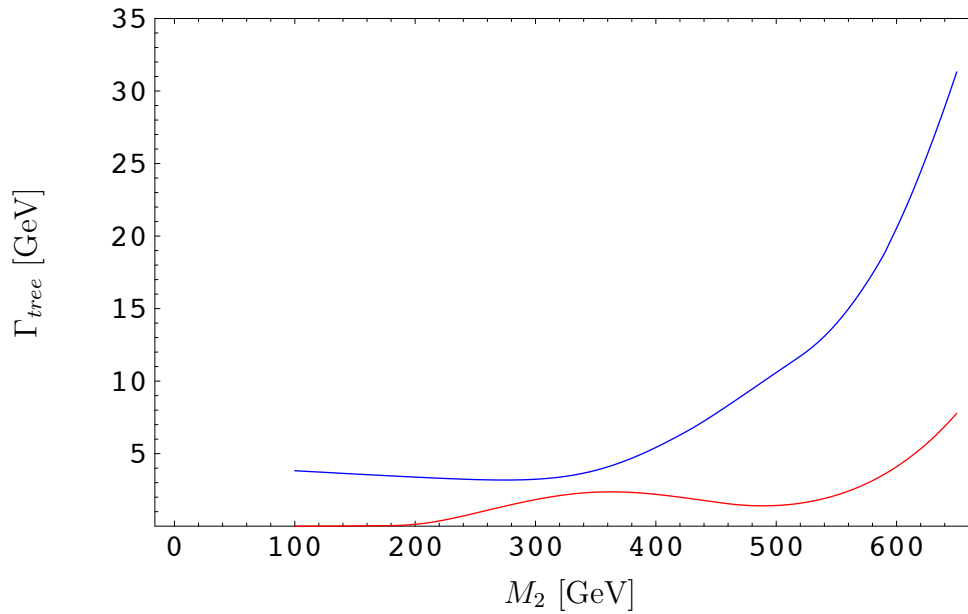


Figure 6.22: The dependence of the total tree-level decay width of $\tilde{\chi}_2^\pm$ and $\tilde{\chi}_1^\pm$ on M_2 .

As already discussed about the neutralinos, in Fig. 6.23, Fig. 6.24 and Fig. 6.25 most of the kinks and peaks can be explained by the opening or closing of different decay channels. At $M_2 = 515$ GeV several channels of the type $\tilde{\chi}_2^\pm \rightarrow q\tilde{q}_2$ are opening, at $M_2 = 560$ GeV $\tilde{\chi}_2^\pm \rightarrow b\tilde{t}_1$ shows a minimum.

The kink of the $\tilde{\chi}_1^\pm$ line at $M_2 = 465$ GeV is caused by the opening of the channel $\tilde{\chi}_1^\pm \rightarrow b\tilde{t}_1$, also well visible in Fig. 6.27.

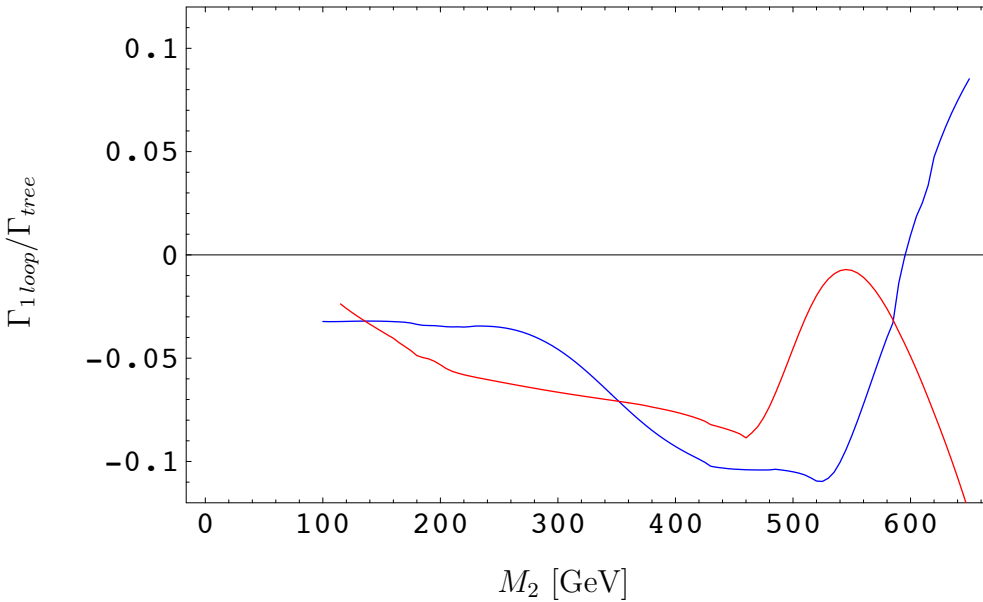


Figure 6.23: The dependence of the one-loop level corrections to the total decay width of $\tilde{\chi}_2^\pm$ and $\tilde{\chi}_1^\pm$ on M_2 .

Table 6.12 shows the legend to the colors used in Fig. 6.25 and Fig. 6.27. Solid lines stand again for the one-loop corrected, dashed lines for the tree level branching ratios.

dark blue	$\tilde{\chi}^\pm \rightarrow l\tilde{\nu}$	light green	$\tilde{\chi}^\pm \rightarrow \tilde{\chi}^0 H^+$
light blue	$\tilde{\chi}^\pm \rightarrow \nu\tilde{l}$	dark green	$\tilde{\chi}^\pm \rightarrow \tilde{\chi}^0 Z^0$
orange	$\tilde{\chi}^\pm \rightarrow q\tilde{q}$	violet	$\tilde{\chi}^\pm \rightarrow \tilde{\chi}^0 W^+$
red	$\tilde{\chi}^\pm \rightarrow \tilde{\chi}^\pm H^0$	yellow	$\tilde{\chi}^\pm \rightarrow \tilde{\chi}^\pm \gamma$

Table 6.12: Colors used for Figures 6.25, 6.27, 6.31, 6.32, 6.36, 6.37.

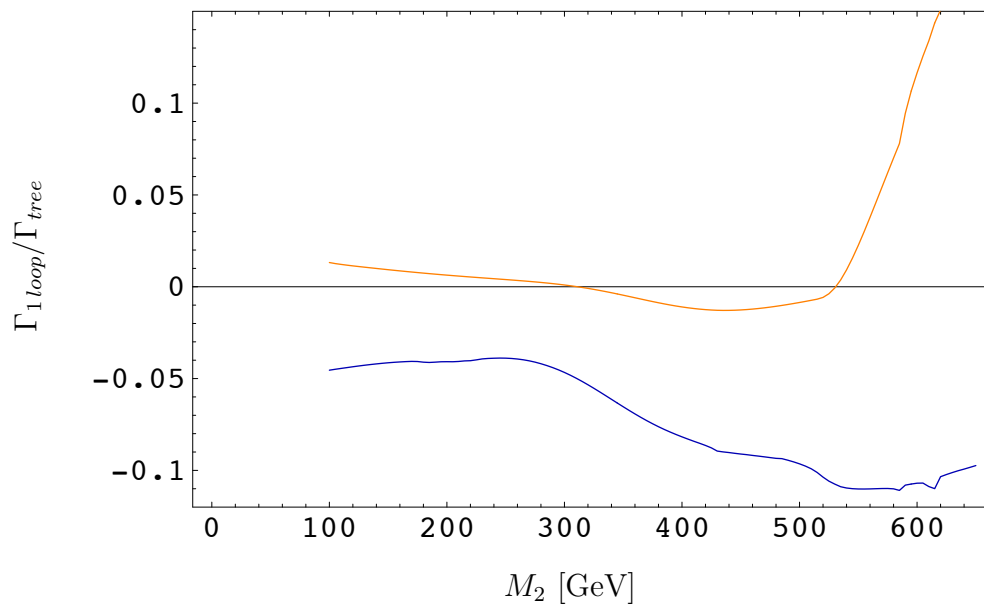


Figure 6.24: The dependence of the [electroweak](#) and the [QCD](#) corrections to the total decay width of the $\tilde{\chi}_2^\pm$ on M_2 .

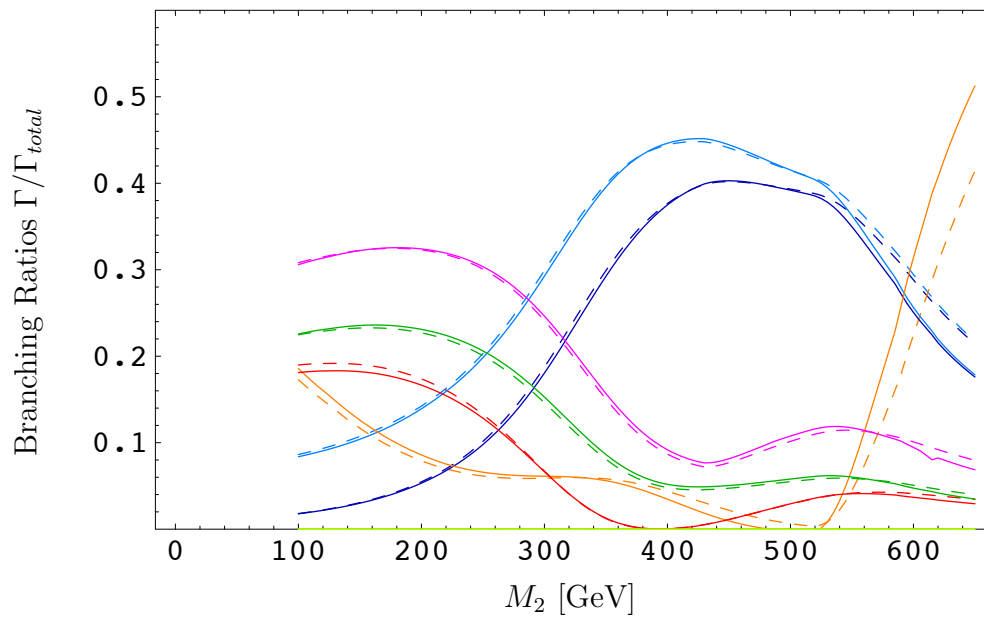


Figure 6.25: The dependence of the branching ratios of $\tilde{\chi}_2^\pm$ on M_2 .

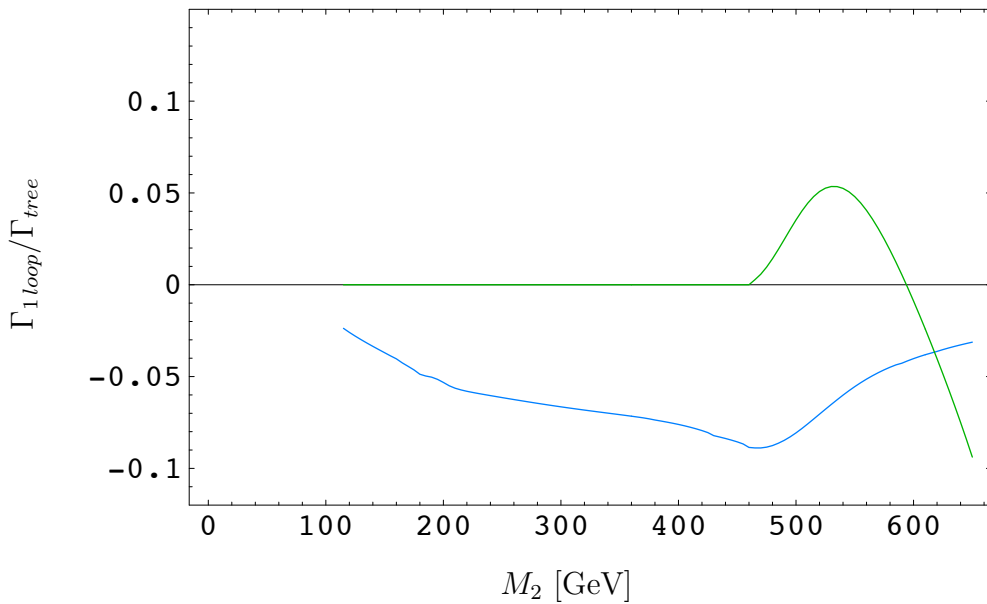


Figure 6.26: The dependence of the [electroweak](#) and the [QCD](#) corrections to the total decay width of the $\tilde{\chi}_1^\pm$ on M_2 .

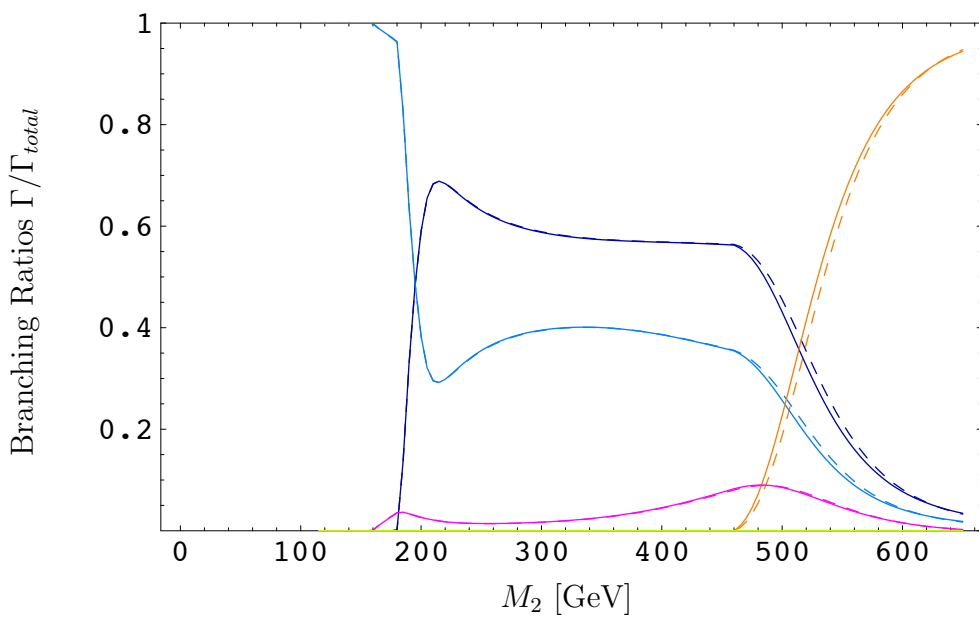


Figure 6.27: The dependence of the branching ratios of $\tilde{\chi}_1^\pm$ on M_2 .

6.4.2 Variation of μ

The following figures show the dependence of tree-level decay widths, relative One-Loop corrections and branching ratios on the variation of μ .

The kinks and peaks visible in Fig. 6.28, Fig. 6.29, Fig. 6.30 and Fig. 6.31 correspond to the appearance of the channels $\tilde{\chi}_2^\pm \rightarrow b\tilde{t}_1$ at $\mu = 350$ GeV, $\tilde{\chi}_2^\pm \rightarrow t\tilde{b}_1$ at $\mu = 680$ GeV, $\tilde{\chi}_2^\pm \rightarrow \tilde{\chi}_1^\pm H_0$ and $\tilde{\chi}_2^\pm \rightarrow \tilde{\chi}_1^\pm A_0$ at $\mu = 650$ GeV and $\tilde{\chi}_2^\pm \rightarrow t\tilde{b}_1$ at $\mu = 680$ GeV.

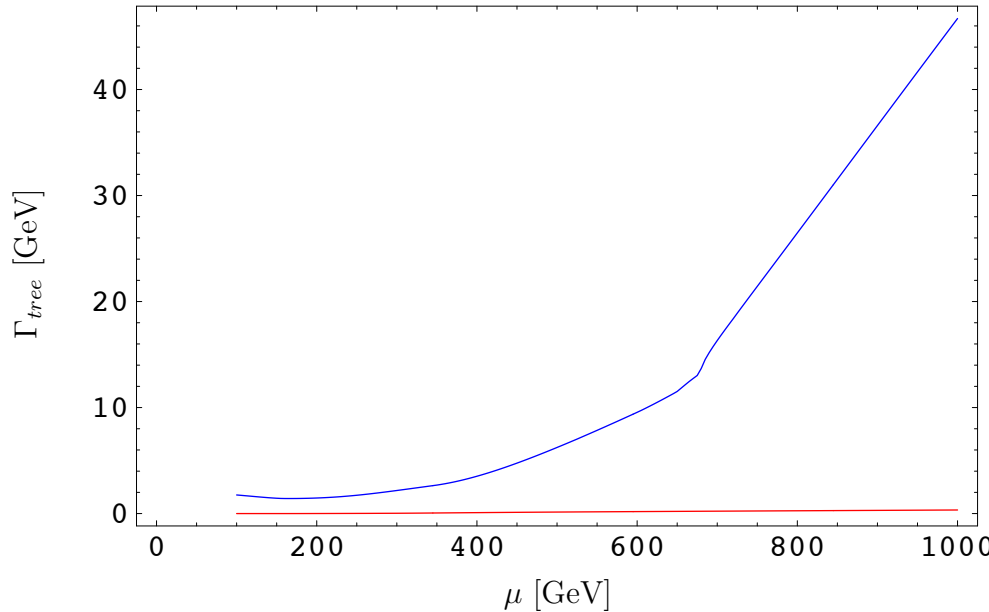


Figure 6.28: The dependence of the total tree-level decay width of $\tilde{\chi}_2^\pm$ and $\tilde{\chi}_1^\pm$ on μ .

In Figure 6.29, the kink of the $\tilde{\chi}_1^\pm$ line at $\mu = 265$ GeV is due to the appearance channel $\tilde{\chi}_1^\pm \rightarrow \tilde{\chi}_1^0 W^\pm$, the kink at $\mu = 295$ GeV due to the opening of the channels $\tilde{\chi}_1^\pm \rightarrow l\tilde{\nu}$.

Since there are no decays of $\tilde{\chi}_1^0$ into quarks and squarks kinematically allowed, there only exist electroweak one-loop corrections to the $\tilde{\chi}_1^0$ decays, without any QCD contributions.

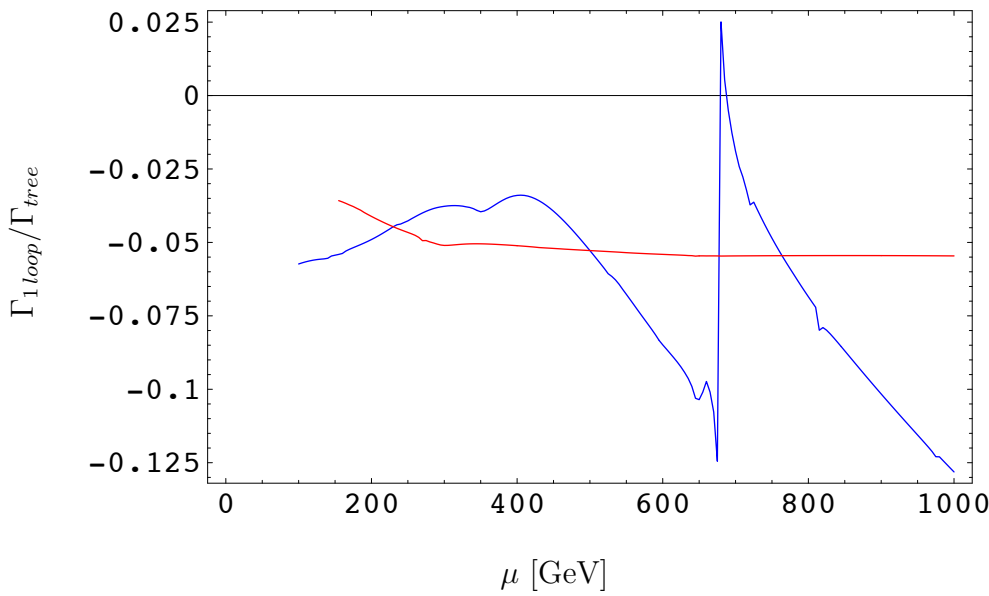


Figure 6.29: The dependence of the one-loop level corrections to the total decay width of $\tilde{\chi}_2^\pm$ and $\tilde{\chi}_1^\pm$ on μ .

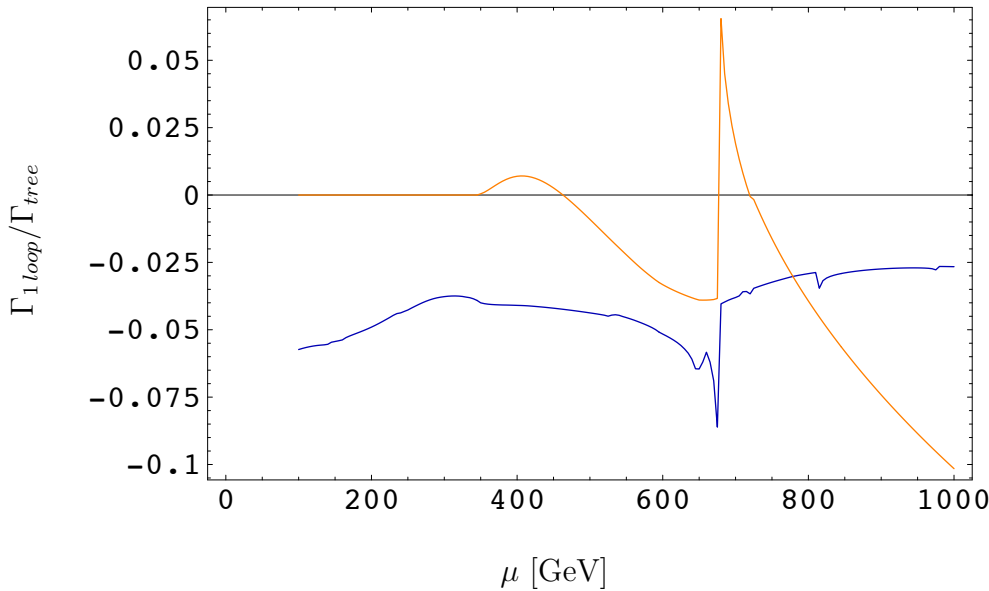


Figure 6.30: The dependence of the **electroweak** and the **QCD** corrections to the total decay width of the $\tilde{\chi}_2^\pm$ on μ .

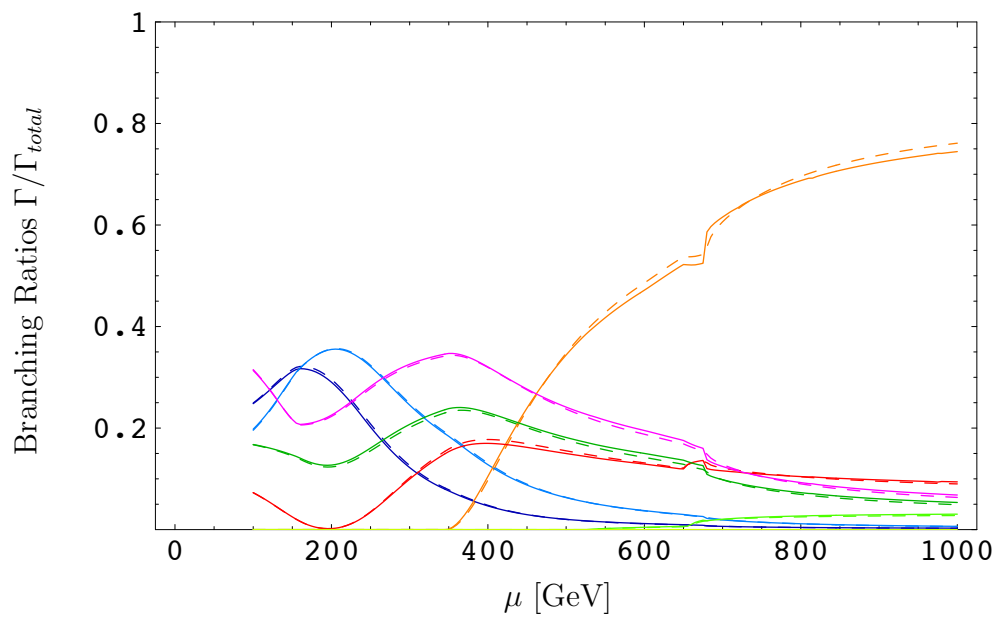


Figure 6.31: The dependence of the branching ratios of $\tilde{\chi}_2^\pm$ on μ .

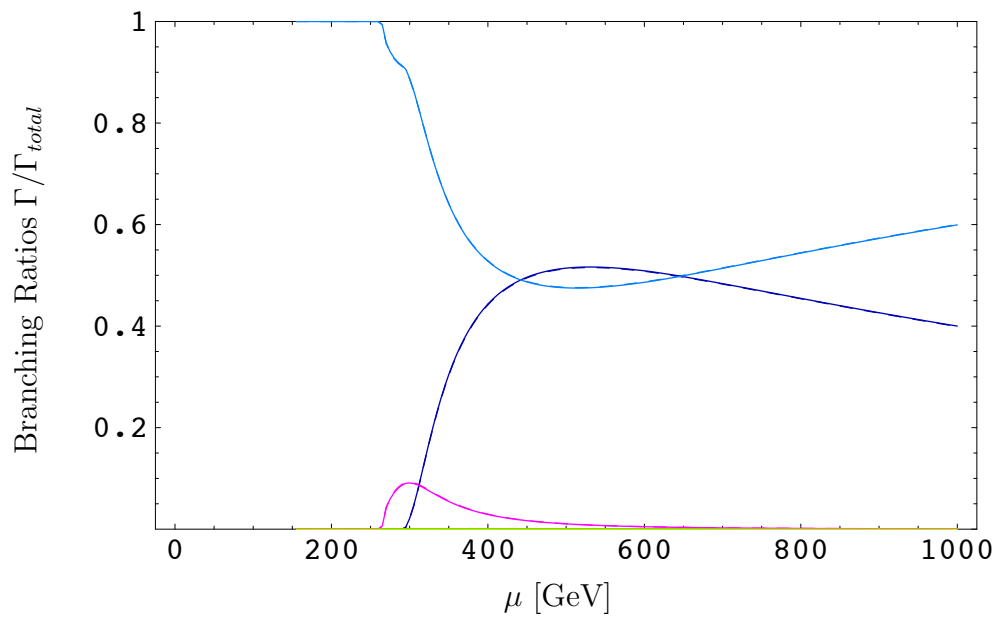


Figure 6.32: The dependence of the branching ratios of $\tilde{\chi}_1^\pm$ on μ .

6.4.3 Variation of $\tan \beta$

Similar to the neutralino decays, the dependence of the branching ratios of $\tilde{\chi}_2^\pm$ on $\tan \beta$ is rather small, shown in Fig 6.36. On the other hand, the branching ratios of $\tilde{\chi}_2^\pm$ (see Fig. 6.37) are of the same shape as the branching ratios of $\tilde{\chi}_2^0$ (see Fig. 6.21).

Again there are no decays of $\tilde{\chi}_1^\pm$ to quarks and squarks kinematically allowed, so there are only electroweak corrections.

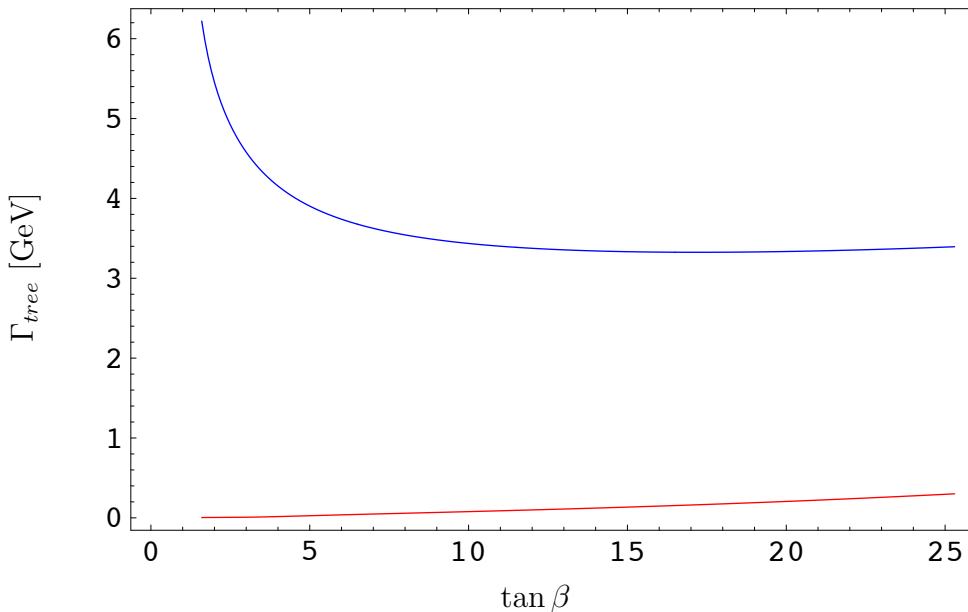


Figure 6.33: The dependence of the total tree-level decay width of $\tilde{\chi}_2^\pm$ and $\tilde{\chi}_1^\pm$ on $\tan \beta$.

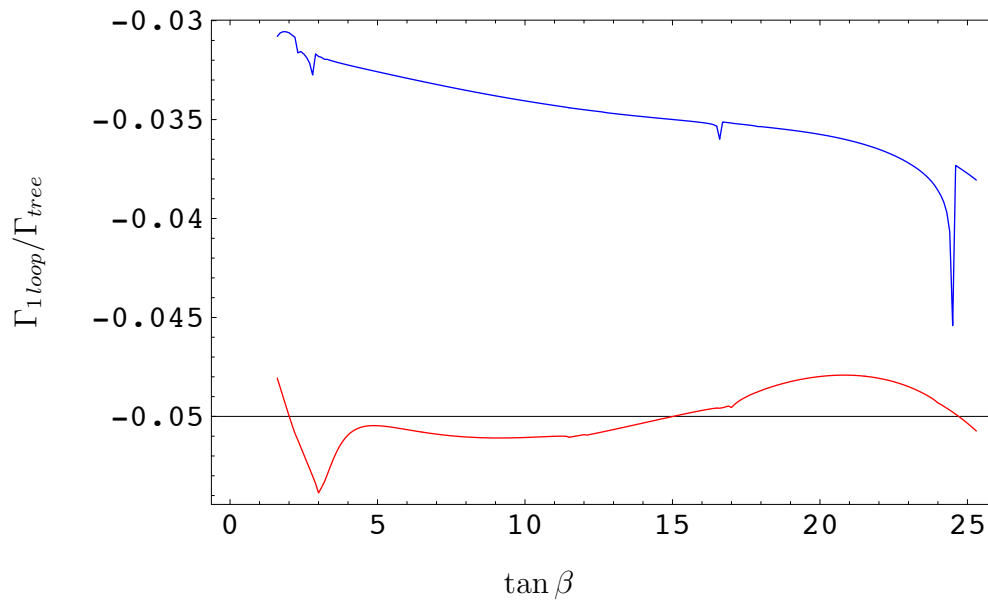


Figure 6.34: The dependence of the one-loop level corrections to the total decay width of $\tilde{\chi}_2^\pm$ and $\tilde{\chi}_1^\pm$ on $\tan \beta$.

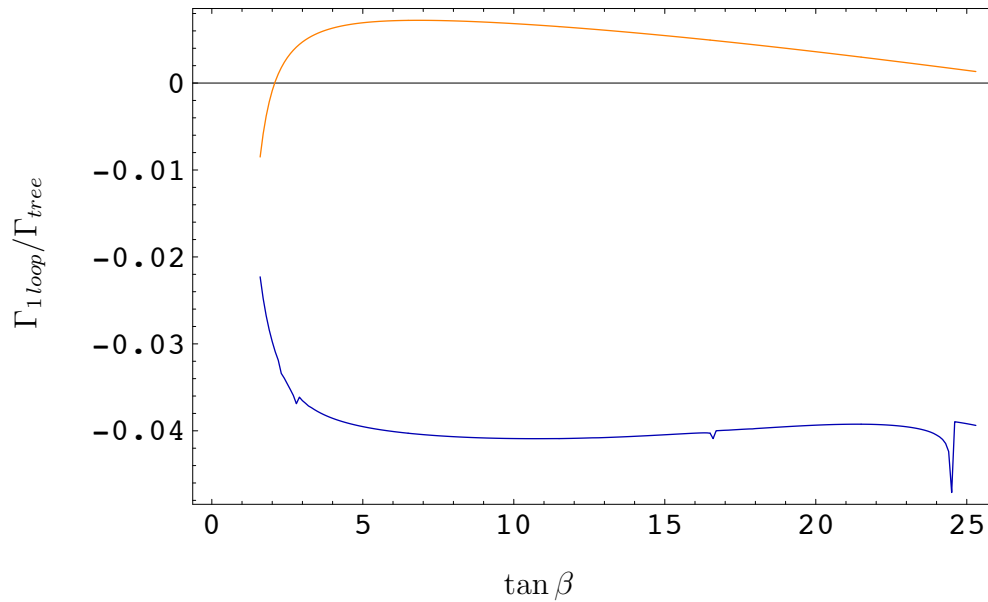


Figure 6.35: The dependence of the electroweak and the QCD corrections to the total decay width of the $\tilde{\chi}_2^\pm$ on $\tan \beta$.

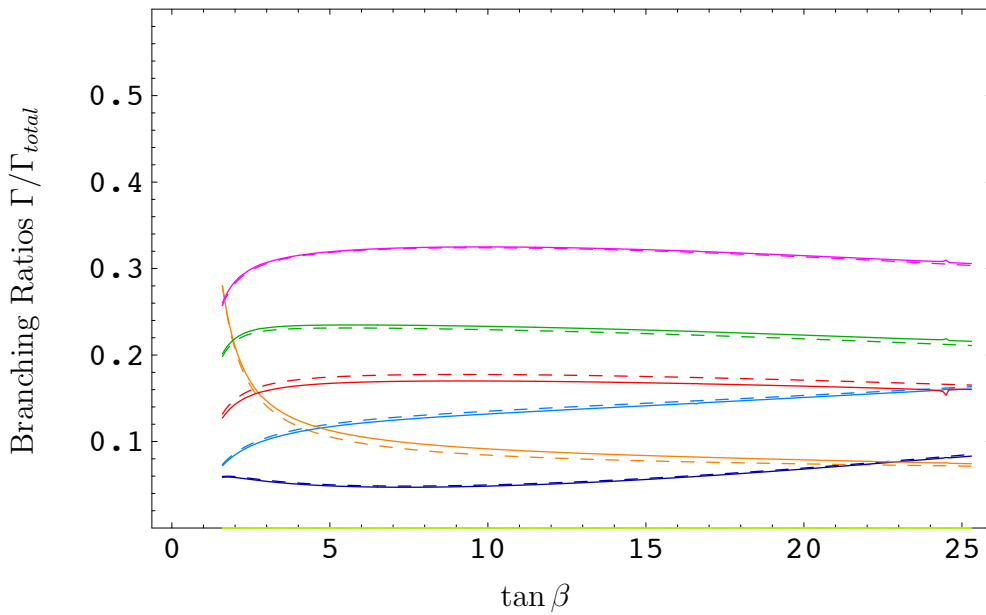


Figure 6.36: The dependence of the branching ratios of $\tilde{\chi}_2^\pm$ on $\tan \beta$.

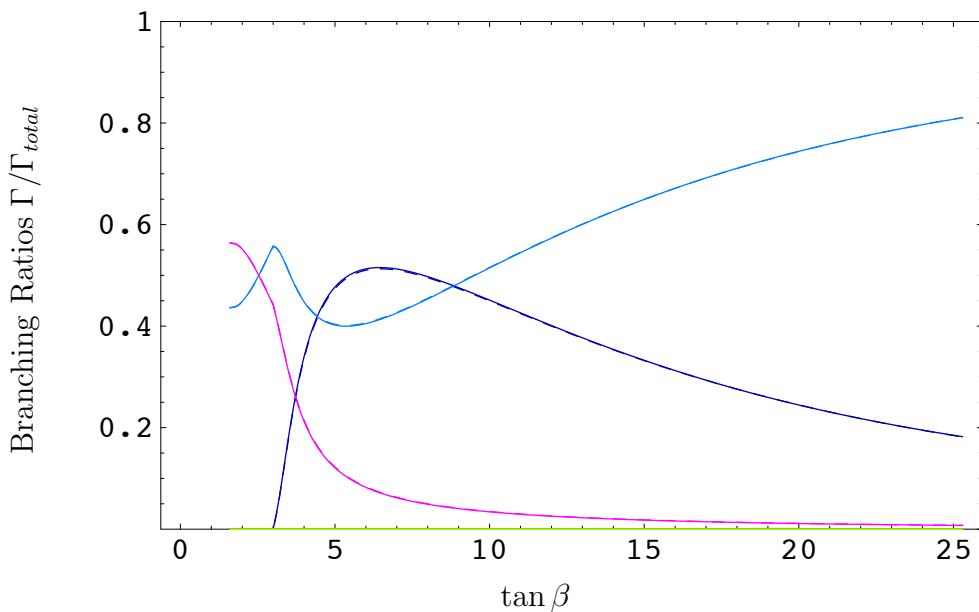


Figure 6.37: The dependence of the branching ratios of $\tilde{\chi}_1^\pm$ on $\tan \beta$.

Appendix A

Tree-level Couplings and Counterterms

Following we list the treelevel couplings and the corresponding counterterms. The mixing matrices U_{ij} , V_{ij} , N_{ij} and R_{ij} are defined in Chapter 2. The complex conjugated of δZ is denoted by δZ^C . Generic forms of all counterterms may be found in Chapter 3.

Tab.A.1 can be used to find the generic forms of the counterterms in Chapter 3 by the equation reference numbers.

Counterterm	Equation	Counterterm	Equation
$\delta m(\text{fermion})$	3.22	$\delta R_{ij}^{\tilde{f}}$	3.36
$\delta Z_{ij}^{L,R}(\text{fermion})$	3.23	$\delta R_{ij}^{\tilde{f}}$	3.36
$\delta Z_{ii}^{L,R}(\text{fermion})$	3.24	$\delta \tan \beta$	3.41
$\delta U_{ij}, \delta V_{ij}$	3.25	$\delta Z(\text{vector})$	3.53
δN_{ij}	3.26	$\delta m(\text{vector})$	3.54
$\delta m(\text{scalar})$	3.33	$\delta \cos \theta_W$	3.55
$\delta Z_{ij}(\text{scalar})$	3.34	$\delta \sin \theta_W$	3.55
$\delta Z_{ii}(\text{scalar})$	3.35	δe	3.61

Table A.1: References of the generic forms of the counterterms.

$$A_{ij}^R = -\frac{g}{2m_W \cos \beta} (2\cos \beta m_W R_{j1}^{\tilde{b}*} U_{i1} - \sqrt{2} R_{j2}^{\tilde{b}*} m_b U_{i2}) \quad (\text{A.1})$$

$$\begin{aligned} \delta A_{ij}^R &= -\frac{g}{2m_W \cos \beta} \left((2\cos \beta m_W R_{j1}^{\tilde{b}*} \delta U_{i1} - \sqrt{2} R_{j2}^{\tilde{b}*} m_b \delta U_{i2}) \right. \\ &\quad + (2\cos \beta m_W \delta R_{j1}^{\tilde{b}*} U_{i1} - \sqrt{2} \delta R_{j2}^{\tilde{b}*} m_b U_{i2}) \\ &\quad + (2\cos \beta m_W R_{j1}^{\tilde{b}*} U_{i1} - \sqrt{2} R_{j2}^{\tilde{b}*} m_b U_{i2}) \left(\frac{\delta e}{e} - \frac{\delta \sin \theta_W}{\sin \theta_W} \right) \\ &\quad + (-\sqrt{2} R_{j2}^{\tilde{b}*} m_b U_{i2}) \left(\frac{\delta m_b}{m_b} - \frac{\delta \cos \beta}{\cos \beta} - \frac{\delta m_W}{m_W} \right) \\ &\quad + \sum_{n=1}^2 \frac{1}{2} \delta Z_{ni}^R(\tilde{\chi}^+) (2\cos \beta m_W R_{j1}^{\tilde{b}*} U_{n1} - \sqrt{2} R_{j2}^{\tilde{b}*} m_b U_{n2}) \\ &\quad + \frac{1}{2} \delta Z^L(t)^C (2\cos \beta m_W R_{j1}^{\tilde{b}*} U_{i1} - \sqrt{2} R_{j2}^{\tilde{b}*} m_b U_{i2}) \\ &\quad \left. + \sum_{s=1}^2 \frac{1}{2} \delta Z_{sj}(\tilde{b}) (2\cos \beta m_W R_{s1}^{\tilde{b}*} U_{i1} - \sqrt{2} R_{s2}^{\tilde{b}*} m_b U_{i2}) \right) \quad (\text{A.2}) \end{aligned}$$

$$A_{ij}^L = \frac{g}{\sqrt{2} m_W \sin \beta} V_{i2}^* R_{j1}^{\tilde{b}*} m_t \quad (\text{A.3})$$

$$\begin{aligned} \delta A_{ij}^L &= \frac{g}{\sqrt{2} m_W \sin \beta} \left(\delta V_{i2}^* R_{j1}^{\tilde{b}*} m_t + V_{i2}^* \delta R_{j1}^{\tilde{b}*} m_t \right. \\ &\quad + V_{i2}^* R_{j1}^{\tilde{b}*} m_t \left(\frac{\delta e}{e} - \frac{\delta \sin \theta_W}{\sin \theta_W} - \frac{\delta m_W}{m_W} - \frac{\sin \beta}{\sin \beta} + \frac{\delta m_t}{m_t} \right) \\ &\quad + \sum_{n=1}^2 \frac{1}{2} \delta Z_{ni}^L(\tilde{\chi}^+) V_{n2}^* R_{j1}^{\tilde{b}*} m_t + \frac{1}{2} \delta Z^R(t)^C V_{i2}^* R_{j1}^{\tilde{b}*} m_t \\ &\quad \left. + \sum_{s=1}^2 \frac{1}{2} \delta Z_{sj}(\tilde{b}) V_{i2}^* R_{s1}^{\tilde{b}*} m_t \right) \quad (\text{A.4}) \end{aligned}$$

$$B_{ij}^R = \frac{g}{\sqrt{2} m_W \sin \beta} (2m_W \sin \beta V_{i1} R_{j1}^{\tilde{t}*} - \sqrt{2} V_{i2} m_t R_{j2}^{\tilde{t}*}) \quad (\text{A.5})$$

$$\begin{aligned} \delta B_{ij}^R &= \frac{g}{\sqrt{2} m_W \sin \beta} \left(2m_W \sin \beta \delta V_{i1} R_{j1}^{\tilde{t}*} - \sqrt{2} \delta V_{i2} m_t R_{j2}^{\tilde{t}*} \right. \\ &\quad + 2m_W \sin \beta V_{i1} \delta R_{j1}^{\tilde{t}*} - \sqrt{2} V_{i2} m_t \delta R_{j2}^{\tilde{t}*} \\ &\quad + (2m_W \sin \beta V_{i1} R_{j1}^{\tilde{t}*} - \sqrt{2} V_{i2} m_t R_{j2}^{\tilde{t}*}) \left(\frac{\delta e}{e} - \frac{\delta \sin \theta_W}{\sin \theta_W} \right) \\ &\quad + (-\sqrt{2} V_{i2} m_t R_{j2}^{\tilde{t}*}) \left(\frac{\delta m_t}{m_t} - \frac{\delta \sin \beta}{\sin \beta} - \frac{\delta m_W}{m_W} \right) \\ &\quad + \sum_{n=1}^2 \frac{1}{2} \delta Z_{ni}^L (\tilde{\chi}^+)^C (2m_W \sin \beta V_{n1} R_{j1}^{\tilde{t}*} - \sqrt{2} V_{n2} m_t R_{j2}^{\tilde{t}*}) \\ &\quad + \frac{1}{2} \delta Z^L(b)^C (2m_W \sin \beta V_{i1} R_{j1}^{\tilde{t}*} - \sqrt{2} V_{i2} m_t R_{j2}^{\tilde{t}*}) \\ &\quad \left. + \sum_{s=1}^2 \frac{1}{2} \delta Z_{sj}(\tilde{t}) (2m_W \sin \beta V_{i1} R_{s1}^{\tilde{t}*} - \sqrt{2} V_{i2} m_t R_{s2}^{\tilde{t}*}) \right) \end{aligned} \quad (\text{A.6})$$

$$B_{ij}^L = \frac{g}{\sqrt{2} m_W \cos \beta} (m_b U_{i2}^* R_{j1}^{\tilde{t}*} + m_b U_{i2}^* R_{j1}^{\tilde{t}*}) \quad (\text{A.7})$$

$$\begin{aligned} \delta B_{ij}^L &= \frac{g}{\sqrt{2} m_W \cos \beta} \left(m_b \delta U_{i2}^* R_{j1}^{\tilde{t}*} + m_b U_{i2}^* \delta R_{j1}^{\tilde{t}*} \right. \\ &\quad + m_b U_{i2}^* R_{j1}^{\tilde{t}*} \left(\frac{\delta e}{e} - \frac{\delta \sin \theta_W}{\sin \theta_W} - \frac{\delta m_W}{m_W} - \frac{\cos \beta}{\cos \beta} + \frac{\delta m_b}{m_b} \right) \\ &\quad + \sum_{n=1}^2 \frac{1}{2} \delta Z_{ni}^R (\tilde{\chi}^+)^C m_b U_{n2}^* R_{j1}^{\tilde{t}*} \\ &\quad + \frac{1}{2} \delta Z^R(b)^C m_b U_{i2}^* R_{j1}^{\tilde{t}*} \\ &\quad \left. + \sum_{s=1}^2 \frac{1}{2} \delta Z_{sj}(\tilde{t}) m_b U_{i2}^* R_{s1}^{\tilde{t}*} \right) \end{aligned} \quad (\text{A.8})$$

$$\begin{aligned}
C_{lj}^R &= -\frac{g}{3\sqrt{2}\cos\theta_W m_W \sin\beta} \\
&\quad (m_W \sin\beta \sin\theta_W N_{l1} R_{j1}^{\tilde{t}*} + 3\cos\theta_W (m_W \sin\beta N_{l2} R_{j1}^{\tilde{t}*} + N_{l4} m_t R_{j2}^{\tilde{t}*})) \tag{A.9}
\end{aligned}$$

$$\begin{aligned}
\delta C_{lj}^R &= -\frac{g}{3\sqrt{2}\cos\theta_W m_W \sin\beta} \\
&\quad (m_W \sin\beta \sin\theta_W \delta N_{l1} R_{j1}^{\tilde{t}*} + 3\cos\theta_W (m_W \sin\beta \delta N_{l2} R_{j1}^{\tilde{t}*} + \delta N_{l4} m_t R_{j2}^{\tilde{t}*})) \\
&+ m_W \sin\beta \sin\theta_W N_{l1} \delta R_{j1}^{\tilde{t}*} + 3\cos\theta_W (m_W \sin\beta N_{l2} \delta R_{j1}^{\tilde{t}*} + N_{l4} m_t \delta R_{j2}^{\tilde{t}*}) \\
&+ m_W \sin\beta \sin\theta_W \frac{-\delta \cos\theta_W}{\cos\theta_W} N_{l1} R_{j1}^{\tilde{t}*} \\
&+ 3\cos\theta_W (m_W \sin\beta \frac{-\delta \sin\theta_W}{\sin\theta_W} N_{l2} R_{j1}^{\tilde{t}*} + (-\frac{\delta m_W}{m_W} - \frac{\delta \sin\beta}{\sin\beta} - \frac{\delta \sin\theta_W}{\sin\theta_W} + \frac{\delta m_t}{m_t}) N_{l4} m_t R_{j2}^{\tilde{t}*}) \\
&+ m_W \sin\beta \sin\theta_W N_{l1} R_{j1}^{\tilde{t}*} + 3\cos\theta_W (m_W \sin\beta N_{l2} R_{j1}^{\tilde{t}*} + N_{l4}^* m_t R_{j2}^{\tilde{t}*})(\frac{\delta e}{e}) \\
&+ \sum_{k=1}^4 \frac{1}{2} \delta Z_{kl}^R(\tilde{\chi}^0) [m_W \sin\beta \sin\theta_W N_{k1} R_{j1}^{\tilde{t}*} + 3\cos\theta_W (m_W \sin\beta N_{k2} R_{j1}^{\tilde{t}*} + N_{k4} m_t R_{j2}^{\tilde{t}*})] \\
&+ \sum_{s=1}^2 \frac{1}{2} \delta Z_{sj}(\tilde{t}) [m_W \sin\beta \sin\theta_W N_{l1} R_{s1}^{\tilde{t}*} + 3\cos\theta_W (m_W \sin\beta N_{l2} R_{s1}^{\tilde{t}*} + N_{l4} m_t R_{s2}^{\tilde{t}*})] \\
&+ \frac{1}{2} \delta Z^L(t)^C [m_W \sin\beta \sin\theta_W N_{l1} R_{j1}^{\tilde{t}*} + 3\cos\theta_W (m_W \sin\beta N_{l2} R_{j1}^{\tilde{t}*} + N_{l4} m_t R_{j2}^{\tilde{t}*})] \tag{A.10}
\end{aligned}$$

$$C_{lj}^L = -\frac{g}{3\sqrt{2}\cos\theta_W m_W \sin\beta} (-3\cos\theta_W m_t N_{l4}^* R_{j1}^{\tilde{t}*} + 4m_W \sin\beta \sin\theta_W N_{l1}^* R_{j2}^{\tilde{t}*}) \tag{A.11}$$

$$\begin{aligned}
\delta C_{lj}^L &= -\frac{g}{3\sqrt{2}\cos\theta_W m_W \sin\beta} (-3\cos\theta_W m_t \delta N_{l4}^* R_{j1}^{\tilde{t}*} + 4m_W \sin\beta \sin\theta_W \delta N_{l1}^* R_{j2}^{\tilde{t}*}) \\
&+ -3\cos\theta_W m_t N_{l4}^* \delta R_{j1}^{\tilde{t}*} + 4m_W \sin\beta \sin\theta_W N_{l1}^* \delta R_{j2}^{\tilde{t}*} \\
&+ -3\cos\theta_W (-\frac{\delta m_W}{m_W} - \frac{\delta \sin\beta}{\sin\beta} - \frac{\delta \sin\theta_W}{\sin\theta_W} + \frac{\delta m_t}{m_t}) m_t N_{l4}^* R_{j1}^{\tilde{t}*} \\
&+ 4m_W \sin\beta \sin\theta_W (-\frac{\delta \cos\theta_W}{\cos\theta_W}) N_{l1}^* R_{j2}^{\tilde{t}*} \\
&+ (-3\cos\theta_W m_t N_{l4}^* R_{j1}^{\tilde{t}*} + 4m_W \sin\beta \sin\theta_W N_{l1}^* R_{j2}^{\tilde{t}*})(\frac{\delta e}{e}) \\
&+ \sum_{k=1}^4 \frac{1}{2} \delta Z_{kl}^L(\tilde{\chi}^0)^C [-3\cos\theta_W m_t N_{k4}^* R_{j1}^{\tilde{t}*} + 4m_W \sin\beta \sin\theta_W N_{k1}^* R_{j2}^{\tilde{t}*}] \\
&+ \sum_{s=1}^2 \frac{1}{2} \delta Z_{sj}(\tilde{t}) [-3\cos\theta_W m_t N_{l4}^* R_{s1}^{\tilde{t}*} + 4m_W \sin\beta \sin\theta_W N_{l1}^* R_{s2}^{\tilde{t}*}] \\
&+ \frac{1}{2} \delta Z^R(t)^C [-3\cos\theta_W m_t N_{l4}^* R_{j1}^{\tilde{t}*} + 4m_W \sin\beta \sin\theta_W N_{l1}^* R_{j2}^{\tilde{t}*}] \tag{A.12}
\end{aligned}$$

$$\begin{aligned} D_{lk}^R &= -\frac{g}{3\sqrt{2}\cos\beta\cos\theta_W m_W} \left(-\cos\beta m_W \sin\theta_W N_{l1} R_{k1}^{\tilde{b}*} + 3\cos\theta_W (\cos\beta m_W N_{l2} R_{k1}^{\tilde{b}*} - N_{l3} m_b R_{k2}^{\tilde{b}*}) \right) \end{aligned} \quad (\text{A.13})$$

$$\begin{aligned} \delta D_{lk}^R &= -\frac{g}{3\sqrt{2}\cos\beta\cos\theta_W m_W} \left(-\cos\beta m_W \sin\theta_W \delta N_{l1} R_{k1}^{\tilde{b}*} + 3\cos\theta_W (\cos\beta m_W \delta N_{l2} R_{k1}^{\tilde{b}*} - \delta N_{l3} m_b R_{k2}^{\tilde{b}*}) \right. \\ &+ -\cos\beta m_W \sin\theta_W N_{l1} \delta R_{k1}^{\tilde{b}*} + 3\cos\theta_W (\cos\beta m_W N_{l2} \delta R_{k1}^{\tilde{b}*} - N_{l3} m_b \delta R_{k2}^{\tilde{b}*}) \\ &+ -\cos\beta m_W \sin\theta_W \left(-\frac{\delta\cos\theta_W}{\cos\theta_W}\right) N_{l1} R_{k1}^{\tilde{b}*} \\ &+ 3\cos\theta_W \left(\cos\beta m_W \left(-\frac{\delta\sin\theta_W}{\sin\theta_W}\right) N_{l2} R_{k1}^{\tilde{b}*} - \left(-\frac{\delta m_W}{m_W} - \frac{\delta\cos\beta}{\cos\beta} - \frac{\delta\sin\theta_W}{\sin\theta_W} + \frac{\delta m_b}{m_b}\right) N_{l3} m_b R_{k2}^{\tilde{b}*}\right) \\ &+ \left(-\cos\beta m_W \sin\theta_W N_{l1} R_{k1}^{\tilde{b}*} + 3\cos\theta_W (\cos\beta m_W N_{l2} R_{k1}^{\tilde{b}*} - N_{l3} m_b R_{k2}^{\tilde{b}*})\right) \left(\frac{\delta e}{e}\right) \\ &+ \sum_{n=1}^4 \frac{1}{2} \delta Z_{nl}^R(\tilde{\chi}^0) \left[-\cos\beta m_W \sin\theta_W N_{n1} R_{k1}^{\tilde{b}*} + 3\cos\theta_W (\cos\beta m_W N_{n2} R_{n1}^{\tilde{b}*} - N_{l3} m_b R_{k2}^{\tilde{b}*}) \right] \\ &+ \sum_{s=1}^2 \frac{1}{2} \delta Z_{sk}(\tilde{b}) \left[-\cos\beta m_W \sin\theta_W N_{l1} R_{s1}^{\tilde{b}*} + 3\cos\theta_W (\cos\beta m_W N_{l2} R_{s1}^{\tilde{b}*} - N_{l3} m_b R_{s2}^{\tilde{b}*}) \right] \\ &\left. + \frac{1}{2} \delta Z^L(b)^C \left[-\cos\beta m_W \sin\theta_W N_{l1} R_{k1}^{\tilde{b}*} + 3\cos\theta_W (\cos\beta m_W N_{l2} R_{k1}^{\tilde{b}*} - N_{l3} m_b R_{k2}^{\tilde{b}*}) \right] \right) \end{aligned} \quad (\text{A.14})$$

$$D_{lk}^L = -\frac{g}{3\sqrt{2}\cos\beta\cos\theta_W m_W} \left(3\cos\theta_W m_b N_{l3}^* R_{k1}^{\tilde{b}*} + 2\cos\beta m_W \sin\theta_W N_{l1}^* R_{k2}^{\tilde{b}*} \right) \quad (\text{A.15})$$

$$\begin{aligned} \delta D_{lk}^L &= -\frac{g}{3\sqrt{2}\cos\beta\cos\theta_W m_W} \left(3\cos\theta_W m_b \delta N_{l3}^* R_{k1}^{\tilde{b}*} + 2\cos\beta m_W \sin\theta_W \delta N_{l1}^* R_{k2}^{\tilde{b}*} \right. \\ &+ 3\cos\theta_W m_b N_{l3}^* \delta R_{k1}^{\tilde{b}*} + 2\cos\beta m_W \sin\theta_W N_{l1}^* \delta R_{k2}^{\tilde{b}*} \\ &+ 3\cos\theta_W \left(-\frac{\delta m_W}{m_W} - \frac{\delta\cos\beta}{\cos\beta} - \frac{\delta\sin\theta_W}{\sin\theta_W} + \frac{\delta m_b}{m_b}\right) m_b N_{l3}^* \delta R_{k1}^{\tilde{b}*} \\ &+ 2\cos\beta m_W \sin\theta_W \left(-\frac{\delta\cos\theta_W}{\cos\theta_W}\right) N_{l1}^* \delta R_{k2}^{\tilde{b}*} \\ &+ \left(3\cos\theta_W m_b N_{l3}^* R_{k1}^{\tilde{b}*} + 2\cos\beta m_W \sin\theta_W N_{l1}^* R_{k2}^{\tilde{b}*}\right) \left(\frac{\delta e}{e}\right) \\ &+ \sum_{n=1}^4 \frac{1}{2} \delta Z_{nl}^L(\tilde{\chi}^0) \left[3\cos\theta_W m_b N_{n3}^* R_{k1}^{\tilde{b}*} + 2\cos\beta m_W \sin\theta_W N_{n1}^* R_{k2}^{\tilde{b}*} \right] \\ &+ \sum_{s=1}^2 \frac{1}{2} \delta Z_{sk}(\tilde{b}) \left[3\cos\theta_W m_b N_{l3}^* R_{s1}^{\tilde{b}*} + 2\cos\beta m_W \sin\theta_W N_{l1}^* R_{s2}^{\tilde{b}*} \right] \\ &\left. + \frac{1}{2} \delta Z^R(b)^C \left[3\cos\theta_W m_b N_{l3}^* R_{k1}^{\tilde{b}*} + 2\cos\beta m_W \sin\theta_W N_{l1}^* R_{k2}^{\tilde{b}*} \right] \right) \end{aligned} \quad (\text{A.16})$$

$$A_{is}'^R = \frac{g}{2}(-2R_{s2}^{\tilde{\tau}*}U_{i1} + \frac{\sqrt{2}}{\cos\beta m_W}R_{s2}^{\tilde{\tau}*}m_\tau U_{i2}) \quad (\text{A.17})$$

$$\begin{aligned} \delta A_{is}'^R = & \frac{g}{2}(-2R_{s2}^{\tilde{\tau}*}\delta U_{i1} + \frac{\sqrt{2}}{\cos\beta m_W}R_{s2}^{\tilde{\tau}*}m_\tau\delta U_{i2}) \\ & + \frac{g}{2}(-2\delta R_{s2}^{\tilde{\tau}*}U_{i1} + \frac{\sqrt{2}}{\cos\beta m_W}\delta R_{s2}^{\tilde{\tau}*}m_\tau U_{i2}) \\ & + \frac{g}{2}(-2R_{s2}^{\tilde{\tau}*}U_{i1} + \frac{\sqrt{2}}{\cos\beta m_W}R_{s2}^{\tilde{\tau}*}m_\tau U_{i2})(\frac{\delta e}{e} - \frac{\delta \sin\theta_W}{\sin\theta_W}) \\ & + \frac{g}{2}(\frac{\sqrt{2}}{\cos\beta m_W}R_{s2}^{\tilde{\tau}*}m_\tau U_{i2})(\frac{\delta m_\tau}{m_\tau} - \frac{\delta m_W}{m_W} - \frac{\delta \cos\beta}{\cos\beta}) \\ & + \frac{g}{2}\sum_{n=1}^2 \frac{1}{2}\delta Z_{ni}^R(\tilde{\chi}^+)(-2R_{s2}^{\tilde{\tau}*}U_{n1} + \frac{\sqrt{2}}{\cos\beta m_W}R_{s2}^{\tilde{\tau}*}m_\tau U_{n2}) \\ & + \frac{g}{2}\frac{1}{2}\delta Z^L(\tau)^C(-2R_{s2}^{\tilde{\tau}*}U_{i1} + \frac{\sqrt{2}}{\cos\beta m_W}R_{s2}^{\tilde{\tau}*}m_\tau U_{i2}) \\ & + \frac{g}{2}\sum_{n=1}^2 \frac{1}{2}\delta Z_{ns}(\tilde{\tau})(-2R_{n2}^{\tilde{\tau}*}U_{i1} + \frac{\sqrt{2}}{\cos\beta m_W}R_{n2}^{\tilde{\tau}*}m_\tau U_{i2}) \end{aligned} \quad (\text{A.18})$$

$$A_{is}'^L = 0 \quad (\text{A.19})$$

$$\delta A_{is}'^L = 0 \quad (\text{A.20})$$

$$B_i'^R = -gV_{i1} \quad (\text{A.21})$$

$$\begin{aligned} \delta B_i'^R = & -g\delta V_{i1} - gV_{i1}(\frac{\delta e}{e} - \frac{\delta \sin\theta_W}{\sin\theta_W}) \\ & - g\sum_{k=1}^2 \frac{1}{2}\delta Z_{ki}^L(\tilde{\chi}^+)^C V_{k1} \\ & - g\frac{1}{2}\delta Z^{L*}(\tau)V_{i1} \\ & - g\frac{1}{2}\delta Z(\tilde{\nu})V_{i1} \end{aligned} \quad (\text{A.22})$$

$$B_i'^L = \frac{gm_\tau}{\sqrt{2}m_W \cos \beta} U_{i2}^* \quad (\text{A.23})$$

$$\begin{aligned} \delta B_i'^L &= \frac{gm_\tau}{\sqrt{2}m_W \cos \beta} \delta U_{i2}^* \\ &+ \frac{gm_\tau}{\sqrt{2}m_W \cos \beta} U_{i2}^* \left(\frac{\delta e}{e} - \frac{\delta \sin \theta_W}{\sin \theta_W} - \frac{\delta \cos \beta}{\cos \beta} + \frac{\delta m_\tau}{m_\tau} - \frac{\delta m_W}{m_W} \right) \\ &+ \frac{gm_\tau}{\sqrt{2}m_W \cos \beta} \sum_{k=1}^2 \frac{1}{2} \delta Z_{ki}^R (\tilde{\chi}^+)^C U_{k2}^* \\ &+ \frac{gm_\tau}{\sqrt{2}m_W \cos \beta} \frac{1}{2} \delta Z^{R*}(\tau) V_{i1} \\ &+ \frac{gm_\tau}{\sqrt{2}m_W \cos \beta} \frac{1}{2} \delta Z(\tilde{\nu}) V_{i1} \end{aligned} \quad (\text{A.24})$$

$$C_l'^R = \frac{g}{\sqrt{2} \cos \theta_W} (\sin \theta_W N_{l1} - \cos \theta_W N_{l2}) \quad (\text{A.25})$$

$$\begin{aligned} \delta C_l'^R &= \frac{g}{\sqrt{2} \cos \theta_W} (\sin \theta_W \delta N_{l1} - \cos \theta_W \delta N_{l2}) \\ &+ \frac{g}{\sqrt{2} \cos \theta_W} (\sin \theta_W N_{l1} (-\frac{\delta \cos \theta_W}{\cos \theta_W}) - \cos \theta_W N_{l2} (-\frac{\delta \sin \theta_W}{\sin \theta_W})) \\ &+ \frac{g}{\sqrt{2} \cos \theta_W} (\sin \theta_W N_{l1} - \cos \theta_W N_{l2}) (\frac{\delta e}{e}) \\ &+ \frac{g}{\sqrt{2} \cos \theta_W} \sum_{k=1}^4 \frac{1}{2} \delta Z_{kl}^R (\tilde{\chi}^0) (\sin \theta_W N_{l1} - \cos \theta_W N_{l2}) \\ &+ \frac{g}{\sqrt{2} \cos \theta_W} \frac{1}{2} \delta Z^L(\nu)^C (\sin \theta_W N_{l1} - \cos \theta_W N_{l2}) \\ &+ \frac{g}{\sqrt{2} \cos \theta_W} \frac{1}{2} \delta Z(\tilde{\nu}) (\sin \theta_W N_{l1} - \cos \theta_W N_{l2}) \end{aligned} \quad (\text{A.26})$$

$$C_l'^L = 0 \quad (\text{A.27})$$

$$\delta C_l'^L = 0 \quad (\text{A.28})$$

$$D_{ls}'^R = \frac{g}{\sqrt{2}} \left[-\frac{m_\tau}{m_W \cos \beta} N_{l3} R_{s2}^{\tilde{\tau}*} + (N_{l2} + \tan \theta_W \delta N_{l1}) R_{s1}^{\tilde{\tau}*} \right] \quad (\text{A.29})$$

$$\begin{aligned} \delta D_{ls}'^R &= \frac{g}{\sqrt{2}} \left[-\frac{m_\tau}{m_W \cos \beta} \delta N_{l3} R_{s2}^{\tilde{\tau}*} + (\delta N_{l2} + \tan \theta_W \delta N_{l1}) R_{s1}^{\tilde{\tau}*} \right] \\ &+ \frac{g}{\sqrt{2}} \left[-\frac{m_\tau}{m_W \cos \beta} N_{l3} \delta R_{s2}^{\tilde{\tau}*} + (N_{l2} + \tan \theta_W N_{l1}) \delta R_{s1}^{\tilde{\tau}*} \right] \end{aligned}$$

$$\begin{aligned}
& + \frac{g}{\sqrt{2}} \left[-\frac{m_\tau}{m_W \cos \beta} N_{l3} R_{s2}^{\tilde{\tau}*} \left(\frac{\delta m_\tau}{m_\tau} - \frac{\delta m_W}{m_W} - \frac{\delta \cos \beta}{\cos \beta} - \frac{\delta \sin \theta_W}{\sin \theta_W} \right) \right. \\
& \quad \left. + \left(-\frac{\delta \sin \theta_W}{\sin \theta_W} N_{l2} - \frac{\delta \cos \theta_W}{\cos \theta_W} \tan \theta_W N_{l1} \right) R_{s1}^{\tilde{\tau}*} \right] \\
& + \frac{g}{\sqrt{2}} \left[-\frac{m_\tau}{m_W \cos \beta} N_{l3} R_{s2}^{\tilde{\tau}*} + (N_{l2} + \tan \theta_W N_{l1}) R_{s1}^{\tilde{\tau}*} \right] \frac{\delta e}{e} \\
& + \frac{g}{\sqrt{2}} \sum_{k=1}^4 \frac{1}{2} \delta Z_{kl}^R(\tilde{\chi}^0) \left[-\frac{m_\tau}{m_W \cos \beta} N_{k3} R_{s2}^{\tilde{\tau}*} + (N_{k2} + \tan \theta_W N_{k1}) R_{s1}^{\tilde{\tau}*} \right] \\
& + \frac{g}{\sqrt{2}} \sum_{k=1}^4 \frac{1}{2} \delta Z_{is}(\tilde{\tau}) \left[-\frac{m_\tau}{m_W \cos \beta} N_{l3} R_{i2}^{\tilde{\tau}*} + (N_{l2} + \tan \theta_W N_{l1}) R_{i1}^{\tilde{\tau}*} \right] \\
& + \frac{g}{\sqrt{2}} \frac{1}{2} \delta Z^L(\tau)^C \left[-\frac{m_\tau}{m_W \cos \beta} N_{l3} R_{s2}^{\tilde{\tau}*} + (N_{l2} + \tan \theta_W N_{l1}) R_{s1}^{\tilde{\tau}*} \right]
\end{aligned} \tag{A.30}$$

$$D'_{ls}^L = \frac{g}{\sqrt{2}} \left[-\frac{m_\tau}{m_W \cos \beta} N_{l3}^* R_{s1}^{\tilde{\tau}*} - 2 \tan \theta_W N_{l1}^* R_{s2}^{\tilde{\tau}*} \right] \tag{A.31}$$

$$\begin{aligned}
\delta D'_{ls}^L & = \frac{g}{\sqrt{2}} \left[-\frac{m_\tau}{m_W \cos \beta} \delta N_{l3}^* R_{s1}^{\tilde{\tau}*} - 2 \tan \theta_W \delta N_{l1}^* R_{s2}^{\tilde{\tau}*} \right] \\
& + \frac{g}{\sqrt{2}} \left[-\frac{m_\tau}{m_W \cos \beta} N_{l3}^* \delta R_{s1}^{\tilde{\tau}*} - 2 \tan \theta_W N_{l1}^* \delta R_{s2}^{\tilde{\tau}*} \right] \\
& + \frac{g}{\sqrt{2}} \left[-\frac{m_\tau}{m_W \cos \beta} N_{l3}^* R_{s1}^{\tilde{\tau}*} \left(\frac{\delta m_\tau}{m_\tau} - \frac{\delta m_W}{m_W} - \frac{\delta \cos \beta}{\cos \beta} - \frac{\delta \sin \theta_W}{\sin \theta_W} \right) \right. \\
& \quad \left. - 2 \frac{\delta \cos \beta}{\cos \beta} \tan \theta_W N_{l1}^* R_{s2}^{\tilde{\tau}*} \right] \\
& + \frac{g}{\sqrt{2}} \left[-\frac{m_\tau}{m_W \cos \beta} N_{l3}^* R_{s1}^{\tilde{\tau}*} - 2 \tan \theta_W N_{l1}^* R_{s2}^{\tilde{\tau}*} \right] \frac{\delta e}{e} \\
& + \frac{g}{\sqrt{2}} \sum_{k=1}^4 \frac{1}{2} \delta Z_{kl}^L(\tilde{\chi}^0) \left[-\frac{m_\tau}{m_W \cos \beta} N_{k3}^* R_{s1}^{\tilde{\tau}*} - 2 \tan \theta_W N_{k1}^* R_{s2}^{\tilde{\tau}*} \right] \\
& + \frac{g}{\sqrt{2}} \sum_{i=1}^2 \frac{1}{2} \delta Z_{is}(\tilde{\tau}) \left[-\frac{m_\tau}{m_W \cos \beta} N_{l3}^* R_{i1}^{\tilde{\tau}*} - 2 \tan \theta_W N_{l1}^* R_{i2}^{\tilde{\tau}*} \right] \\
& + \frac{g}{\sqrt{2}} \frac{1}{2} \delta Z^R(\tau)^C \left[-\frac{m_\tau}{m_W \cos \beta} N_{l3}^* R_{s1}^{\tilde{\tau}*} - 2 \tan \theta_W N_{l1}^* R_{s2}^{\tilde{\tau}*} \right]
\end{aligned} \tag{A.32}$$

$$E_{kl}^R = g(U_{k1}N_{l2}^* + \frac{1}{\sqrt{2}}U_{k2}N_{l3}^*) \quad (\text{A.33})$$

$$\begin{aligned} \delta E_{kl}^R &= g(U_{k1}\delta N_{l2}^* + \frac{1}{\sqrt{2}}U_{k2}\delta N_{l3}^*) \\ &+ g(\delta U_{k1}N_{l2}^* + \frac{1}{\sqrt{2}}\delta U_{k2}N_{l3}^*) \\ &+ g(U_{k1}N_{l2}^* + U_{k2}N_{l3}^*)(\frac{\delta e}{e} - \frac{\delta \sin \theta_W}{\sin \theta_W}) \\ &+ g \sum_{j=1}^2 \frac{1}{2} \delta Z_{jk}^R(\tilde{\chi}^+)(U_{k1}N_{l2}^* + \frac{1}{\sqrt{2}}U_{k2}N_{l3}^*) \\ &+ g \sum_{i=1}^4 \frac{1}{2} \delta Z_{il}^L(\tilde{\chi}^0)^C(U_{k1}N_{l2}^* + \frac{1}{\sqrt{2}}U_{k2}N_{l3}^*) \\ &+ g \frac{1}{2} \delta Z(W^+)^C(U_{k1}N_{l2}^* + U_{k2}N_{l3}^*) \end{aligned} \quad (\text{A.34})$$

$$E_{kl}^L = g(N_{l2}V_{k1}^* - \frac{1}{\sqrt{2}}N_{l4}V_{k2}^*) \quad (\text{A.35})$$

$$\begin{aligned} \delta E_{kl}^L &= g(\delta N_{l2}V_{k1}^* - \frac{1}{\sqrt{2}}\delta N_{l4}V_{k2}^*) \\ &+ g(N_{l2}\delta V_{k1}^* - \frac{1}{\sqrt{2}}N_{l4}\delta V_{k2}^*) \\ &+ g(N_{l2}V_{k1}^* - \frac{1}{\sqrt{2}}N_{l4}V_{k2}^*)(\frac{\delta e}{e} - \frac{\delta \sin \theta_W}{\sin \theta_W}) \\ &+ g \sum_{j=1}^2 \frac{1}{2} \delta Z_{jk}^L(\tilde{\chi}^+)([N_{l2}V_{j1}^* - \frac{1}{\sqrt{2}}N_{l4}V_{j2}^*]) \\ &+ g \sum_{i=1}^4 \frac{1}{2} \delta Z_{il}^R(\tilde{\chi}^0)^C(N_{i2}V_{k1}^* - \frac{1}{\sqrt{2}}N_{i4}V_{k2}^*) \\ &+ g \frac{1}{2} \delta Z(W^+)^C(N_{l2}V_{k1}^* - \frac{1}{\sqrt{2}}N_{l4}V_{k2}^*) \end{aligned} \quad (\text{A.36})$$

$$E_{lk}^{0R} = -\frac{g}{2\cos\theta_W} (N_{l4}^* N_{k4} - N_{l3}^* N_{k3}) \quad (\text{A.37})$$

$$\begin{aligned} \delta E_{lk}^{0R} &= -\frac{g}{2\cos\theta_W} (\delta N_{l4}^* N_{k4} - \delta N_{l3}^* N_{k3}) \\ &\quad - \frac{g}{2\cos\theta_W} (N_{l4}^* \delta N_{k4} - N_{l3}^* \delta N_{k3}) \\ &\quad - \frac{g}{2\cos\theta_W} (N_{l4}^* N_{k4} - N_{l3}^* N_{k3}) \left(\frac{\delta e}{e} - \frac{\delta \sin\theta_W}{\sin\theta_W} - \frac{\delta \cos\beta}{\cos\beta} \right) \\ &\quad - \frac{g}{2\cos\theta_W} \sum_{i=1}^4 \frac{1}{2} \delta Z_{il}^L(\tilde{\chi}^0) (N_{i4}^* N_{k4} - N_{i3}^* N_{k3}) \\ &\quad - \frac{g}{2\cos\theta_W} \sum_{j=1}^4 \frac{1}{2} \delta Z_{jk}^L(\tilde{\chi}^0)^C (N_{l4}^* N_{j4} - N_{l3}^* N_{j3}) \\ &\quad - \frac{g}{2\cos\theta_W} \frac{1}{2} \delta Z(Z^0) (N_{l4}^* N_{k4} - N_{l3}^* N_{k3}) \end{aligned} \quad (\text{A.38})$$

$$E_{lk}^{0L} = +\frac{g}{2\cos\theta_W} (N_{l4} N_{k4}^* - N_{l3} N_{k3}^*) \quad (\text{A.39})$$

$$\begin{aligned} \delta E_{lk}^{0L} &= +\frac{g}{2\cos\theta_W} (\delta N_{l4} N_{k4}^* - \delta N_{l3} N_{k3}^*) \\ &\quad + \frac{g}{2\cos\theta_W} (N_{l4} \delta N_{k4}^* - N_{l3} \delta N_{k3}^*) \\ &\quad + \frac{g}{2\cos\theta_W} (N_{l4} N_{k4}^* - N_{l3} N_{k3}^*) \left(\frac{\delta e}{e} - \frac{\delta \sin\theta_W}{\sin\theta_W} - \frac{\delta \cos\beta}{\cos\beta} \right) \\ &\quad + \frac{g}{2\cos\theta_W} \sum_{i=1}^4 \frac{1}{2} \delta Z_{il}^L(\tilde{\chi}^0)^C (N_{i4} N_{k4}^* - N_{i3} N_{k3}^*) \\ &\quad + \frac{g}{2\cos\theta_W} \sum_{j=1}^4 \frac{1}{2} \delta Z_{jk}^L(\tilde{\chi}^0) (N_{l4} N_{j4}^* - N_{l3} N_{j3}^*) \\ &\quad + \frac{g}{2\cos\theta_W} \frac{1}{2} \delta Z(Z^0) (N_{l4} N_{k4}^* - N_{l3} N_{k3}^*) \end{aligned} \quad (\text{A.40})$$

$$E_{ji}^{+R} = -\frac{g}{\cos \theta_W} (U_{j1}^* U_{i1} + \frac{1}{2} U_{j2}^* U_{i2} - \delta_{ij} \sin^2 \theta_W) \quad (\text{A.41})$$

$$\begin{aligned} \delta E_{ji}^{+R} = & -\frac{g}{\cos \theta_W} (\delta U_{j1}^* U_{i1} + \frac{1}{2} \delta U_{j2}^* U_{i2} - \delta_{ij} \sin^2 \theta_W) \\ & - \frac{g}{\cos \theta_W} (U_{j1}^* \delta U_{i1} + \frac{1}{2} U_{j2}^* \delta U_{i2} - \delta_{ij} \sin^2 \theta_W) \\ & - \frac{g}{\cos \theta_W} (U_{j1}^* U_{i1} + \frac{1}{2} U_{j2}^* U_{i2} - \delta_{ij} \sin^2 \theta_W) \left(\frac{\delta e}{e} - \frac{\delta \sin \theta_W}{\sin \theta_W} - \frac{\delta \cos \beta}{\cos \beta} \right) \\ & - \frac{g}{\cos \theta_W} \sum_{k=1}^2 \frac{1}{2} \delta Z_{kj}^L (\tilde{\chi}^+)^C (U_{k1}^* U_{i1} + \frac{1}{2} U_{k2}^* U_{i2} - \delta_{kj} \sin^2 \theta_W) \\ & - \frac{g}{\cos \theta_W} \sum_{l=1}^2 \frac{1}{2} \delta Z_{li}^R (\tilde{\chi}^+) (U_{j1}^* U_{l1} + \frac{1}{2} U_{j2}^* U_{l2} - \delta_{li} \sin^2 \theta_W) \\ & - \frac{g}{\cos \theta_W} \frac{1}{2} \delta Z(Z^0) (U_{j1}^* U_{i1} + \frac{1}{2} U_{j2}^* U_{i2} - \delta_{ij} \sin^2 \theta_W) \end{aligned} \quad (\text{A.42})$$

$$E_{ji}^{+L} = -\frac{g}{\cos \theta_W} (V_{j1} V_{i1}^* + \frac{1}{2} V_{j2} V_{i2}^* - \delta_{ij} \sin^2 \theta_W) \quad (\text{A.43})$$

$$\begin{aligned} \delta E_{ji}^{+L} = & -\frac{g}{\cos \theta_W} (\delta V_{j1} V_{i1}^* + \frac{1}{2} \delta V_{j2} V_{i2}^* - \delta_{ij} \sin^2 \theta_W) \\ & - \frac{g}{\cos \theta_W} (V_{j1} \delta V_{i1}^* + \frac{1}{2} V_{j2} \delta V_{i2}^* - \delta_{ij} \sin^2 \theta_W) \\ & - \frac{g}{\cos \theta_W} (V_{j1} V_{i1}^* + \frac{1}{2} V_{j2} V_{i2}^* - \delta_{ij} \sin^2 \theta_W) \left(\frac{\delta e}{e} - \frac{\delta \sin \theta_W}{\sin \theta_W} - \frac{\delta \cos \beta}{\cos \beta} \right) \\ & - \frac{g}{\cos \theta_W} \sum_{k=1}^2 \frac{1}{2} \delta Z_{kj}^R (\tilde{\chi}^+)^C (V_{k1} V_{i1}^* + \frac{1}{2} V_{k2} V_{i2}^* - \delta_{kj} \sin^2 \theta_W) \\ & - \frac{g}{\cos \theta_W} \sum_{i=1}^2 \frac{1}{2} \delta Z_{li}^L (\tilde{\chi}^+) (V_{j1} V_{l1}^* + \frac{1}{2} V_{j2} V_{l2}^* - \delta_{li} \sin^2 \theta_W) \\ & - \frac{g}{\cos \theta_W} \frac{1}{2} \delta Z(Z^0) (V_{j1} V_{i1}^* + \frac{1}{2} V_{j2} V_{i2}^* - \delta_{ij} \sin^2 \theta_W) \end{aligned} \quad (\text{A.44})$$

$$K_{ji1}^+ = \frac{g}{\sqrt{2}}(-\cos \alpha V_{j2} U_{i1} + \sin \alpha V_{j1} U_{i2}) \quad (\text{A.45})$$

$$\begin{aligned} \delta K_{ji1}^+ &= \frac{g}{\sqrt{2}} \left[(-\cos \alpha \delta V_{j2} U_{i1} + \sin \alpha \delta V_{j1} U_{i2}) + (-\cos \alpha V_{j2} \delta U_{i1} + \sin \alpha V_{j1} \delta U_{i2}) \right. \\ &\quad + (-\cos \alpha V_{j2} U_{i1} + \sin \alpha V_{j1} U_{i2}) \left(\frac{\delta e}{e} - \frac{\delta \sin \theta_W}{\sin \theta_W} \right) \\ &\quad + (-\delta \cos \alpha V_{j2} U_{i1} + \delta \sin \alpha V_{j1} U_{i2}) \\ &\quad + \sum_{n=1}^2 \frac{1}{2} \delta Z_{nj}^L(\tilde{\chi}^+)^C (-\cos \alpha \delta V_{n2} U_{i1} + \sin \alpha V_{n1} U_{i2}) \\ &\quad + \sum_{n=1}^2 \frac{1}{2} \delta Z_{ni}^R(\tilde{\chi}^+) (-\cos \alpha \delta V_{j2} U_{n1} + \sin \alpha \delta V_{j1} U_{n2}) \\ &\quad + \frac{1}{2} \delta Z(h_0, h_0) (-\cos \alpha \delta V_{j2} U_{i1} + \sin \alpha \delta V_{j1} U_{i2}) \\ &\quad \left. + \frac{1}{2} \delta Z(h_0, H_0) (\sin \alpha \delta V_{j2} U_{i1} + \cos \alpha \delta V_{j1} U_{i2}) \right] \end{aligned} \quad (\text{A.46})$$

$$K_{ji2}^+ = \frac{g}{\sqrt{2}}(\sin \alpha V_{j2} U_{i1} + \cos \alpha V_{j1} U_{i2}) \quad (\text{A.47})$$

$$\begin{aligned} \delta K_{ji2}^+ &= \frac{g}{\sqrt{2}} \left[(\sin \alpha \delta V_{j2} U_{i1} + \cos \alpha \delta V_{j1} U_{i2}) + (\sin \alpha V_{j2} \delta U_{i1} + \cos \alpha V_{j1} \delta U_{i2}) \right. \\ &\quad + (\sin \alpha V_{j2} U_{i1} + \cos \alpha V_{j1} U_{i2}) \left(\frac{\delta e}{e} - \frac{\delta \sin \theta_W}{\sin \theta_W} \right) \\ &\quad + (\delta \sin \alpha V_{j2} U_{i1} + \delta \cos \alpha V_{j1} U_{i2}) \\ &\quad + \sum_{n=1}^2 \frac{1}{2} \delta Z_{nj}^L(\tilde{\chi}^+)^C (\sin \alpha V_{n2} U_{i1} + \cos \alpha V_{n1} U_{i2}) \\ &\quad + \sum_{n=1}^2 \frac{1}{2} \delta Z_{ni}^R(\tilde{\chi}^+) (\sin \alpha V_{j2} U_{n1} + \cos \alpha V_{j1} U_{n2}) \\ &\quad + \frac{1}{2} \delta Z(h_0, H_0) (-\cos \alpha V_{j2} U_{i1} + \sin \alpha V_{j1} U_{i2}) \\ &\quad \left. + \frac{1}{2} \delta Z(H_0, H_0) (\sin \alpha V_{j2} U_{i1} + \cos \alpha V_{j1} U_{i2}) \right] \end{aligned} \quad (\text{A.48})$$

$$K_{ji3}^+ = \frac{ig}{\sqrt{2}}(\sin \beta U_{i2} V_{j1} + \cos \beta U_{i1} V_{j2}) \quad (\text{A.49})$$

$$\begin{aligned} \delta K_{ji3}^+ &= \frac{ig}{\sqrt{2}} \left[(\sin \beta \delta U_{i2} V_{j1} + \cos \beta \delta U_{i1} V_{j2}) + (\sin \beta U_{i2} \delta V_{j1} + \cos \beta U_{i1} \delta V_{j2}) \right. \\ &\quad + (\sin \beta U_{i2} V_{j1} + \cos \beta U_{i1} V_{j2}) \left(\frac{\delta e}{e} - \frac{\delta \sin \theta_W}{\sin \theta_W} \right) \end{aligned}$$

$$\begin{aligned}
& + (\delta \sin \beta U_{i2} V_{j1} + \delta \cos \beta U_{i1}) \\
& + \sum_{n=1}^2 \frac{1}{2} \delta Z_{nj}^L (\tilde{\chi}^+)^C (\sin \beta U_{i2} V_{n1} + \cos \beta U_{i1} V_{n2}) \\
& + \sum_{n=1}^2 \frac{1}{2} \delta Z_{ni}^R (\tilde{\chi}^+) (\sin \beta U_{n2} V_{j1} + \cos \beta U_{n1} V_{j2}) \\
& + \frac{1}{2} \delta Z(A_0, A_0) (\sin \beta U_{i2} V_{j1} + \cos \beta U_{i1} V_{j2}) \\
& + \frac{1}{2} \delta Z(G_0, A_0) (-\cos \beta U_{i2} V_{j1} + \sin \beta U_{i1} V_{j2}) \\
& + \frac{m_{A_0}^2 - m_Z^2}{M_Z} \delta Z(Z_0, A_0) (-\cos \beta U_{i2} V_{j1} + \sin \beta U_{i1} V_{j2}) \Big] \tag{A.50}
\end{aligned}$$

$$\begin{aligned}
K_{lk1}^0 & = -g \left(\frac{-\sin \alpha}{2} [N_{l3} N_{k2} + N_{k3} N_{l2} - \tan \theta_W (N_{l3} N_{k1} + N_{k3} N_{l1})] \right. \\
& \quad \left. + \frac{-\cos \alpha}{2} [N_{l4} N_{k2} + N_{k4} N_{l2} - \tan \theta_W (N_{l4} N_{k1} + N_{k4} N_{l1})] \right) \tag{A.51}
\end{aligned}$$

$$\begin{aligned}
\delta K_{lk1}^0 & = -g \left(\frac{-\sin \alpha}{2} [\delta N_{l3} N_{k2} + \delta N_{k3} N_{l2} - \tan \theta_W (\delta N_{l3} N_{k1} + \delta N_{k3} N_{l1})] \right. \\
& \quad \left. + \frac{-\cos \alpha}{2} [\delta N_{l4} N_{k2} + \delta N_{k4} N_{l2} - \tan \theta_W (\delta N_{l4} N_{k1} + \delta N_{k4} N_{l1})] \right. \\
& \quad \left. + \frac{-\sin \alpha}{2} [N_{l3} \delta N_{k2} + N_{k3} \delta N_{l2} - \tan \theta_W (N_{l3} \delta N_{k1} + N_{k3} \delta N_{l1})] \right. \\
& \quad \left. + \frac{-\cos \alpha}{2} [N_{l4} \delta N_{k2} + N_{k4} \delta N_{l2} - \tan \theta_W (N_{l4} \delta N_{k1} + N_{k4} \delta N_{l1})] \right. \\
& \quad \left. + \left(\frac{-\sin \alpha}{2} [N_{l3} N_{k2} + N_{k3} N_{l2} - \tan \theta_W (N_{l3} N_{k1} + N_{k3} N_{l1})] \right. \right. \\
& \quad \left. \left. + \frac{-\cos \alpha}{2} [N_{l4} N_{k2} + N_{k4} N_{l2} - \tan \theta_W (N_{l4} N_{k1} + N_{k4} N_{l1})] \right) \left(\frac{\delta e}{e} \right) \right. \\
& \quad \left. + \frac{-\delta \sin \alpha}{2} [N_{l3} N_{k2} + N_{k3} N_{l2} - \tan \theta_W (N_{l3} N_{k1} + N_{k3} N_{l1})] \right. \\
& \quad \left. + \frac{-\delta \cos \alpha}{2} [N_{l4} N_{k2} + N_{k4} N_{l2} - \tan \theta_W (N_{l4} N_{k1} + N_{k4} N_{l1})] \right. \\
& \quad \left. + \frac{-\sin \alpha}{2} \left[\left(\frac{-\delta \sin \theta_W}{\sin \theta_W} \right) (N_{l3} N_{k2} + N_{k3} N_{l2}) - \left(\frac{-\delta \cos \theta_W}{\cos \theta_W} \right) \tan \theta_W (N_{l3} N_{k1} + N_{k3} N_{l1}) \right] \right. \\
& \quad \left. + \frac{-\cos \alpha}{2} \left[\left(\frac{-\delta \sin \theta_W}{\sin \theta_W} \right) (N_{l4} N_{k2} + N_{k4} N_{l2}) - \left(\frac{-\delta \cos \theta_W}{\cos \theta_W} \right) \tan \theta_W (N_{l4} N_{k1} + N_{k4} N_{l1}) \right] \right. \\
& \quad \left. + \sum_{j=1}^4 \frac{1}{2} \delta Z_{jl}^L (\tilde{\chi}^0)^C \left(\frac{-\sin \alpha}{2} [N_{j3} N_{k2} + N_{k3} N_{j2} - \tan \theta_W (N_{j3} N_{k1} + N_{k3} N_{j1})] \right. \right. \\
& \quad \left. \left. + \frac{-\cos \alpha}{2} [N_{j4} N_{k2} + N_{k4} N_{j2} - \tan \theta_W (N_{j4} N_{k1} + N_{k4} N_{j1})] \right) \right] \tag{A.51}
\end{aligned}$$

$$\begin{aligned}
& + \frac{-\cos \alpha}{2} [N_{j4}N_{k2} + N_{k4}N_{j2} - \tan \theta_W(N_{j4}N_{k1} + N_{k4}N_{j1})] \Big) \\
& + \sum_{i=1}^4 \frac{1}{2} \delta Z_{ik}^L(\tilde{\chi}^0)^C \left(\frac{-\sin \alpha}{2} [N_{l3}N_{i2} + N_{i3}N_{l2} - \tan \theta_W(N_{l3}N_{i1} + N_{i3}N_{l1})] \right. \\
& \quad \left. + \frac{-\cos \alpha}{2} [N_{l4}N_{i2} + N_{i4}N_{l2} - \tan \theta_W(N_{l4}N_{i1} + N_{i4}N_{l1})] \right) \\
& + \delta Z(h_0, h_0) \left(\frac{-\sin \alpha}{2} [N_{l3}N_{k2} + N_{k3}N_{l2} - \tan \theta_W(N_{l3}N_{k1} + N_{k3}N_{l1})] \right. \\
& \quad \left. + \frac{-\cos \alpha}{2} [N_{l4}N_{k2} + N_{k4}N_{l2} - \tan \theta_W(N_{l4}N_{k1} + N_{k4}N_{l1})] \right) \\
& + \delta Z(h_0, H_0) \left(\frac{\cos \alpha}{2} [N_{l3}N_{k2} + N_{k3}N_{l2} - \tan \theta_W(N_{l3}N_{k1} + N_{k3}N_{l1})] \right. \\
& \quad \left. + \frac{-\sin \alpha}{2} [N_{l4}N_{k2} + N_{k4}N_{l2} - \tan \theta_W(N_{l4}N_{k1} + N_{k4}N_{l1})] \right) \tag{A.52}
\end{aligned}$$

$$\begin{aligned}
K_{lk2}^0 & = -g \left(\frac{\cos \alpha}{2} [N_{l3}N_{k2} + N_{k3}N_{l2} - \tan \theta_W(N_{l3}N_{k1} + N_{k3}N_{l1})] \right. \\
& \quad \left. + \frac{-\sin \alpha}{2} [N_{l4}N_{k2} + N_{k4}N_{l2} - \tan \theta_W(N_{l4}N_{k1} + N_{k4}N_{l1})] \right) \tag{A.53}
\end{aligned}$$

$$\begin{aligned}
\delta K_{lk2}^0 & = -g \left(\frac{\cos \alpha}{2} [\delta N_{l3}N_{k2} + \delta N_{k3}N_{l2} - \tan \theta_W(\delta N_{l3}N_{k1} + \delta N_{k3}N_{l1})] \right. \\
& \quad \left. + \frac{-\sin \alpha}{2} [\delta N_{l4}N_{k2} + \delta N_{k4}N_{l2} - \tan \theta_W(\delta N_{l4}N_{k1} + \delta N_{k4}N_{l1})] \right) \\
& + \frac{\cos \alpha}{2} [N_{l3}\delta N_{k2} + N_{k3}\delta N_{l2} - \tan \theta_W(N_{l3}\delta N_{k1} + N_{k3}\delta N_{l1})] \\
& \quad + \frac{-\sin \alpha}{2} [N_{l4}\delta N_{k2} + N_{k4}\delta N_{l2} - \tan \theta_W(N_{l4}\delta N_{k1} + N_{k4}\delta N_{l1})] \\
& + \left(\frac{\cos \alpha}{2} [N_{l3}N_{k2} + N_{k3}N_{l2} - \tan \theta_W(N_{l3}N_{k1} + N_{k3}N_{l1})] \right. \\
& \quad \left. + \frac{-\sin \alpha}{2} [N_{l4}N_{k2} + N_{k4}N_{l2} - \tan \theta_W(N_{l4}N_{k1} + N_{k4}N_{l1})] \right) \left(\frac{\delta e}{e} \right) \\
& + \frac{\delta \cos \alpha}{2} [N_{l3}N_{k2} + N_{k3}N_{l2} - \tan \theta_W(N_{l3}N_{k1} + N_{k3}N_{l1})] \\
& \quad + \frac{-\delta \sin \alpha}{2} [N_{l4}N_{k2} + N_{k4}N_{l2} - \tan \theta_W(N_{l4}N_{k1} + N_{k4}N_{l1})] \\
& + \frac{\cos \alpha}{2} \left[\left(\frac{-\delta \sin \theta_W}{\sin \theta_W} \right) (N_{l3}N_{k2} + N_{k3}N_{l2}) - \left(\frac{-\delta \cos \theta_W}{\cos \theta_W} \right) \tan \theta_W(N_{l3}N_{k1} + N_{k3}N_{l1}) \right] \\
& \quad + \frac{-\sin \alpha}{2} \left[\left(\frac{-\delta \sin \theta_W}{\sin \theta_W} \right) (N_{l4}N_{k2} + N_{k4}N_{l2}) - \left(\frac{-\delta \cos \theta_W}{\cos \theta_W} \right) \tan \theta_W(N_{l4}N_{k1} + N_{k4}N_{l1}) \right]
\end{aligned}$$

$$\begin{aligned}
& + \sum_{j=1}^4 \frac{1}{2} \delta Z_{jl}^L (\tilde{\chi}^0)^C \left(\frac{\cos \alpha}{2} [N_{j3}N_{k2} + N_{k3}N_{j2} - \tan \theta_W (N_{j3}N_{k1} + N_{k3}N_{j1})] \right. \\
& \quad \left. + \frac{-\sin \alpha}{2} [N_{j4}N_{k2} + N_{k4}N_{j2} - \tan \theta_W (N_{j4}N_{k1} + N_{k4}N_{j1})] \right) \\
& + \sum_{i=1}^4 \frac{1}{2} \delta Z_{ik}^L (\tilde{\chi}^0)^C \left(\frac{\cos \alpha}{2} [N_{l3}N_{i2} + N_{i3}N_{l2} - \tan \theta_W (N_{l3}N_{i1} + N_{i3}N_{l1})] \right. \\
& \quad \left. + \frac{-\sin \alpha}{2} [N_{l4}N_{i2} + N_{i4}N_{l2} - \tan \theta_W (N_{l4}N_{i1} + N_{i4}N_{l1})] \right) \\
& + \delta Z(H_0, H_0) \left(\frac{\cos \alpha}{2} [N_{l3}N_{k2} + N_{k3}N_{l2} - \tan \theta_W (N_{l3}N_{k1} + N_{k3}N_{l1})] \right. \\
& \quad \left. + \frac{-\sin \alpha}{2} [N_{l4}N_{k2} + N_{k4}N_{l2} - \tan \theta_W (N_{l4}N_{k1} + N_{k4}N_{l1})] \right) \\
& + \delta Z(h_0, H_0) \left(\frac{-\sin \alpha}{2} [N_{l3}N_{k2} + N_{k3}N_{l2} - \tan \theta_W (N_{l3}N_{k1} + N_{k3}N_{l1})] \right. \\
& \quad \left. + \frac{-\cos \alpha}{2} [N_{l4}N_{k2} + N_{k4}N_{l2} - \tan \theta_W (N_{l4}N_{k1} + N_{k4}N_{l1})] \right) \tag{A.54}
\end{aligned}$$

$$\begin{aligned}
K_{lk3}^0 & = -ig \left(\frac{\sin \beta}{2} [N_{l3}N_{k2} + N_{k3}N_{l2} - \tan \theta_W (N_{l3}N_{k1} + N_{k3}N_{l1})] \right. \\
& \quad \left. + \frac{-\cos \beta}{2} [N_{l4}N_{k2} + N_{k4}N_{l2} - \tan \theta_W (N_{l4}N_{k1} + N_{k4}N_{l1})] \right) \tag{A.55}
\end{aligned}$$

$$\begin{aligned}
\delta K_{lk3}^0 & = -ig \left(\frac{\sin \beta}{2} [\delta N_{l3}N_{k2} + \delta N_{k3}N_{l2} - \tan \theta_W (\delta N_{l3}N_{k1} + \delta N_{k3}N_{l1})] \right. \\
& \quad \left. + \frac{-\cos \beta}{2} [\delta N_{l4}N_{k2} + \delta N_{k4}N_{l2} - \tan \theta_W (\delta N_{l4}N_{k1} + \delta N_{k4}N_{l1})] \right) \\
& + \frac{\sin \beta}{2} [N_{l3}\delta N_{k2} + N_{k3}\delta N_{l2} - \tan \theta_W (N_{l3}\delta N_{k1} + N_{k3}\delta N_{l1})] \\
& \quad + \frac{-\cos \beta}{2} [N_{l4}\delta N_{k2} + N_{k4}\delta N_{l2} - \tan \theta_W (N_{l4}\delta N_{k1} + N_{k4}\delta N_{l1})] \\
& + \left(\frac{\sin \beta}{2} [N_{l3}N_{k2} + N_{k3}N_{l2} - \tan \theta_W (N_{l3}N_{k1} + N_{k3}N_{l1})] \right. \\
& \quad \left. + \frac{-\cos \beta}{2} [N_{l4}N_{k2} + N_{k4}N_{l2} - \tan \theta_W (N_{l4}N_{k1} + N_{k4}N_{l1})] \right) \left(\frac{\delta e}{e} \right) \\
& + \frac{\delta \sin \beta}{2} [N_{l3}N_{k2} + N_{k3}N_{l2} - \tan \theta_W (N_{l3}N_{k1} + N_{k3}N_{l1})] \\
& \quad + \frac{-\delta \cos \beta}{2} [N_{l4}N_{k2} + N_{k4}N_{l2} - \tan \theta_W (N_{l4}N_{k1} + N_{k4}N_{l1})] \\
& + \frac{\sin \beta}{2} \left[\left(\frac{-\delta \sin \theta_W}{\sin \theta_W} \right) (N_{l3}N_{k2} + N_{k3}N_{l2}) - \left(\frac{-\delta \cos \theta_W}{\cos \theta_W} \right) \tan \theta_W (N_{l3}N_{k1} + N_{k3}N_{l1}) \right]
\end{aligned}$$

$$\begin{aligned}
& + \frac{-\cos \beta}{2} \left[\left(\frac{-\delta \sin \theta_W}{\sin \theta_W} \right) (N_{l4}N_{k2} + N_{k4}N_{l2}) - \left(\frac{-\delta \cos \theta_W}{\cos \theta_W} \right) \tan \theta_W (N_{l4}N_{k1} + N_{k4}N_{l1}) \right] \\
& + \sum_{j=1}^4 \frac{1}{2} \delta Z_{jl}^L (\tilde{\chi}^0)^C \left(\frac{\sin \beta}{2} \left[N_{j3}N_{k2} + N_{k3}N_{j2} - \tan \theta_W (N_{j3}N_{k1} + N_{k3}N_{j1}) \right] \right. \\
& \quad \left. + \frac{-\cos \beta}{2} \left[N_{j4}N_{k2} + N_{k4}N_{j2} - \tan \theta_W (N_{j4}N_{k1} + N_{k4}N_{j1}) \right] \right) \\
& + \sum_{i=1}^4 \frac{1}{2} \delta Z_{ik}^L (\tilde{\chi}^0)^C \left(\frac{\sin \beta}{2} \left[N_{l3}N_{i2} + N_{i3}N_{l2} - \tan \theta_W (N_{l3}N_{i1} + N_{i3}N_{l1}) \right] \right. \\
& \quad \left. + \frac{-\cos \beta}{2} \left[N_{l4}N_{i2} + N_{i4}N_{l2} - \tan \theta_W (N_{l4}N_{i1} + N_{i4}N_{l1}) \right] \right) \\
& + \delta Z(A_0, A_0) \left(\frac{\sin \beta}{2} \left[N_{l3}N_{k2} + N_{k3}N_{l2} - \tan \theta_W (N_{l3}N_{k1} + N_{k3}N_{l1}) \right] \right. \\
& \quad \left. + \frac{-\cos \beta}{2} \left[N_{l4}N_{k2} + N_{k4}N_{l2} - \tan \theta_W (N_{l4}N_{k1} + N_{k4}N_{l1}) \right] \right) \\
& + \delta Z(G_0, A_0) \left(\frac{-\cos \beta}{2} \left[N_{l3}N_{k2} + N_{k3}N_{l2} - \tan \theta_W (N_{l3}N_{k1} + N_{k3}N_{l1}) \right] \right. \\
& \quad \left. + \frac{-\sin \beta}{2} \left[N_{l4}N_{k2} + N_{k4}N_{l2} - \tan \theta_W (N_{l4}N_{k1} + N_{k4}N_{l1}) \right] \right) \\
& + \frac{m_{A_0}^2 - m_Z^2}{M_Z} \delta Z(Z_0, A_0) \left(\frac{-\cos \beta}{2} \left[N_{l3}N_{k2} + N_{k3}N_{l2} - \tan \theta_W (N_{l3}N_{k1} + N_{k3}N_{l1}) \right] \right. \\
& \quad \left. + \frac{-\sin \beta}{2} \left[N_{l4}N_{k2} + N_{k4}N_{l2} - \tan \theta_W (N_{l4}N_{k1} + N_{k4}N_{l1}) \right] \right) \tag{A.56}
\end{aligned}$$

$$K_{jl}^{1R} = -g\cos\beta(V_{j1}N_{l4} + \frac{1}{\sqrt{2}}(N_{l2} + N_{l1}\tan\theta_W)V_{j2}) \quad (\text{A.57})$$

$$\begin{aligned} \delta K_{jl}^{1R} = & -g\cos\beta(V_{j1}\delta N_{l4} + \frac{1}{\sqrt{2}}(\delta N_{l2} + \delta N_{l1}\tan\theta_W)V_{j2}) \\ & - g\cos\beta(\delta V_{j1}N_{l4} + \frac{1}{\sqrt{2}}(N_{l2} + N_{l1}\tan\theta_W)\delta V_{j2}) \\ & - g\cos\beta(V_{j1}N_{l4} + \frac{1}{\sqrt{2}}(N_{l2} + N_{l1}\tan\theta_W)V_{j2})(\frac{\delta e}{e} - \frac{\delta\sin\theta_W}{\sin\theta_W} + \frac{\delta\cos\beta}{\cos\beta}) \\ & - g\cos\beta\sum_{i=1}^2\frac{1}{2}\delta Z_{ij}^R(\tilde{\chi}^\pm)(V_{i1}N_{l4} + \frac{1}{\sqrt{2}}(N_{l2} + N_{l1}\tan\theta_W)V_{i2}) \\ & - g\cos\beta\sum_{k=1}^4\frac{1}{2}\delta Z_{kl}^L(\tilde{\chi}^0)^C(V_{j1}N_{k4} + \frac{1}{\sqrt{2}}(N_{l2} + N_{k1}\tan\theta_W)V_{j2}) \\ & - g\cos\beta\frac{1}{2}\delta Z_{11}(H^+)(V_{j1}N_{l4} + \frac{1}{\sqrt{2}}(\delta N_{l2} + N_{l1}\tan\theta_W)V_{j2}) \\ & - g\sin\beta\frac{1}{2}\delta Z_{21}(H^+)(V_{j1}N_{l4} + \frac{1}{\sqrt{2}}(\delta N_{l2} + N_{l1}\tan\theta_W)V_{j2}) \\ & - g\sin\beta\frac{m_{H^+} - m_W}{m_W}\delta Z(WH^+)(V_{j1}N_{l4} + \frac{1}{\sqrt{2}}(\delta N_{l2} + N_{l1}\tan\theta_W)V_{j2}) \end{aligned} \quad (\text{A.58})$$

$$K_{jl}^{1L} = -g\sin\beta(V_{j1}^*N_{l4}^* + \frac{1}{\sqrt{2}}(N_{l2}^* + N_{l1}^*\tan\theta_W)V_{j2}^*) \quad (\text{A.59})$$

$$\begin{aligned} \delta K_{jl}^{1L} = & -g\sin\beta(V_{j1}^*\delta N_{l4}^* + \frac{1}{\sqrt{2}}(\delta N_{l2}^* + \delta N_{l1}^*\tan\theta_W)V_{j2}^*) \\ & - g\sin\beta(\delta V_{j1}N_{l4}^* + \frac{1}{\sqrt{2}}(N_{l2}^* + N_{l1}^*\tan\theta_W)\delta V_{j2}^*) \\ & - g\sin\beta(V_{j1}^*N_{l4}^* + \frac{1}{\sqrt{2}}(N_{l2}^* + N_{l1}^*\tan\theta_W)V_{j2}^*)(\frac{\delta e}{e}) \\ & - g\sin\beta\sum_{i=1}^2\frac{1}{2}\delta Z_{ij}^L(\tilde{\chi}^\pm)(V_{i1}^*N_{l4}^* + \frac{1}{\sqrt{2}}(N_{l2}^* + N_{l1}^*\tan\theta_W)V_{i2}^*) \\ & - g\sin\beta\sum_{k=1}^4\frac{1}{2}\delta Z_{kl}^L(\tilde{\chi}^0)^C(V_{j1}^*N_{k4}^* + \frac{1}{\sqrt{2}}(N_{l2}^* + N_{k1}^*\tan\theta_W)V_{j2}^*) \\ & - g\sin\beta\frac{1}{2}\delta Z_{11}(H^+)(V_{j1}^*N_{l4}^* + \frac{1}{\sqrt{2}}(N_{l2}^* + N_{l1}^*\tan\theta_W)V_{j2}^*) \\ & - g\cos\beta\frac{1}{2}\delta Z_{21}(H^+)(V_{j1}^*N_{l4}^* + \frac{1}{\sqrt{2}}(N_{l2}^* + N_{l1}^*\tan\theta_W)V_{j2}^*) \\ & - g\cos\beta\frac{m_{H^+} - m_W}{m_W}\delta Z(WH^+)(V_{j1}^*N_{l4}^* + \frac{1}{\sqrt{2}}(N_{l2}^* + N_{l1}^*\tan\theta_W)V_{j2}^*) \end{aligned} \quad (\text{A.60})$$

Appendix B

Calculations for Bremsstrahlung

B.1 Matrixelements

$$\begin{aligned}\mathcal{M}_a &= \bar{u}(p_2)(-iQ_2e)\gamma^\mu\epsilon_\mu^*(q)\frac{i(\not{p}_2 + \not{q} + m_2)}{(p_2 + q)^2 - m_2^2} i(g^R P_R + g^L P_L)u(p_0) \\ &= \frac{iQ_2e}{2p_2 \cdot q} \bar{u}(p_2)\gamma^\mu\epsilon_\mu^*(q)(\not{p}_2 + \not{q} + m_2)(g^R P_R + g^L P_L)u(p_0)\end{aligned}\quad (\text{B.1})$$

$$\begin{aligned}\mathcal{M}_a^\dagger &= \frac{-iQ_2e}{2p_2 \cdot q} u^\dagger(p_0)(g^{R*} P_R + g^{L*} P_L)(\not{p}_2^\dagger + \not{q}^\dagger + m_2)\gamma^{\nu\dagger}\epsilon_\nu(q)\bar{u}^\dagger(p_2) \\ &= \frac{-iQ_2e}{2p_2 \cdot q} \bar{u}(p_0)\gamma^0(g^{R*} P_R + g^{L*} P_L)\gamma^0(\not{p}_2 + \not{q} + m_2)\gamma^0\gamma^\nu\gamma^0\epsilon_\nu(q)\gamma^0u(p_2) \\ &= \frac{-iQ_2e}{2p_2 \cdot q} \bar{u}(p_0)(g^{R*} P_L + g^{L*} P_R)(\not{p}_2 + \not{q} + m_2)\gamma^\nu\epsilon_\nu(q)u(p_2)\end{aligned}\quad (\text{B.2})$$

$$\begin{aligned}\mathcal{M}_b &= \bar{u}(p_2)(-iQ_1e)(2p_1 + q)^\mu\epsilon_\mu^*(q)\frac{i}{(p_1 + q)^2 - m_1^2} i(g^R P_R + g^L P_L)u(p_0) \\ &= \frac{iQ_1e}{2p_1 \cdot q} \bar{u}(p_1)(2p_1 + q)^\mu\epsilon_\mu^*(q)(g^R P_R + g^L P_L)u(p_0)\end{aligned}\quad (\text{B.3})$$

$$\begin{aligned}\mathcal{M}_b^\dagger &= \frac{-iQ_1e}{2p_1 \cdot q} u^\dagger(p_0)(g^{R*} P_R + g^{L*} P_L)(2p_1 + q)^\nu\epsilon_\nu(q)\bar{u}^\dagger(p_2) \\ &= \frac{-iQ_1e}{2p_1 \cdot q} \bar{u}(p_0)\gamma^0(g^{R*} P_R + g^{L*} P_L)(2p_1 + q)^\nu\epsilon_\nu(q)\gamma^0u(p_2) \\ &= \frac{-iQ_1e}{2p_1 \cdot q} \bar{u}(p_0)(g^{R*} P_L + g^{L*} P_R)(2p_1 + q)^\nu\epsilon_\nu(q)u(p_2)\end{aligned}\quad (\text{B.4})$$

$$\begin{aligned}\mathcal{M}_c &= \bar{u}(p_2)i(g^R P_R + g^L P_L)\frac{i(\not{p}_0 - \not{q} + m_0)}{(p_0 - q)^2 - m_0^2}(-iQ_0e)\gamma^\mu\epsilon_\mu^*(q)u(p_0) \\ &= \frac{-iQ_0e}{2p_0 \cdot q} \bar{u}(p_2)(g^R P_R + g^L P_L)(\not{p}_0 - \not{q} + m_0)\gamma^\mu\epsilon_\mu^*(q)u(p_0)\end{aligned}\quad (\text{B.5})$$

$$\begin{aligned}
\mathcal{M}_c^\dagger &= \frac{i Q_0 e}{2p_0 \cdot q} u^\dagger(p_0) \gamma^{\mu\dagger} \epsilon_\mu(q) (\not{p}_0^\dagger - \not{q}^\dagger + m_0) (g^{R*} P_R + g^{L*} P_L) \bar{u}(p_2) \\
&= \frac{i Q_0 e}{2p_0 \cdot q} \bar{u}(p_0) \gamma^0 \gamma^0 \gamma^\mu \gamma^0 \epsilon_\mu(q) \gamma^0 (\not{p}_0 - \not{q} + m_0) \gamma^0 (g^{R*} P_R + g^{L*} P_L) \gamma^0 u(p_2) \\
&= \frac{i Q_0 e}{2p_0 \cdot q} \bar{u}(p_0) \gamma^\nu \epsilon_\nu(q) (\not{p}_0 - \not{q} + m_0) (g^{R*} P_L + g^{L*} P_R) u(p_2)
\end{aligned} \tag{B.6}$$

B.2 $a \times a$

$$\begin{aligned}
\mathcal{M}_a^\dagger \mathcal{M}_a &= \frac{Q_2^2 e^2}{(2p_2 \cdot q)^2} \bar{u}(p_0) (g^{R*} P_L + g^{L*} P_R) (\not{p}_2 + \not{q} + m_2) \gamma^\nu \epsilon_\nu(q) u(p_2) \\
&\quad \bar{u}(p_2) \gamma^\mu \epsilon_\mu^*(q) (\not{p}_2 + \not{q} + m_2) (g^R P_R + g^L P_L) u(p_0)
\end{aligned} \tag{B.7}$$

$$\begin{aligned}
\left(\frac{Q_2^2 e^2}{(2p_2 \cdot q)^2} \right)^{-1} Tr(\mathcal{M}_a^\dagger \mathcal{M}_a) &= Tr \left[-g_{\mu\nu} (\not{p}_0 + m_0) (g^{R*} P_L + g^{L*} P_R) (\not{p}_2 + \not{q} + m_2) \gamma^\nu \right. \\
&\quad \left. (\not{p}_2 + m_2) \gamma^\mu (\not{p}_2 + \not{q} + m_2) (g^R P_R + g^L P_L) \right] \\
&= 8(g^{R*} g^R + g^{L*} g^L) \left(m_2^2 \left(-\frac{Y}{2} + p_1 \cdot q - p_0 \cdot q \right) + p_0 \cdot q p_2 \cdot q \right) \\
&\quad + 8(g^{R*} g^L + g^{L*} g^R) m_0 m_2 \left(-p_2 \cdot q - m_2^2 \right) \\
&= 8(g^{R*} g^R + g^{L*} g^L) \left(m_2^2 \left(-\frac{Y}{2} - p_2 \cdot q \right) + p_0 \cdot q p_2 \cdot q \right) \\
&\quad + 8(g^{R*} g^L + g^{L*} g^R) m_0 m_2 \left(-p_2 \cdot q - m_2^2 \right)
\end{aligned} \tag{B.8}$$

$$\begin{aligned}
\left(\frac{Q_2^2 e^2}{(2p_2 \cdot q)^2} \right)^{-1} \frac{1}{\pi^2} \int \frac{d^3 p_1}{2E_1} \frac{d^3 p_2}{2E_2} \frac{d^3 q}{2E_q} \delta^4(p_0 - p_1 - p_2 - q) Tr(\mathcal{M}_a^\dagger \mathcal{M}_a) \\
&= \left(8(g^{R*} g^R + g^{L*} g^L) \left(-\frac{m_2^2 Y}{2} I_{22} - \frac{m_2^2}{2} I_2 - \frac{1}{4} I_2^0 \right) \right. \\
&\quad \left. + 8(g^{R*} g^L + g^{L*} g^R) m_0 m_2 \left(-\frac{1}{2} I_2 - m_2^2 I_{22} \right) \right)
\end{aligned} \tag{B.9}$$

B.3 $b \times b$

$$\begin{aligned} \mathcal{M}_b^\dagger \mathcal{M}_b &= \frac{Q_1^2 e^2}{(2p_1 \cdot q)^2} \bar{u}(p_0)(g^{R*}P_L + g^{L*}P_R)(2p_1 + q)^\nu \epsilon_\nu(q) u(p_2) \\ &\quad \bar{u}(p_2)(2p_1 + q)^\mu \epsilon_\mu^*(q)(g^R P_R + g^L P_L) u(p_0) \end{aligned} \quad (\text{B.10})$$

$$\begin{aligned} \left(\frac{Q_1^2 e^2}{(2p_1 \cdot q)^2} \right)^{-1} Tr(\mathcal{M}_b^\dagger \mathcal{M}_b) &= Tr \left[-g_{\mu\nu}(\not{p}_0 + m_0)(g^{R*}P_L + g^{L*}P_R)(2p_1 + q)^\nu \right. \\ &\quad \left. (\not{p}_2 + m_2)(2p_1 + q)^\mu (g^R P_R + g^L P_L) \right] \\ &= 8(g^{R*}g^R + g^{L*}g^L) \left(-p_0 \cdot p_2 (m_1^2 + p_1 \cdot q) \right) \\ &\quad + 8(g^{R*}g^L + g^{L*}g^R)m_0m_2 \left(-p_1 \cdot q - m_1^2 \right) \\ &= 8(g^{R*}g^R + g^{L*}g^L) \left(\left(-\frac{Y}{2} + p_1 \cdot q \right) (m_1^2 + p_1 \cdot q) \right) \\ &\quad + 8(g^{R*}g^L + g^{L*}g^R)m_0m_2 \left(-p_1 \cdot q - m_1^2 \right) \end{aligned} \quad (\text{B.11})$$

$$\begin{aligned} \left(\frac{Q_1^2 e^2}{(2p_1 \cdot q)^2} \right)^{-1} \frac{1}{\pi^2} \int \frac{d^3 p_1}{2E_1} \frac{d^3 p_2}{2E_2} \frac{d^3 q}{2E_q} \delta^4(p_0 - p_1 - p_2 - q) Tr(\mathcal{M}_b^\dagger \mathcal{M}_b) \\ = \left(2(g^{R*}g^R + g^{L*}g^L) \left(-2m_1^2 Y I_{11} - Y I_1 + 2m_1^2 I_1 + I \right) \right. \\ \left. + 8(g^{R*}g^L + g^{L*}g^R)m_0m_2 \left(-\frac{1}{2}I_1 - m_1^2 I_{11} \right) \right) \end{aligned} \quad (\text{B.12})$$

B.4 $c \times c$

$$\begin{aligned} \mathcal{M}_c^\dagger \mathcal{M}_c &= \frac{Q_0^2 e^2}{(-2p_0 \cdot q)^2} \bar{u}(p_0) \gamma^\nu \epsilon_\nu(q) (g^{R*} P_L + g^{L*} P_R) (\not{p}_0 - \not{q} + m_0) u(p_2) \\ &\quad \bar{u}(p_2) (\not{p}_0 - \not{q} + m_0) (g^R P_R + g^L P_L) \gamma^\mu \epsilon_\mu^*(q) u(p_0) \end{aligned} \quad (\text{B.13})$$

$$\begin{aligned} \left(\frac{Q_0^2 e^2}{(-2p_0 \cdot q)^2} \right)^{-1} Tr(\mathcal{M}_c^\dagger \mathcal{M}_c) &= Tr \left[-g_{\mu\nu} (\not{p}_0 + m_0) \gamma^\nu (\not{p}_0 - \not{q} + m_0) (g^{R*} P_L + g^{L*} P_R) \right. \\ &\quad \left. (\not{p}_2 + m_2) (g^R P_R + g^L P_L) (\not{p}_0 - \not{q} + m_0) \gamma^\mu \right] \\ &= 8(g^{R*} g^R + g^{L*} g^L) \left(m_0^2 \left(-\frac{Y}{2} + p_1 \cdot q + p_2 \cdot q \right) + p_0 \cdot q p_2 \cdot q \right) \\ &\quad + 8(g^{R*} g^L + g^{L*} g^R) m_0 m_2 \left(p_0 \cdot q - m_0^2 \right) \\ &= 8(g^{R*} g^R + g^{L*} g^L) \left(m_0^2 \left(-\frac{Y}{2} + p_0 \cdot q \right) + p_0 \cdot q p_2 \cdot q \right) \\ &\quad + 8(g^{R*} g^L + g^{L*} g^R) m_0 m_2 \left(p_0 \cdot q - m_0^2 \right) \end{aligned} \quad (\text{B.14})$$

$$\begin{aligned} \left(\frac{Q_0^2 e^2}{(-2p_0 \cdot q)^2} \right)^{-1} \frac{1}{\pi^2} \int \frac{d^3 p_1}{2E_1} \frac{d^3 p_2}{2E_2} \frac{d^3 q}{2E_q} \delta^4(p_0 - p_1 - p_2 - q) Tr(\mathcal{M}_c^\dagger \mathcal{M}_c) \\ = \left(8(g^{R*} g^R + g^{L*} g^L) \left(-\frac{m_0^2 Y}{2} I_{00} - \frac{m_0^2}{2} I_0 - \frac{1}{4} I_0^2 \right) \right. \\ \left. + 8(g^{R*} g^L + g^{L*} g^R) m_0 m_2 \left(-\frac{1}{2} I_0 - m_0^2 I_{00} \right) \right) \end{aligned} \quad (\text{B.15})$$

B.5 $a \times b$

$$\begin{aligned} \mathcal{M}_a^\dagger \mathcal{M}_b &= \frac{Q_1 Q_2 e^2}{(2p_1 \cdot q)(2p_2 \cdot q)} \bar{u}(p_0) (g^{R*} P_L + g^{L*} P_R) (\not{p}_2 + \not{q} + m_2) \gamma^\nu \epsilon_\nu(q) u(p_2) \\ &\quad \bar{u}(p_2) (2p_1 + q)^\mu \epsilon_\mu^*(q) (g^R P_R + g^L P_L) u(p_0) \end{aligned} \quad (\text{B.16})$$

$$\begin{aligned} \mathcal{M}_b^\dagger \mathcal{M}_a &= \frac{Q_1 Q_2 e^2}{(2p_1 \cdot q)(2p_2 \cdot q)} \bar{u}(p_0) (g^{R*} P_L + g^{L*} P_R) (2p_1 + q)^\nu \epsilon_\nu(q) u(p_2) \\ &\quad \bar{u}(p_2) \gamma^\mu \epsilon_\mu^*(q) (\not{p}_2 + \not{q} + m_2) (g^R P_R + g^L P_L) u(p_0) \end{aligned} \quad (\text{B.17})$$

$$\begin{aligned} Tr(\mathcal{M}_a^\dagger \mathcal{M}_b) &= \frac{Q_1 Q_2 e^2}{(2p_1 \cdot q)(2p_2 \cdot q)} Tr \left[-g_{\mu\nu}(\not{p}_0 + m_0) (g^{R*} P_L + g^{L*} P_R) (\not{p}_2 + \not{q} + m_2) \gamma^\nu \right. \\ &\quad \left. (\not{p}_2 + m_2) (2p_1 + q)^\mu (g^R P_R + g^L P_L) \right] \end{aligned} \quad (\text{B.18})$$

$$\begin{aligned} Tr(\mathcal{M}_b^\dagger \mathcal{M}_a) &= \frac{Q_1 Q_2 e^2}{(2p_1 \cdot q)(2p_2 \cdot q)} Tr \left[-g_{\mu\nu}(\not{p}_0 + m_0) (g^{R*} P_L + g^{L*} P_R) (2p_1 + q)^\nu \right. \\ &\quad \left. (\not{p}_2 + m_2) \gamma^\mu (\not{p}_2 + \not{q} + m_2) (g^R P_R + g^L P_L) \right] \end{aligned} \quad (\text{B.19})$$

$$\begin{aligned} &\left(\frac{Q_1 Q_2 e^2}{(2p_1 \cdot q)(2p_2 \cdot q)} \right)^{-1} (Tr(\mathcal{M}_a^\dagger \mathcal{M}_b) + Tr(\mathcal{M}_b^\dagger \mathcal{M}_a)) = \\ &4(g^{R*} g^R + g^{L*} g^L) \left(-XY + Yp_1 \cdot q + Yp_2 \cdot q + Xp_1 \cdot q + Wp_2 \cdot q - Xp_2 \cdot q + 2p_1 \cdot q p_2 \cdot q \right) \\ &+ (g^{R*} g^L + g^{L*} g^R) m_0 m_2 \left(-X + p_1 \cdot q + p_2 \cdot q \right) \end{aligned} \quad (\text{B.20})$$

$$\begin{aligned} &\left(\frac{Q_1 Q_2 e^2}{(2p_1 \cdot q)(2p_2 \cdot q)} \right)^{-1} \frac{1}{\pi^2} \int \frac{d^3 p_1}{2E_1} \frac{d^3 p_2}{2E_2} \frac{d^3 q}{2E_q} \delta^4(p_0 - p_1 - p_2 - q) (Tr(\mathcal{M}_a^\dagger \mathcal{M}_b) + Tr(\mathcal{M}_b^\dagger \mathcal{M}_a)) \\ &= \left(2(g^{R*} g^R + g^{L*} g^L) \left(-2XYI_{12} + Y(I_2 + I_1) + X(I_2 - I_1) + WI_1 + I \right) \right. \\ &\quad \left. + 4(g^{R*} g^L + g^{L*} g^R) m_0 m_2 \left(-2XI_{12} + I_2 + I_1 \right) \right) \end{aligned} \quad (\text{B.21})$$

B.6 $a \times c$

$$\begin{aligned} \mathcal{M}_a^\dagger \mathcal{M}_c &= \frac{Q_0 Q_2 e^2}{(-2p_0 \cdot q)(2p_2 \cdot q)} \bar{u}(p_0) (g^{R*} P_L + g^{L*} P_R) (\not{p}_2 + \not{q} + m_2) \gamma^\nu \epsilon_\nu(q) u(p_2) \\ &\quad \bar{u}(p_2) (g^R P_R + g^L P_L) (\not{p}_0 - \not{q} + m_0) \gamma^\mu \epsilon_\mu^*(q) u(p_0) \end{aligned} \quad (\text{B.22})$$

$$\begin{aligned} \mathcal{M}_c^\dagger \mathcal{M}_a &= \frac{Q_0 Q_2 e^2}{(-2p_0 \cdot q)(2p_2 \cdot q)} \bar{u}(p_0) (g^{R*} P_L + g^{L*} P_R) (2p_1 + q)^\nu \epsilon_\nu(q) u(p_2) \\ &\quad \bar{u}(p_2) \gamma^\mu \epsilon_\mu^*(q) (\not{p}_2 + \not{q} + m_2) (g^R P_R + g^L P_L) u(p_0) \end{aligned} \quad (\text{B.23})$$

$$\begin{aligned} Tr(\mathcal{M}_a^\dagger \mathcal{M}_c) &= \frac{Q_0 Q_2 e^2}{(-2p_0 \cdot q)(2p_2 \cdot q)} Tr \left[-g_{\mu\nu} (\not{p}_0 + m_0) (g^{R*} P_L + g^{L*} P_R) (\not{p}_2 + \not{q} + m_2) \gamma^\nu \right. \\ &\quad \left. (\not{p}_2 + m_2) (g^R P_R + g^L P_L) (\not{p}_0 - \not{q} + m_0) \gamma^\mu \right] \end{aligned} \quad (\text{B.24})$$

$$\begin{aligned} Tr(\mathcal{M}_c^\dagger \mathcal{M}_a) &= \frac{Q_0 Q_2 e^2}{(-2p_0 \cdot q)(2p_2 \cdot q)} Tr \left[-g_{\mu\nu} (\not{p}_0 + m_0) \gamma^\nu (\not{p}_0 - \not{q} + m_0) (g^{R*} P_L + g^{L*} P_R) \right. \\ &\quad \left. (\not{p}_2 + m_2) \gamma^\mu (\not{p}_2 + \not{q} + m_2) (g^R P_R + g^L P_L) \right] \end{aligned} \quad (\text{B.25})$$

$$\begin{aligned} \left(\frac{Q_0 Q_2 e^2}{(-2p_0 \cdot q)(2p_2 \cdot q)} \right)^{-1} (Tr(\mathcal{M}_a^\dagger \mathcal{M}_c) + Tr(\mathcal{M}_c^\dagger \mathcal{M}_a)) &= \\ 8(g^{R*} g^R + g^{L*} g^L) \left(m_0^2 p_2 \cdot q - \frac{Y^2}{2} - m_2^2 p_0 \cdot q + Y p_0 \cdot q - Y p_2 \cdot q + 2p_0 \cdot q p_2 \cdot q \right) \\ + 8(g^{R*} g^L + g^{L*} g^R) m_0 m_2 \left(p_0 \cdot q - p_2 \cdot q - Y \right) \end{aligned} \quad (\text{B.26})$$

$$\begin{aligned} \left(\frac{Q_0 Q_2 e^2}{(-2p_0 \cdot q)(2p_2 \cdot q)} \right)^{-1} \frac{1}{\pi^2} \int \frac{d^3 p_1}{2E_1} \frac{d^3 p_2}{2E_2} \frac{d^3 q}{2E_q} \delta^4(p_0 - p_1 - p_2 - q) (Tr(\mathcal{M}_a^\dagger \mathcal{M}_c) + Tr(\mathcal{M}_c^\dagger \mathcal{M}_a)) \\ = \left(4(g^{R*} g^R + g^{L*} g^L) \left(m_0^2 I_0 - Y^2 I_{02} + m_2^2 I_2 - Y I_2 - Y I_0 - \frac{1}{2} I \right) \right. \\ \left. + 4(g^{R*} g^L + g^{L*} g^R) m_0 m_2 \left(-I_2 - I_0 - 2Y I_{02} \right) \right) \end{aligned} \quad (\text{B.27})$$

B.7 $b \times c$

$$\begin{aligned} \mathcal{M}_b^\dagger \mathcal{M}_c &= \frac{Q_0 Q_1 e^2}{(-2p_0 \cdot q)(2p_1 \cdot q)} \bar{u}(p_0) (g^{R*} P_L + g^{L*} P_R) (2p_1 + q)^\nu \epsilon_\nu(q) u(p_2) \\ &\quad \bar{u}(p_2) (g^R P_R + g^L P_L) (\not{p}_0 - \not{q} + m_0) \gamma^\mu \epsilon_\mu^*(q) u(p_0) \end{aligned} \quad (B.28)$$

$$\begin{aligned} \mathcal{M}_c^\dagger \mathcal{M}_b &= \frac{Q_0 Q_1 e^2}{(-2p_0 \cdot q)(2p_1 \cdot q)} \bar{u}(p_0) \gamma^\mu \epsilon_\mu(q) (\not{p}_0 - \not{q} + m_0) (g^{R*} P_L + g^{L*} P_R) u(p_2) \\ &\quad \bar{u}(p_2) (2p_1 + q)^\mu \epsilon_\mu^*(q) (g^R P_R + g^L P_L) u(p_0) \end{aligned} \quad (B.29)$$

$$\begin{aligned} Tr(\mathcal{M}_b^\dagger \mathcal{M}_c) &= \frac{Q_0 Q_1 e^2}{(-2p_0 \cdot q)(2p_1 \cdot q)} Tr \left[-g_{\mu\nu} (\not{p}_0 + m_0) (g^{R*} P_L + g^{L*} P_R) (2p_1 + q)^\nu \right. \\ &\quad \left. (\not{p}_2 + m_2) (g^R P_R + g^L P_L) (\not{p}_0 - \not{q} + m_0) \gamma^\mu \right] \end{aligned} \quad (B.30)$$

$$\begin{aligned} Tr(\mathcal{M}_c^\dagger \mathcal{M}_b) &= \frac{Q_0 Q_1 e^2}{(-2p_0 \cdot q)(2p_1 \cdot q)} Tr \left[-g_{\mu\nu} (\not{p}_0 + m_0) \gamma^\nu (\not{p}_0 - \not{q} + m_0) (g^{R*} P_L + g^{L*} P_R) \right. \\ &\quad \left. (\not{p}_2 + m_2) (2p_1 + q)^\mu (g^R P_R + g^L P_L) \right] \end{aligned} \quad (B.31)$$

$$\begin{aligned} &\left(\frac{Q_0 Q_1 e^2}{(-2p_0 \cdot q)(2p_1 \cdot q)} \right)^{-1} (Tr(\mathcal{M}_b^\dagger \mathcal{M}_c) + Tr(\mathcal{M}_c^\dagger \mathcal{M}_b)) = \\ &8(g^{R*} g^R + g^{L*} g^L) \left(-\left(\frac{X}{2} - p_0 \cdot q \right) p_0 \cdot q - \left(\frac{Y}{2} - p_1 \cdot q \right) p_0 \cdot q \right. \\ &\quad \left. + \left(\frac{Y}{2} - p_1 \cdot q \right) p_1 \cdot q - 2\left(\frac{Y}{2} - p_1 \cdot q \right) \left(\frac{W}{2} - p_2 \cdot q \right) + \left(\frac{W}{2} - p_2 \cdot q \right) p \cdot q \right) \\ &+ 8(g^{R*} g^L + g^{L*} g^R) m_0 m_2 \left(p_1 \cdot q - 2p_0 \cdot p_1 - p_0 \cdot q \right) \end{aligned} \quad (B.32)$$

$$\begin{aligned} &\left(\frac{Q_0 Q_1 e^2}{(-2p_0 \cdot q)(2p_1 \cdot q)} \right)^{-1} \frac{1}{\pi^2} \int \frac{d^3 p_1}{2E_1} \frac{d^3 p_2}{2E_2} \frac{d^3 q}{2E_q} \delta^4(p_0 - p_1 - p_2 - q) (Tr(\mathcal{M}_b^\dagger \mathcal{M}_c) + Tr(\mathcal{M}_c^\dagger \mathcal{M}_b)) \\ &= \left(2(g^{R*} g^R + g^{L*} g^L) \left(-I + W(I_0 - I_1) + XI_1 - Y(I_0 + YI_1) - 2WI_{01} \right) \right. \\ &\quad \left. + 4(g^{R*} g^L + g^{L*} g^R) m_0 m_2 \left(-I_0 - I_1 - 2WI_{01} \right) \right) \end{aligned} \quad (B.33)$$

B.8 Bremsstrahlung integrals for processes with an outgoing neutrino

$$\beta_2 = \frac{m_0^2 + m_1^2 - m_2^2 - \kappa}{2m_0m_1} \quad (\text{B.34})$$

$$I_0 = \frac{1}{4m_0^2} \left(-2m_1^2 \ln(\beta_2) - \kappa \right) \quad (\text{B.35})$$

$$I_1 = \frac{1}{4m_0^2} \left(-2m_0^2 \ln(\beta_2) - \kappa \right) \quad (\text{B.36})$$

$$\begin{aligned} I_{00} = & -\frac{1}{4m_0^4} \left[m_0^2 \ln \left(\frac{m_0}{m_1} - \frac{m_1}{m_0} \right) - (m_0 - m_1)(m_0 + m_1) \left(-1 + \ln^2 \left(\frac{m_0^2 - m_1^2}{\lambda m_0^2 m_1} \right) \right) \right. \\ & \left. + m_1^2 \ln \left(\frac{m_0^3}{m_0^2 m_1 - m_1^3} \right) \right] \end{aligned} \quad (\text{B.37})$$

$$\begin{aligned} I_{11} = & -\frac{1}{4m_0^2 m_1^2} \left[m_0^2 \ln \left(-1 + \frac{m_0^2}{m_1^2} \right) + m_1^2 \ln \left(\frac{m_0^2}{m_0^2 - m_1^2} \right) \right. \\ & \left. - (m_0 - m_1)(m_0 + m_1) \left(-1 + \ln \left(\frac{(m_0^2 - m_1^2)^2}{\lambda m_0^2 m_1} \right) \right) \right] \\ I_{01} = & \frac{1}{4m_0^2} \left[6 \ln^2 \left(\frac{m_1}{m_0} \right) + \ln^2 \left(\frac{m_0}{m_1} - \frac{m_1}{m_0} \right) - 2 \ln \left(\frac{m_1}{m_0} \right) \ln \left(\frac{\lambda m_0^2 m_1}{(m_0^2 - m_1^2)^2} \right) \right. \\ & \left. - \ln^2 \left(\frac{m_0^2}{(m_0^2 - m_1^2)^2} \right) + 2 Sp \left(1 - \frac{m_0^2}{m_1^2} \right) \right] \\ I_0^2 = & \frac{1}{4m_0^2} \left[-m_1^2 (2m_0^2 + m_1^2) \ln(\beta_2) - \frac{\kappa}{4} (m_0^2 + 5m_1^2) \right] \\ I = & \frac{1}{4m_0^2} \left[\frac{\kappa}{2} (m_0^2 + m_1^2) + 2m_0^2 m_1^2 \ln(\beta_2) \right] \end{aligned} \quad (\text{B.38})$$

$$\begin{aligned} X &= (m_0^2 - m_1^2) \\ Y &= (m_0^2 - m_1^2) \\ W &= (m_0^2 + m_1^2) \end{aligned} \quad (\text{B.39})$$

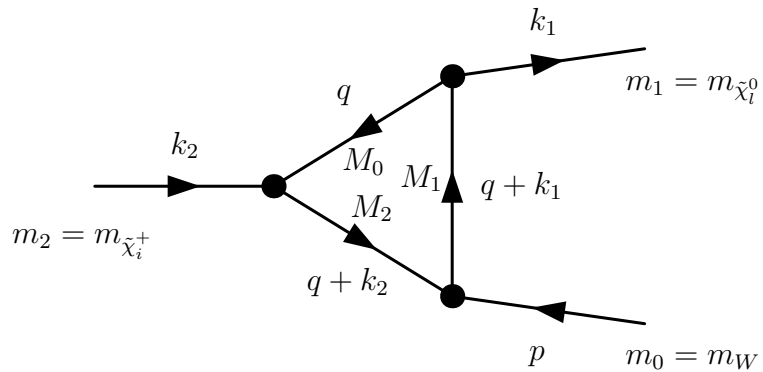
Appendix C

Generic Vertex Structures

All the following form factors are calculated in the SUSY invariant Dimensional Reduction regularisation scheme ($\overline{\text{DR}}$) [33]. As the vector boson propagators are taken in the $\xi = 1$ gauge, $m_{G^+} = m_{W^+}$ and $m_{G^0} = m_{Z^0}$. According to the on-shell relations, $p^2 = m_0^2$, $k_1^2 = m_1^2$ and $k_2^2 = m_2^2$. For the calculation of the loop integrals, we use the formalism of Passarino-Veltman-Integrals [61],[48] (" B -, C -functions"). The matrix elements, conventions for momenta and masses are given in [48]:

$$\mathcal{M}_{f \rightarrow fv} = \frac{i}{(4\pi)^2} \bar{u}(k_1) [\gamma^\mu \Lambda^{R,L} - k_2^\mu \Pi^{R,L}] P_{R,L} u(k_2) \epsilon_\mu^*(-p) \quad (\text{C.1})$$

$$\mathcal{M}_{f \rightarrow fs} = \frac{i}{(4\pi)^2} \bar{u}(k_1) [\Lambda^R P_R + \Lambda^L P_L] u(k_2) \quad (\text{C.2})$$



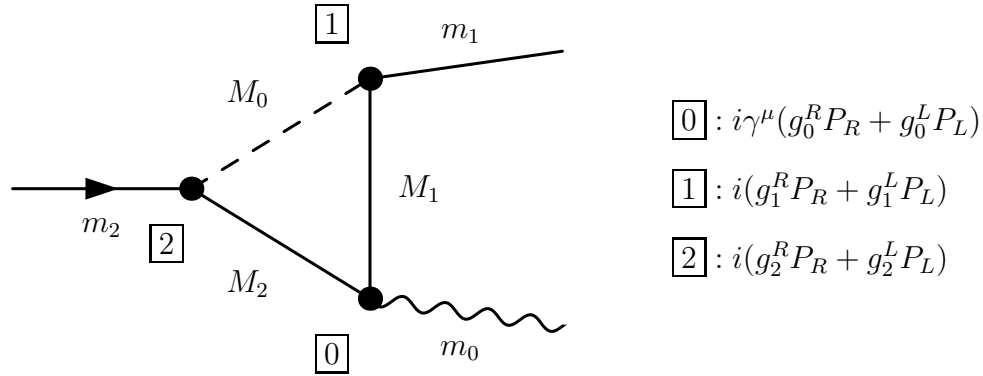
The occurring C -functions are defined in [48]

$$C_{i,ik} = C_{i,ik}(m_1^2, m_0^2, m_2^2, M_0^2, M_1^2, M_2^2) \quad (C.3)$$

Note, that in the following subsections the form factors Λ and Π are not written as functions of m_1 , m_0 and m_2 , because these are always the same: $m_1 = m_{\tilde{\chi}_l^0}$, $m_0 = m_W$ and $m_2 = m_{\tilde{\chi}_i^+}$.

We only provide Λ^R and Π^R , since Λ^L and Π^L can be easily obtained by exchanging right- and lefthanded couplings ($g_{0,1,2}^R \rightarrow g_{0,1,2}^L$, $g_{0,1,2}^L \rightarrow g_{0,1,2}^R$).

C.1 Generic structure I



Generic graph I: $f \rightarrow fv$, sff loop

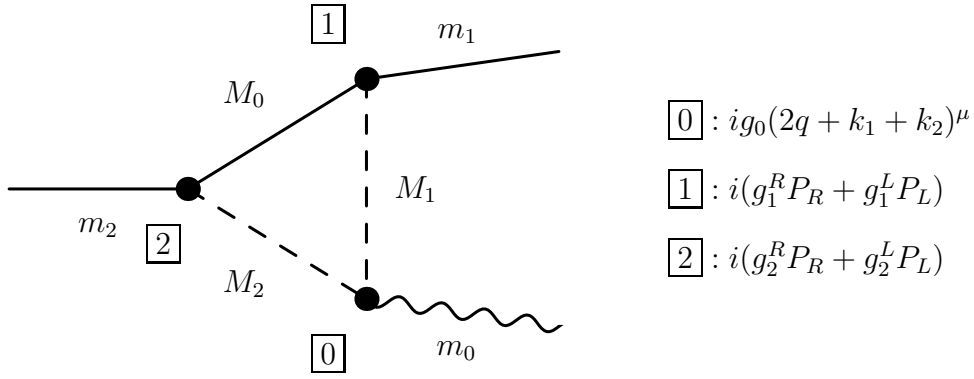
$$\begin{aligned} \Lambda_I^R(f) &= - \left(g_0^L g_1^L g_2^R \left(2C_{00} - B_0(m_0^2, M_1^2, M_2^2) \right) + (g_0^R h_1^{RL} h_2^{LR} - g_0^L g_1^L g_2^R M_0^2) C_0 + \right. \\ &\quad \left. (g_0^R g_1^R h_2^{LR} - g_0^L g_2^R h_1^{LR}) m_1 C_1 - (g_0^L g_1^L h_2^{RL} - g_0^R g_2^L h_1^{RL}) m_2 C_2 \right) \end{aligned} \quad (C.4)$$

$$\begin{aligned} \Pi_I^R(f) &= 2 \left(g_0^L g_2^R h_1^{LR} C_1 + g_0^R g_1^R h_2^{LR} C_2 + \right. \\ &\quad \left. g_0^L g_1^L g_2^R m_1 (C_{11} + C_{12}) + g_0^R g_1^R g_2^L m_2 (C_{22} + C_{12}) \right) \end{aligned} \quad (C.5)$$

$$f = (M_0, M_1, M_2, g_0^R, g_0^L, g_1^R, g_1^L, g_2^R, g_2^L) \quad (C.6)$$

$$\text{with } h_i^{jk} = g_i^j m_i + g_i^k M_i \quad i = 1, 2; j, k = L, R \quad (C.7)$$

C.2 Generic structure II



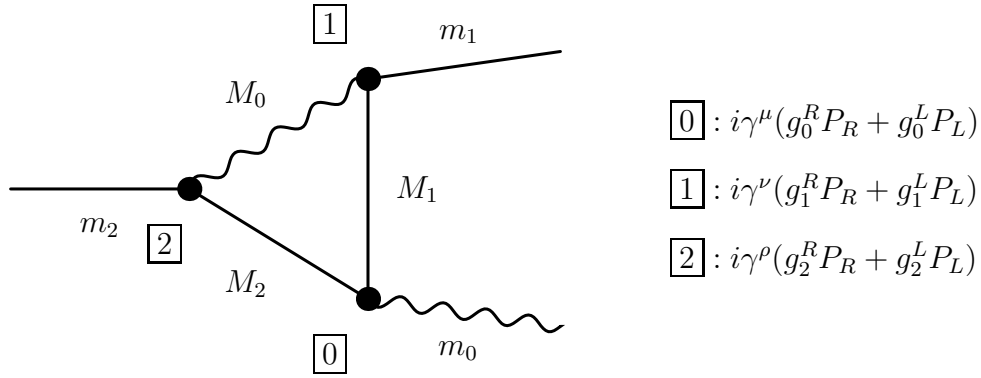
Generic graph II: $f \rightarrow fv, fss$ loop

$$\Lambda_{II}^R(f) = 2 C_{00} g_0 g_1^L g_2^R \quad (\text{C.8})$$

$$\begin{aligned} \Pi_{II}^R(f) = & -2g_0 \left[m_1 g_1^L g_2^R (C_1 + C_{11} + C_{12}) + m_2 g_1^R g_2^L (C_2 + C_{22} + C_{12}) \right. \\ & \left. - M_0 g_1^R g_2^R (C_0 + C_1 + C_2) \right] \end{aligned} \quad (\text{C.9})$$

$$f = (M_0, M_1, M_2, g_0, g_1^R, g_1^L, g_2^R, g_2^L) \quad (\text{C.10})$$

C.3 Generic structure III



Generic graph III: $f \rightarrow fv, vff$ loop

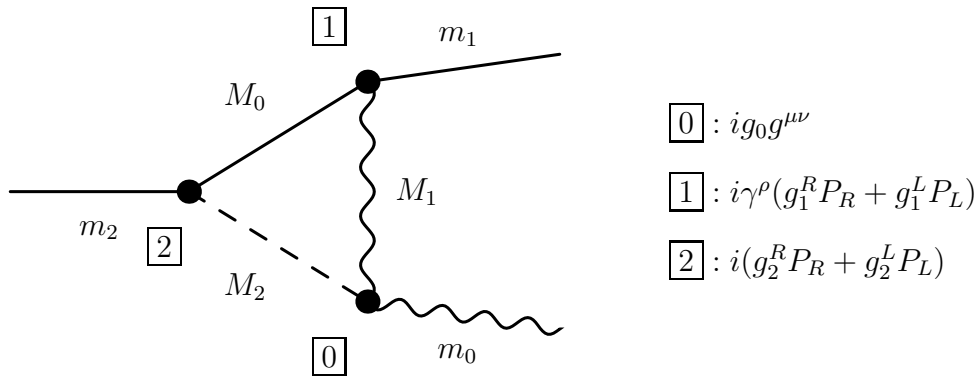
$$\begin{aligned} \Lambda_{III}^R(f) = & -2 \left\{ g_0^R g_1^R g_2^R [2C_{00} - B_0(m_0^2, M_1^2, M_2^2) + \frac{r}{2} \right. \\ & + (m_0^2 - m_1^2 - m_2^2)(C_0 + C_1 + C_2) - M_0^2 C_0 - m_1^2 C_1 - m_2^2 C_2] \\ & \left. g_0^L g_1^R g_2^R M_1 M_2 C_0 - g_0^L g_1^L g_2^L m_1 m_2 (C_0 + C_1 + C_2) \right\} \end{aligned} \quad (\text{C.11})$$

$$\begin{aligned} \Pi_{III}^R(f) = & 4 \left\{ [g_0^R g_2^R (g_1^R m_1 - g_1^L M_1) + g_0^L g_1^L (g_2^L m_2 - g_2^R M_2)] (C_0 + C_1 + C_2) \right. \\ & \left. g_0^R g_1^R g_2^R m_1 (C_1 + C_{11} + C_{12}) + g_0^L g_1^L g_2^L m_2 (C_2 + C_{22} + C_{12}) \right\} \end{aligned} \quad (\text{C.12})$$

$$f = (M_0, M_1, M_2, g_0^R, g_0^L, g_1^R, g_1^L, g_2^R, g_2^L) \quad (\text{C.13})$$

$$r = 0 \text{ (because of the application of the } \overline{\text{DR}} \text{ regularisation scheme [33])} \quad (\text{C.14})$$

C.4 Generic structure IV

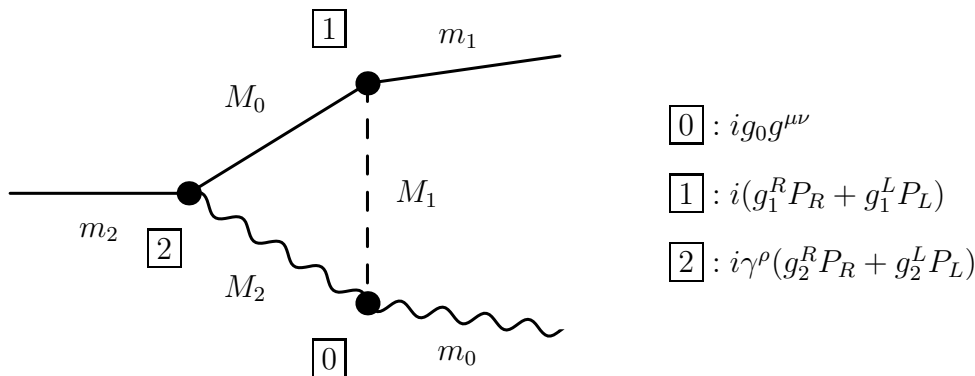
Generic graph IV: $f \rightarrow fv, fvs$ loop

$$\Lambda_{IV}^R(f) = g_0(g_1^R g_2^R M_0 C_0 + g_1^L g_2^R m_1 C_1 - g_1^R g_2^L m_2 C_2) \quad (\text{C.15})$$

$$\Pi_{IV}^R(f) = 2g_0 g_1^L g_2^R C_1 \quad (\text{C.16})$$

$$f = (M_0, M_1, M_2, g_0, g_1^R, g_1^L, g_2^R, g_2^L) \quad (\text{C.17})$$

C.5 Generic structure V

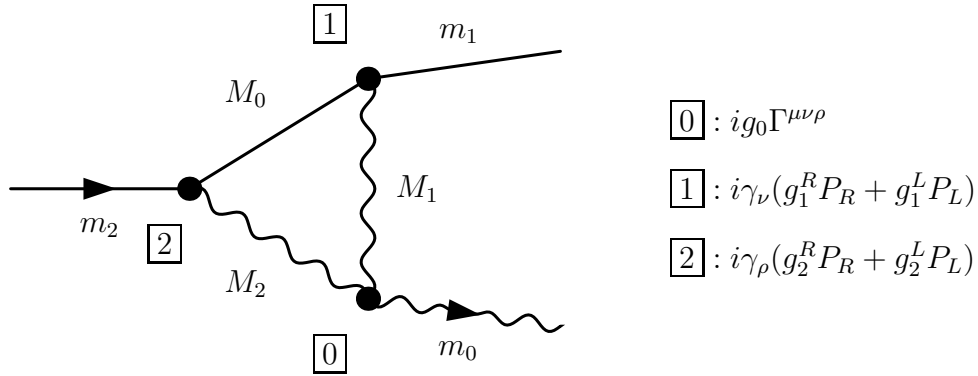
Generic graph V: $f \rightarrow fv, fsv$ loop

$$\Lambda_V^R(f) = g_0(g_1^L g_2^R M_0 C_0 - g_1^R g_2^R m_1 C_1 + g_1^L g_2^L m_2 C_2) \quad (\text{C.18})$$

$$\Pi_V^R(f) = 2g_0 g_1^R g_2^R C_2 \quad (\text{C.19})$$

$$f = (M_0, M_1, M_2, g_0, g_1^R, g_1^L, g_2^R, g_2^L) \quad (\text{C.20})$$

C.6 Generic structure VI



Generic graph VI: $f \rightarrow fv, fvv$ loop

$$\Gamma^{\mu\nu\rho} = -(2k_1 - k_2 + q)^\rho g^{\mu\nu} + (k_1 + k_2 + 2q)^\mu g^{\nu\rho} + (k_1 - 2k_2 - q)^\nu g^{\mu\rho} \quad (\text{C.21})$$

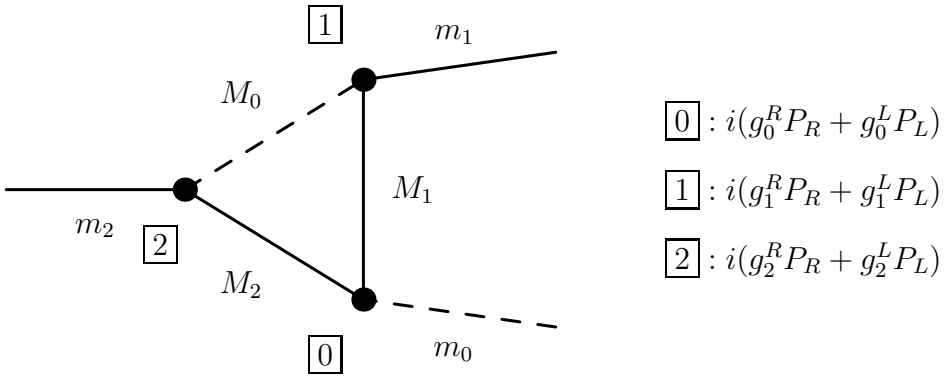
$$\begin{aligned} \Lambda_{VI}^R(f) = & g_0 \left\{ g_1^R g_2^R [2B_0(m_0^2, M_1^2, M_2^2) - r + 4C_{00} + 2M_0^2 C_0 \right. \\ & (3m_1^2 + 2m_2^2 - 2m_0^2)C_1 + (2m_1^2 + 3m_2^2 - 2m_0^2)C_2] \\ & \left. + 3(g_1^L g_2^R m_1 + g_1^R g_2^L m_2)M_0 C_0 + 3g_1^L g_2^L m_1 m_2 (C_1 + C_2) \right\} \end{aligned} \quad (\text{C.22})$$

$$\begin{aligned} \Pi_{VI}^R(f) = & -2g_0 \left\{ 3g_1^L g_2^R M_0 (C_1 + C_2) - g_1^R g_2^R m_1 (C_2 - 2C_{11} - 2C_{12}) \right. \\ & \left. - g_1^L g_2^L m_2 (C_1 - 2C_{22} - 2C_{12}) \right\} \end{aligned} \quad (\text{C.23})$$

$$f = (M_0, M_1, M_2, g_0, g_1^R, g_1^L, g_2^R, g_2^L) \quad (\text{C.24})$$

$$r = 0 \text{ (for the } \overline{\text{DR}} \text{ regularisation scheme [33])} \quad (\text{C.25})$$

C.7 Generic structure VII

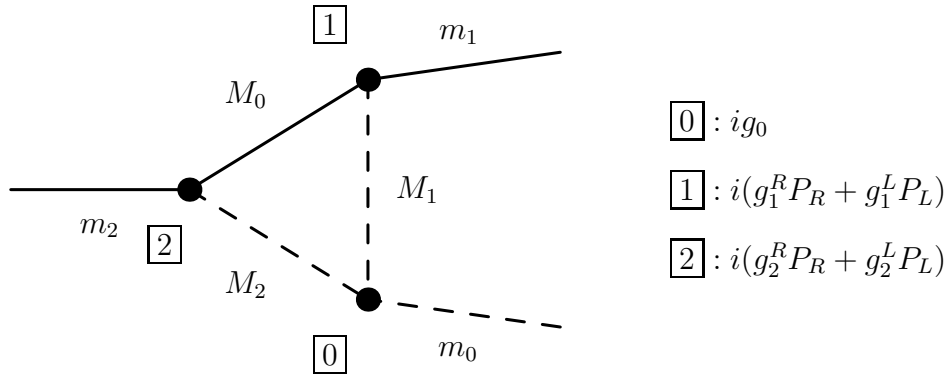


Generic graph VII: Scalar-fermion-fermion loop

$$\begin{aligned} \Lambda_{VII}^R(f) = & [g_0^L g_2^R (g_1^R m_1 + g_1^L M_1) + g_0^R g_1^L (g_2^L m_2 + g_2^R M_2)] m_1 C_1 \\ & + [g_0^R g_2^L (g_1^L m_1 + g_1^R M_1) + g_0^L g_1^R (g_2^R m_2 + g_2^L M_2)] m_2 C_2 \\ & + g_0^R [g_1^L g_2^L m_1 m_2 + g_1^R g_2^R M_1 M_2 + g_1^L g_2^R m_1 M_2 + g_1^R g_2^L m_2 M_1] C_0 \\ & + g_0^L g_1^R g_2^R [B_0(m_0^2, M_1^2, M_2^2) + M_0^2 C_0] \end{aligned} \quad (\text{C.26})$$

$$f = (M_0, M_1, M_2, g_0^R, g_0^L, g_1^R, g_1^L, g_2^R, g_2^L) \quad (\text{C.27})$$

C.8 Generic structure VIII

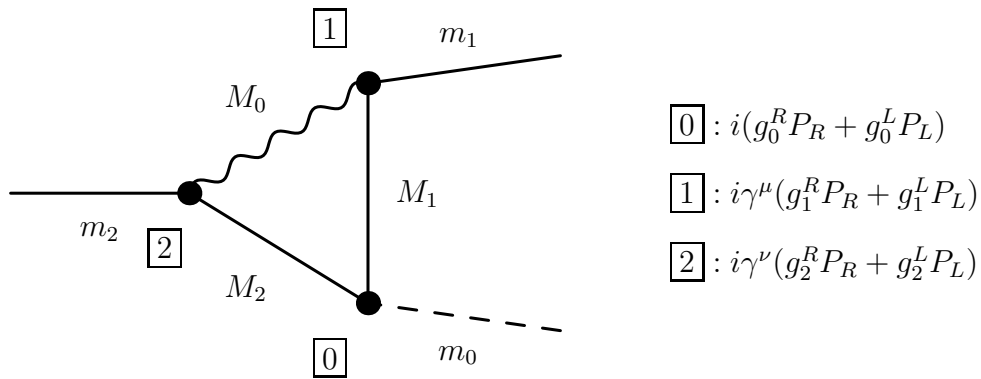


Generic graph VIII: Fermion-scalar-scalar loop

$$\Lambda_{VIII}^R(f) = g_0(-g_1^R g_2^R M_0 C_0 + g_1^L g_2^R m_1 C_1 + g_1^R g_2^L m_2 C_2) \quad (\text{C.28})$$

$$f = (M_0, M_1, M_2, g_0, g_1^R, g_1^L, g_2^R, g_2^L) \quad (\text{C.29})$$

C.9 Generic structure IX



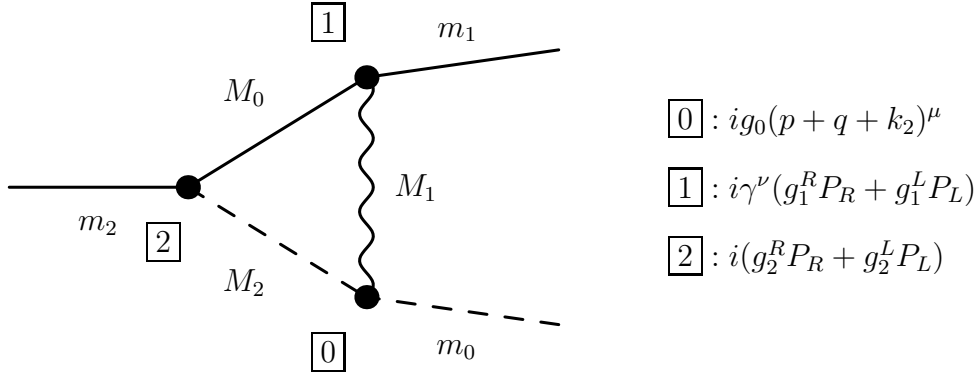
Generic graph IX: Vector-fermion-fermion loop

$$\Lambda_{IX}^R(f) = 2g_0^R g_1^L g_2^R [B_0(m_1^2, M_0^2, M_1^2) + B_0(m_2^2, M_0^2, M_2^2) + (M_1^2 + M_2^2 - m_0^2)C_0] \quad (\text{C.30})$$

$$\begin{aligned} & -2g_0^L [g_1^L g_2^L M_1 m_2 + g_1^R g_2^R m_1 M_2 - 2g_1^L g_2^R M_1 M_2] C_0 \\ & -2g_1^R g_2^R m_1 (g_0^L M_2 + g_0^R M_1) C_1 - 2g_1^L g_2^L m_2 (g_0^L M_1 + g_0^R M_2) C_2 \end{aligned} \quad (\text{C.30})$$

$$f = (M_0, M_1, M_2, g_0^R, g_0^L, g_1^R, g_1^L, g_2^R, g_2^L) \quad (\text{C.31})$$

C.10 Generic structure X

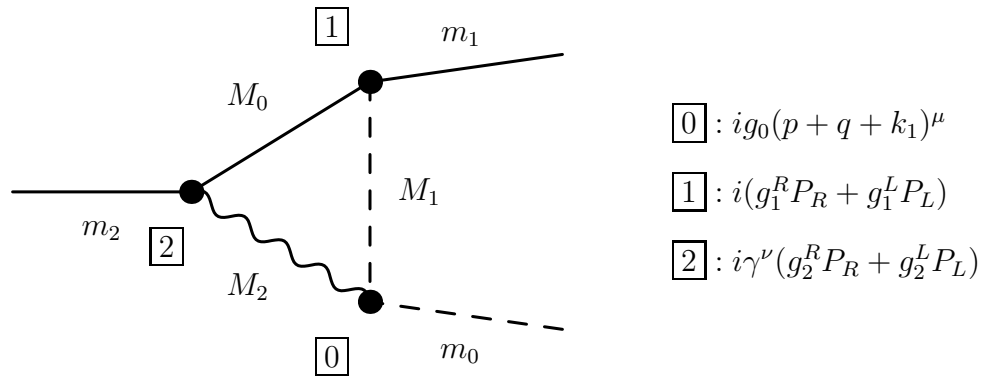


Generic graph X: Fermion-vector-scalar loop

$$\begin{aligned} \Lambda_X^R(f) = & g_0 \left\{ 2(C_1 + C_2)g_1^L g_2^R m_2^2 - g_2^L [(2C_0 + C_2)g_1^L M_0 + (C_1 + C_2)g_1^R m_1] m_2 \right. \\ & + g_2^R [C_0 M_0 (g_1^L M_0 + g_1^R m_1) + C_1 (-2g_1^L m_0^2 + g_1^L m_1^2 - g_1^R M_0 m_1)] \\ & \left. + g_1^L g_2^R B_0(m_0^2, M_1^2, M_2^2) \right\} \end{aligned} \quad (\text{C.32})$$

$$f = (M_0, M_1, M_2, g_0, g_1^R, g_1^L, g_2^R, g_2^L) \quad (\text{C.33})$$

C.11 Generic structure XI

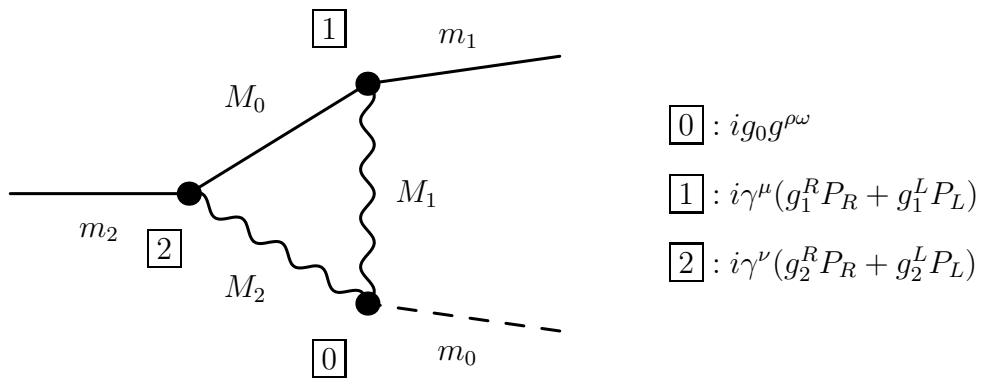


Generic graph XI: Fermion-scalar-vector loop

$$\begin{aligned} \Lambda_{XI}^R(f) = & g_0 \left\{ -C_2 g_1^R g_2^R m_2^2 + g_2^L \left[-C_0 g_1^R M_0 + C_2 g_1^R M_0 + (C_1 + 2C_2) g_1^L m_1 \right] m_2 \right. \\ & + g_2^R \left[-2(C_1 + C_2) g_1^R m_1^2 + (2C_0 + C_1) g_1^L M_0 m_1 + g_1^R (2C_2 m_0^2 - C_0 M_0^2) \right] \\ & \left. - g_1^R g_2^R B_0(m_0^2, M_1^2, M_2^2) \right\} \end{aligned} \quad (\text{C.34})$$

$$f = (M_0, M_1, M_2, g_0, g_1^R, g_1^L, g_2^R, g_2^L) \quad (\text{C.35})$$

C.12 Generic structure XII



Generic graph XII: Fermion-vector-vector loop

$$\Lambda_{XII}^R(f) = -2g_0(2C_0g_1^Lg_2^RM_0 + C_1g_1^Rg_2^Rm_1 + C_2g_1^Lg_2^Lm_2) \quad (\text{C.36})$$

$$f = (M_0, M_1, M_2, g_0, g_1^R, g_1^L, g_2^R, g_2^L) \quad (\text{C.37})$$

Appendix D

Generic Selfenergies (SE)

D.1 Fermion SE: Fermion-Scalar-Loop

:



$$\Pi^R = \frac{1}{(4\pi)^2} g_1^R g_2^L (B_0 + B_1), \quad \Pi^{S,R} = \frac{1}{(4\pi)^2} g_1^R g_2^L B_0 \quad (\text{D.1})$$

$$\begin{aligned} B_0 &= B_0(m_2, M_1^2, M_2^2) \\ B_1 &= B_1(m_2, M_1^2, M_2^2) \end{aligned} \quad (\text{D.2})$$

D.2 Fermion SE: Fermion-Vector-Loop



$$\Pi^R = \frac{1}{(2\pi)^2} g_1^R g_2^R (B_0 + B_1), \quad \Pi^{S,R} = -\frac{1}{(\pi)^2} g_1^R g_2^L B_0 \quad (\text{D.3})$$

$$\begin{aligned} B_0 &= B_0(m_2, M_1^2, M_2^2) \\ B_1 &= B_1(m_2, M_1^2, M_2^2) \end{aligned} \quad (\text{D.4})$$

D.3 Vector SE: Fermion-Fermion-Loop

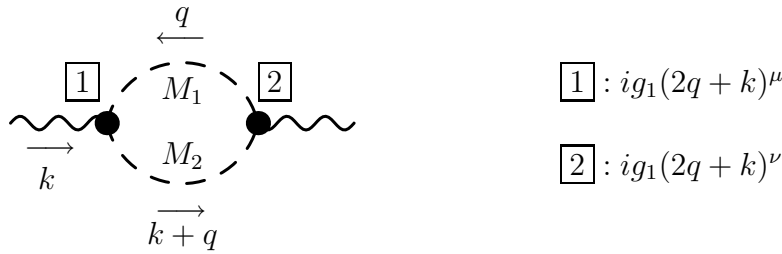


$$\begin{aligned} \Pi_T = & - \frac{1}{(4\pi)^2} \left\{ B_0 \left[(g_L g_L^* + g_R g_R^*) (M_1^2 + M_2^2 - m_2) - 2g_R g_L^* M_1 M_2 - 2g_R^* g_L M_1 M_2 \right] \right. \\ & \left. + (g_L g_L^* + g_R g_R^*) \left[-4B_{00} + A_0(M_1^2) + A_0(M_2^2) \right] \right\} \end{aligned} \quad (\text{D.5})$$

$$\begin{aligned} \delta \Pi_T = & - \frac{1}{(4\pi)^2} \left\{ \delta B_0 \left[(g_L g_L^* + g_R g_R^*) (M_1^2 + M_2^2 - m_2) - 2g_R g_L^* M_1 M_2 - 2g_R^* g_L M_1 M_2 \right] \right. \\ & \left. + (g_L g_L^* + g_R g_R^*) \left[-4\delta B_{00} - \delta B_0 \right] \right\} \end{aligned} \quad (\text{D.6})$$

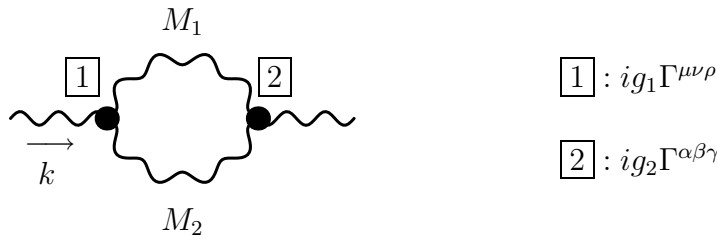
$$\begin{aligned} B_0 &= B_0(m_2, M_1^2, M_2^2) \\ B_{00} &= B_{00}(m_2, M_1^2, M_2^2) \end{aligned} \quad (\text{D.7})$$

D.4 Vector SE: Scalar-Scalar-Loop



$$\Pi_T = - \frac{1}{(4\pi)^2} g_1 g_2 B_{00}, \quad B_{00} = B_{00}(m_2, M_1^2, M_2^2) \quad (\text{D.8})$$

D.5 Vector SE: Vector-Vector-Loop

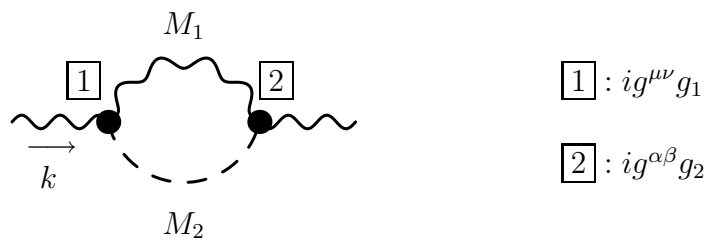


$$\Gamma^{\mu\nu\rho} = -(2k_1 - k_2 + q)^\rho g^{\mu\nu} + (k_1 + k_2 + 2q)^\mu g^{\nu\rho} + (k_1 - 2k_2 - q)^\nu g^{\mu\rho} \quad (\text{D.9})$$

$$\Pi_T = - \frac{1}{(4\pi)^2} g_1 g_2 (10B_{00} + 5k^2 B_0 + 2k^2 B_1 + 2M_1^2 B_0 + 2A_0) \quad (\text{D.10})$$

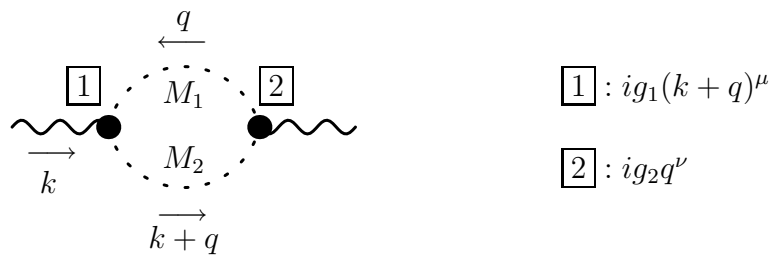
$$\begin{aligned} B_{00} &= B_{00}(k^2, M_1^2, M_2^2) \\ B_0 &= B_0(k^2, M_1^2, M_2^2) \\ B_1 &= B_1(k^2, M_1^2, M_2^2) \\ A_0 &= A_0(M_2^2) \end{aligned} \quad (\text{D.11})$$

D.6 Vector SE: Vector-Scalar-Loop



$$\Pi_T = \frac{1}{(4\pi)^2} g_1 g_2 B_0, \quad B_0 = B_0(k^2, M_1^2, M_2^2) \quad (\text{D.12})$$

D.7 Vector SE: Ghost-Ghost-Loop



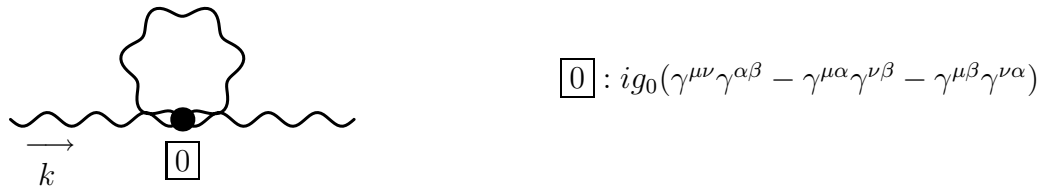
$$\Pi_T = \frac{1}{(4\pi)^2} g_1 g_2 B_{00}, \quad B_{00} = B_{00}(k^2, M_1^2, M_2^2) \quad (\text{D.13})$$

D.8 Vector SE: Scalar-Loop



$$\Pi_T = \frac{1}{(4\pi)^2} g_0 A_0, \quad A_0 = A_0(M_0^2) \quad (\text{D.14})$$

D.9 Vector SE: Vector-Loop



$$\Pi_T = \frac{6}{(4\pi)^2} g_0 A_0, \quad A_0 = A_0(M_0^2) \quad (\text{D.15})$$

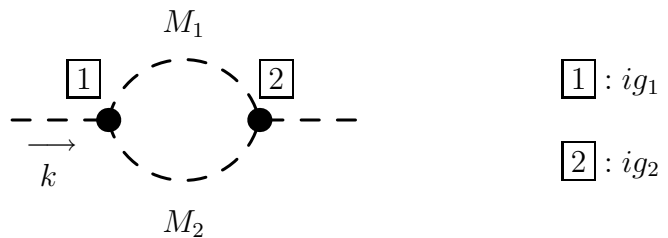
D.10 Scalar SE: Fermion-Fermion-Loop



$$\begin{aligned} \Pi = & - \frac{1}{(4\pi)^2} \left\{ -(g_1^L g_2^R + g_1^R g_2^L) [A_0(M_1^2) + A_0(M_2^2) + B_0(M_1^2 + M_2^2 - k^2)] \right. \\ & \left. - 2M_1 M_2 (g_1^R g_2^R + g_1^L g_2^L) B_0 \right\} \end{aligned} \quad (\text{D.16})$$

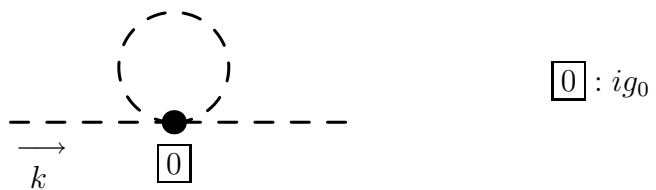
$$B_0 = B_0(m_2, M_1^2, M_2^2) \quad (\text{D.17})$$

D.11 Scalar SE: Fermion-Fermion-Loop



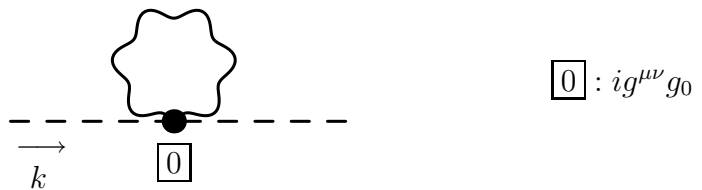
$$\Pi = - \frac{1}{(4\pi)^2} (g_1 g_2 B_0), \quad B_0 = B_0(m_2, M_1^2, M_2^2) \quad (\text{D.18})$$

D.12 Scalar SE: Scalar-Loop



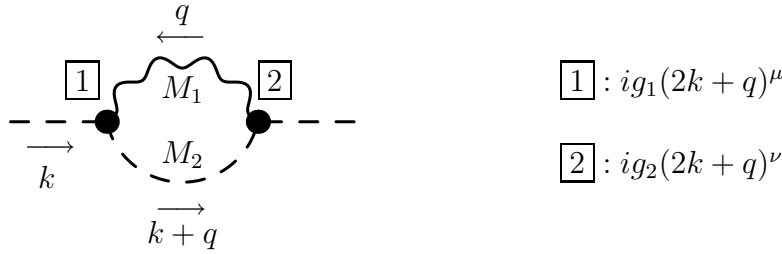
$$\Pi = - \frac{1}{(4\pi)^2} g_0 A_0, \quad A_0 = A_0(M_0^2) \quad (\text{D.19})$$

D.13 Scalar SE: Vector-Loop



$$\Pi = \frac{4}{(4\pi)^2} g_0 A_0, \quad A_0 = A_0(M_0^2) \quad (\text{D.20})$$

D.14 Scalar SE: Vector-Scalar-Loop



$$\Pi = \frac{1}{(4\pi)^2} \left\{ -g_1 g_2 [2A_0(M_1^2) - A_0(M_2^2) + (2k^2 + 2M_2^2 - M_1^2)B_0] \right\} \quad (\text{D.21})$$

$$B_0 = B_0(m_2, M_1^2, M_2^2) \quad (\text{D.22})$$

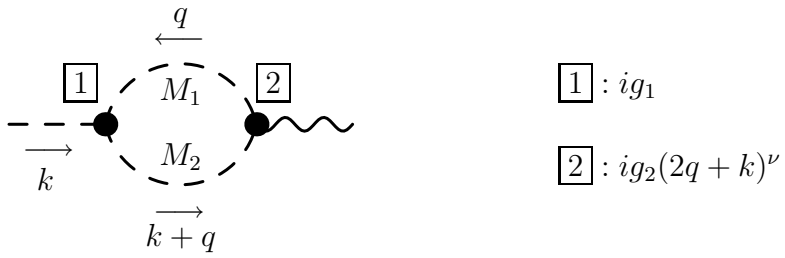
D.15 Scalar/Vector SE: Fermion-Fermion-Loop



$$\Pi = \frac{1}{(8\pi)^2} \left\{ (g_1^R g_2^L + g_1^L g_2^R) M_2 B_0 + [(g_1^R g_2^L + g_1^L g_2^R) M_2 + (g_1^L g_2^L + g_1^R g_2^R) M_1] B_1 \right\} \quad (\text{D.23})$$

$$\begin{aligned} B_0 &= B_0(k2, M_2^2, M_1^2) \\ B_1 &= B_1(k^2, M_2^2, M_1^2) \end{aligned} \quad (\text{D.24})$$

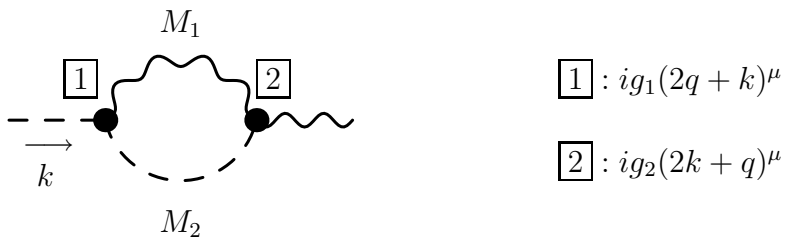
D.16 Scalar/Vector SE: Scalar-Scalar-Loop



$$\Pi = -\frac{1}{(4\pi)^2} g_1 g_2 (B_0 + 2B_1) \quad (\text{D.25})$$

$$\begin{aligned} B_0 &= B_0(k^2, M_2^2, M_1^2) \\ B_1 &= B_1(k^2, M_2^2, M_1^2) \end{aligned} \quad (\text{D.26})$$

D.17 Scalar/VectorSE: Vector-Scalar-Loop



$$\Pi = \frac{1}{(4\pi)^2} g_1 g_2 (2B_0 + B_1) \quad (\text{D.27})$$

$$\begin{aligned} B_0 &= B_0(k^2, M_1^2, M_2^2) \\ B_1 &= B_1(k^2, M_1^2, M_2^2) \end{aligned} \quad (\text{D.28})$$

Appendix E

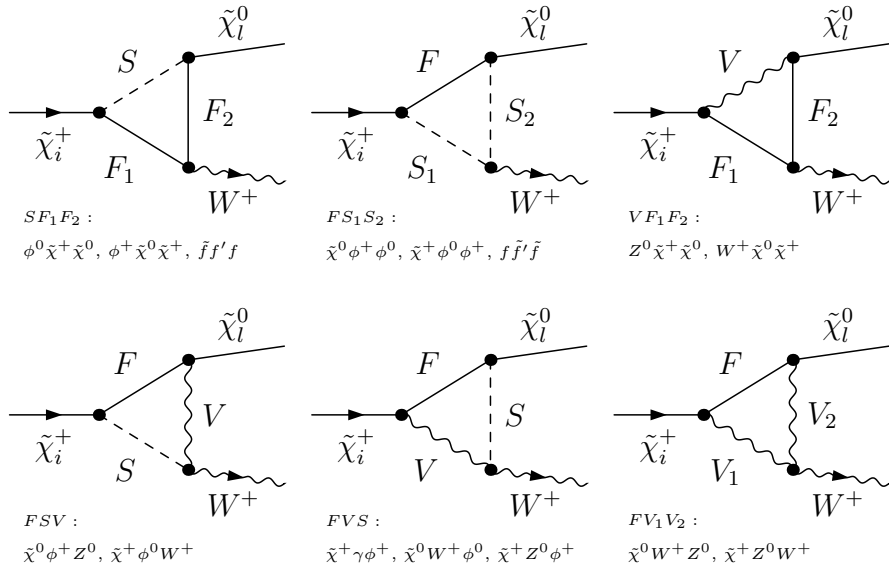
Vertex-Contributions

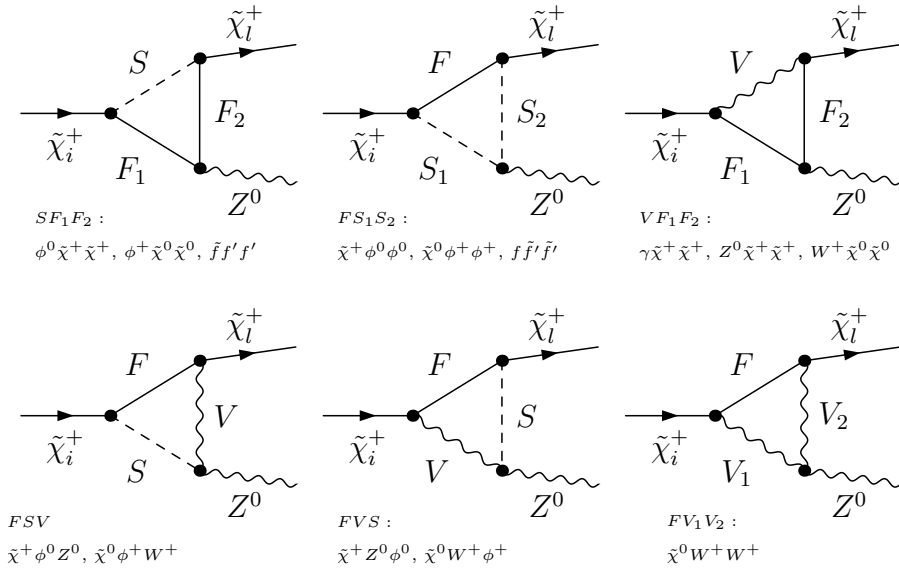
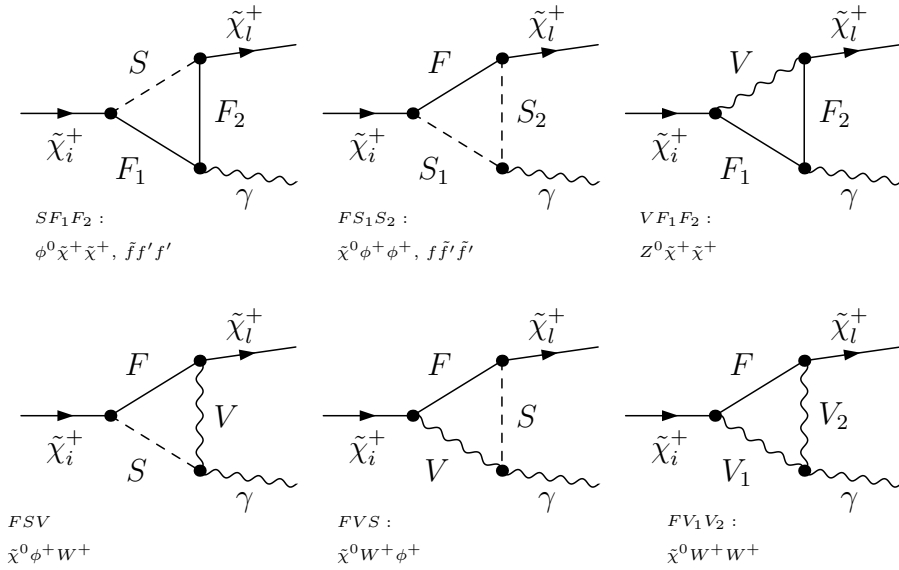
For the listing of the contributing vertex-corrections and the selfenergies we use the abbreviations

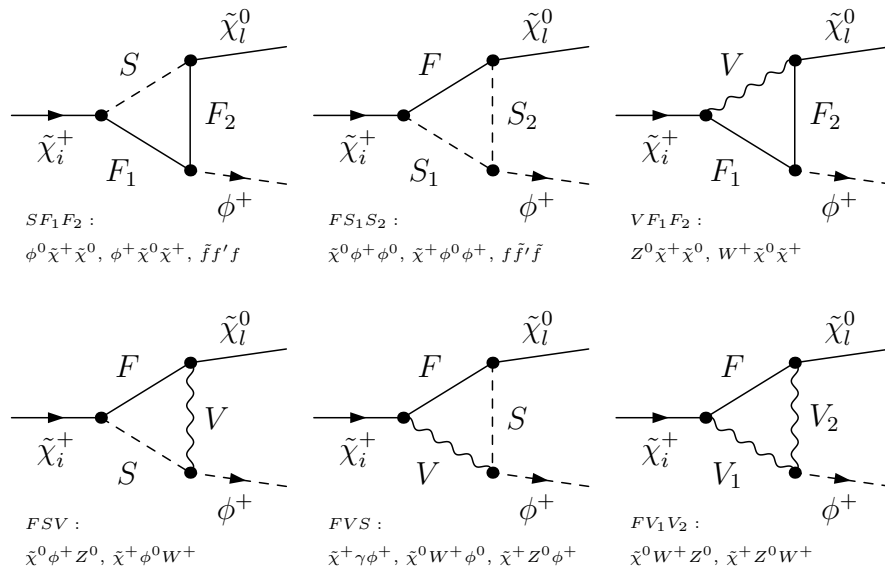
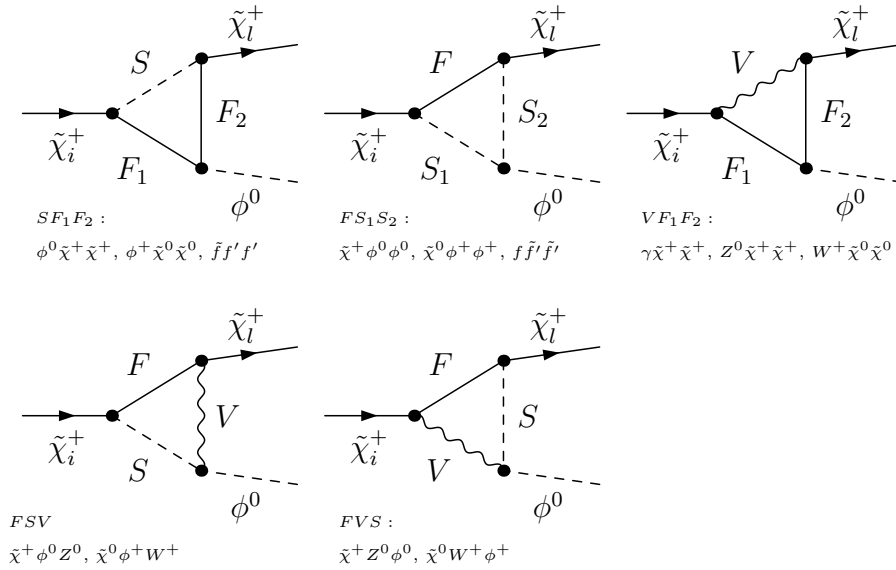
$$\begin{aligned} \phi^0 &= (h^0, H^0, A^0, G^0), & \phi^+ &= (H^+, G^+), \\ f &= (u_g, d_g, \nu_g, l_g), & \tilde{f} &= (\tilde{u}_g, \tilde{d}_g, \tilde{\nu}_g, \tilde{l}_g). \end{aligned} \quad (\text{E.1})$$

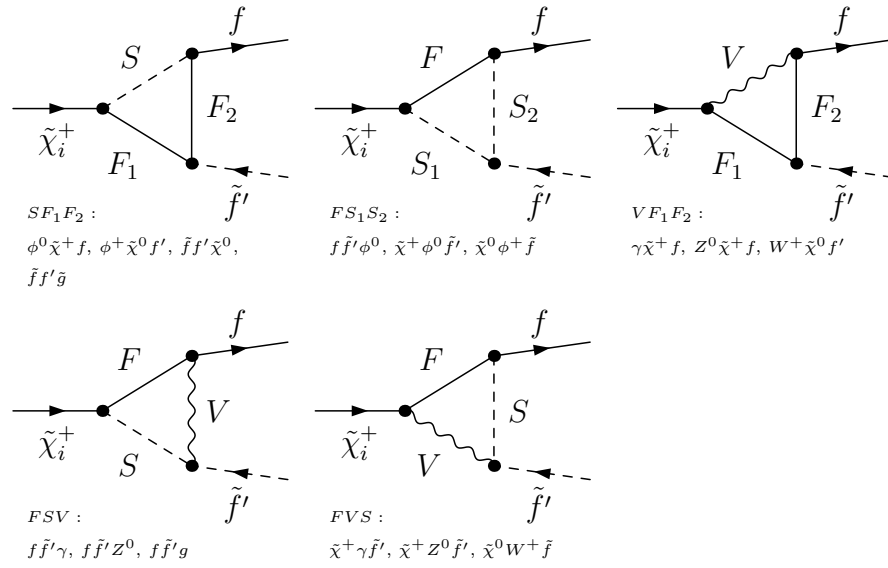
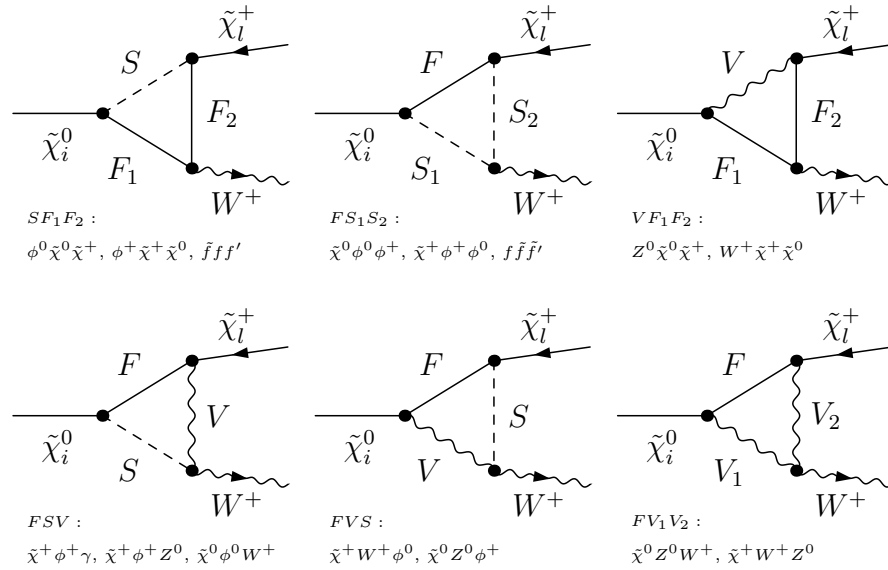
Since not all particles couple to each other, the number of possible diagrams is restricted by the existence of the particular couplings.

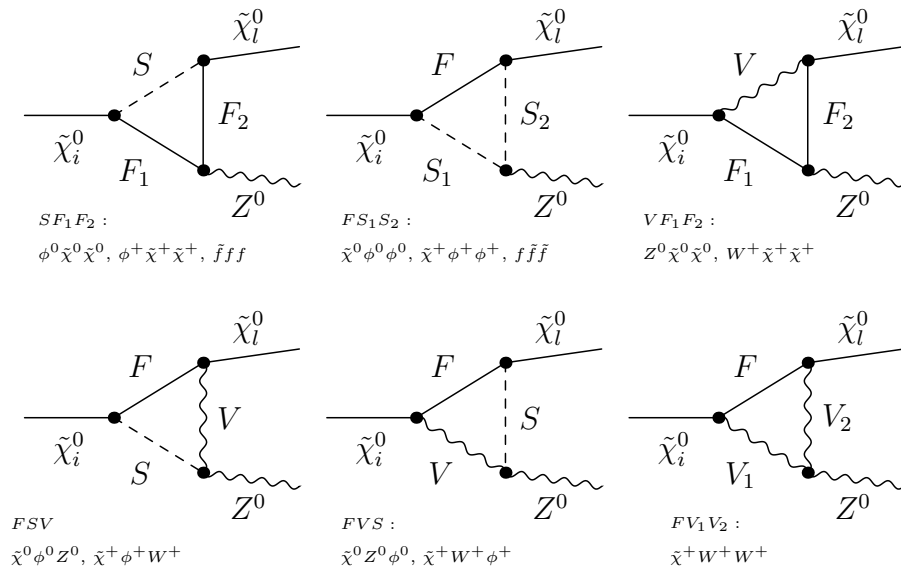
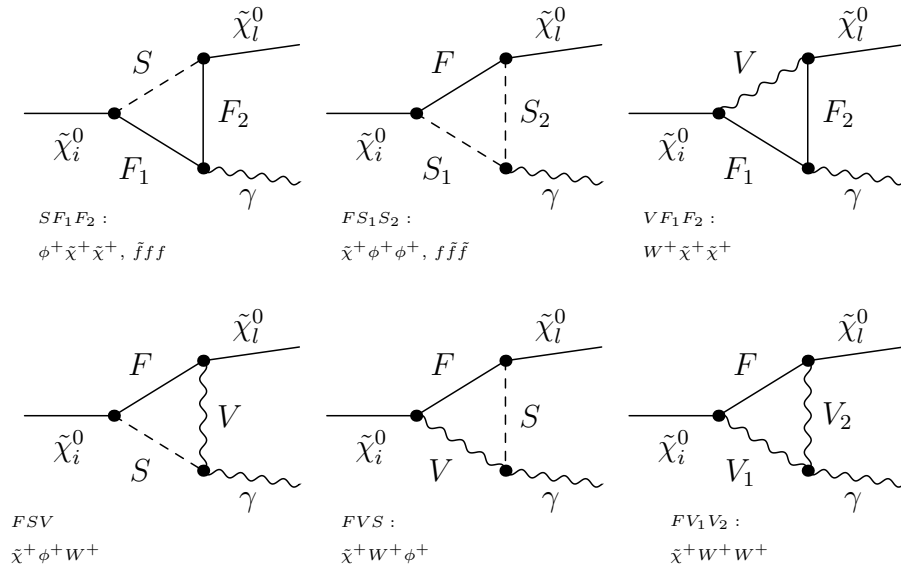
E.1 $\tilde{\chi}_i^+ \rightarrow \tilde{\chi}_l^0 W^+$

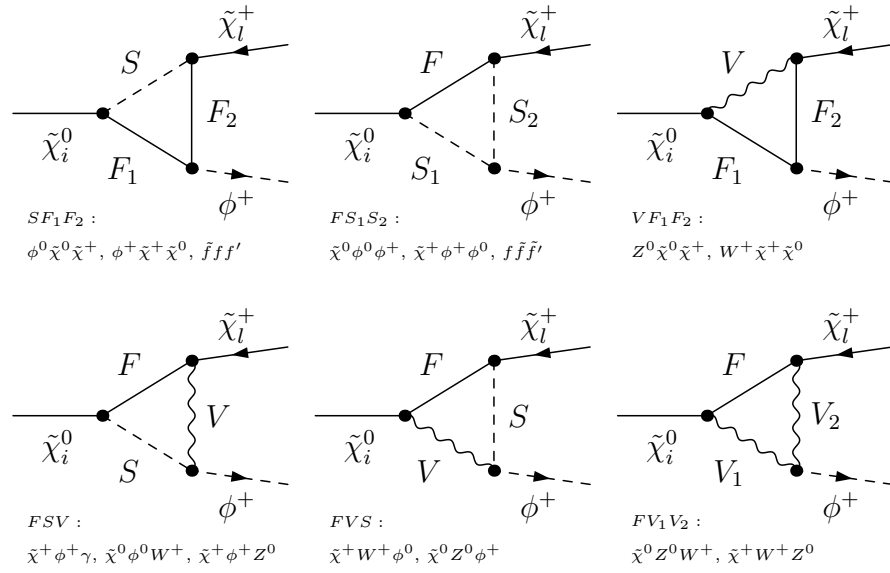
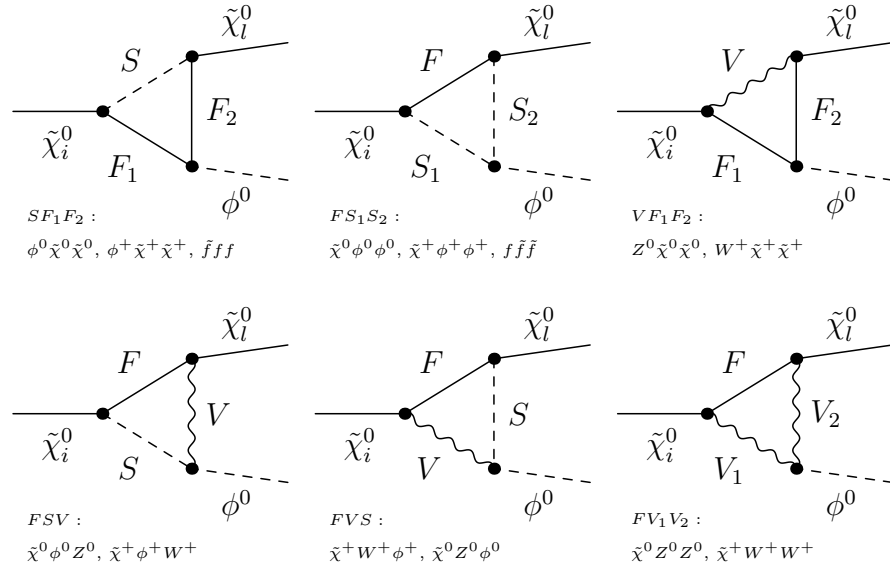


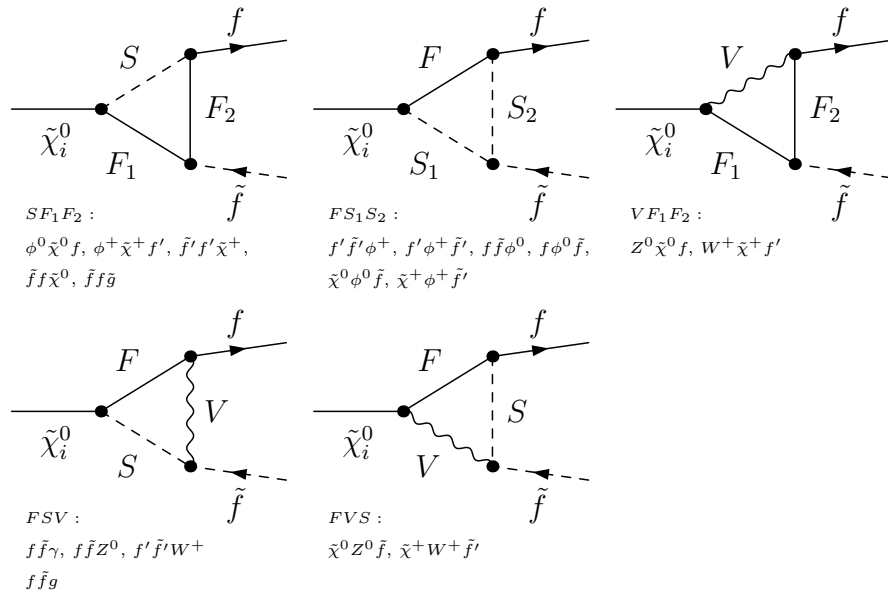
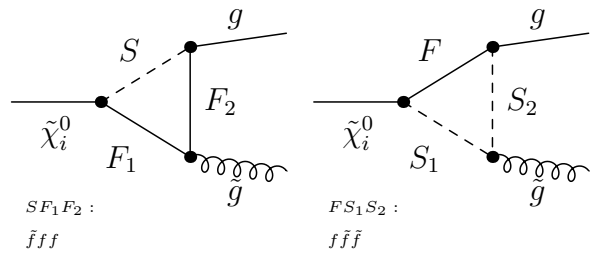
E.2 $\tilde{\chi}^+ \rightarrow \tilde{\chi}_l^+ Z^0$ **E.3** $\tilde{\chi}^+ \rightarrow \tilde{\chi}_l^+ \gamma$ 

E.4 $\tilde{\chi}^+ \rightarrow \tilde{\chi}_l^0 \phi^+$

E.5 $\tilde{\chi}^+ \rightarrow \tilde{\chi}_l^+ \phi^0$


E.6 $\tilde{\chi}^+ \rightarrow f\tilde{f}'$ **E.7** $\tilde{\chi}^+ \rightarrow \tilde{\chi}_l^0 W^+$ 

E.8 $\tilde{\chi}_i^0 \rightarrow \tilde{\chi}_l^0 Z^0$

E.9 $\tilde{\chi}_i^0 \rightarrow \tilde{\chi}_l^0 \gamma$


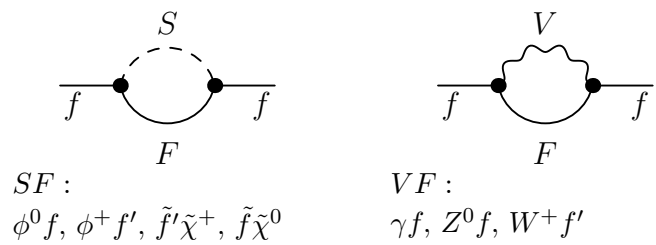
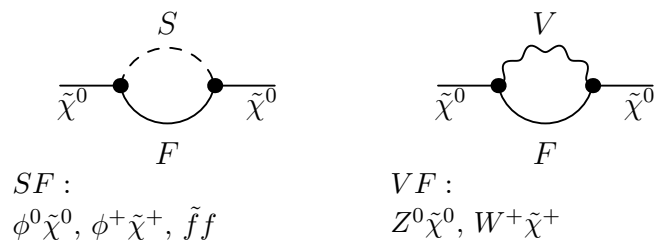
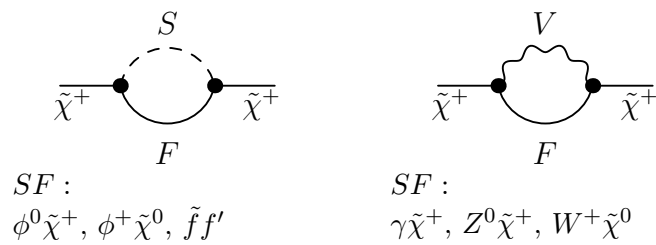
E.10 $\tilde{\chi}^0 \rightarrow \tilde{\chi}^+ \phi^+$ **E.11** $\tilde{\chi}^0 \rightarrow \tilde{\chi}_l^0 \phi^0$ 

E.12 $\tilde{\chi}_i^0 \rightarrow f\tilde{f}$ **E.13** $\tilde{\chi}_i^0 \rightarrow g\tilde{g}$ 

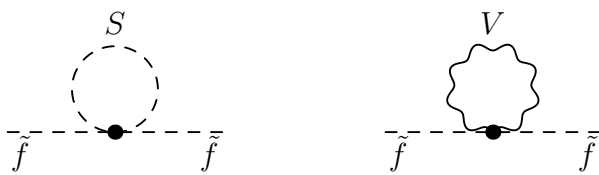
Appendix F

Selfenergy-Contributions

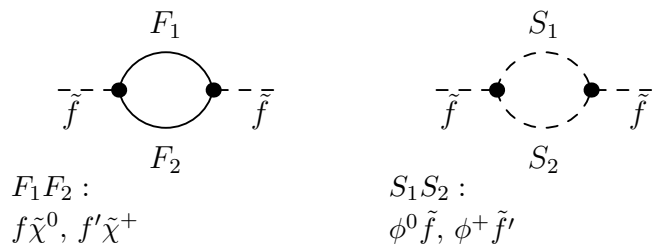
F.1 Selfenergies for $\tilde{\chi}^+, \tilde{\chi}^0, f = (u_g, d_g, \nu_g, e_g)$



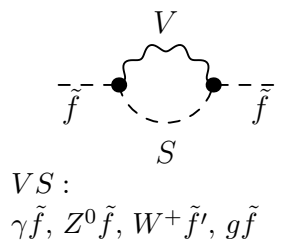
F.2 Selfenergies for $\tilde{f} = (\tilde{u}_g, \tilde{d}_g, \tilde{\nu}_g, \tilde{e}_g)$



$$\begin{array}{ll} S : & V : \\ \phi^0, \phi^+, \tilde{f}, \tilde{f}' & \gamma, Z^0, W^+, g \end{array}$$

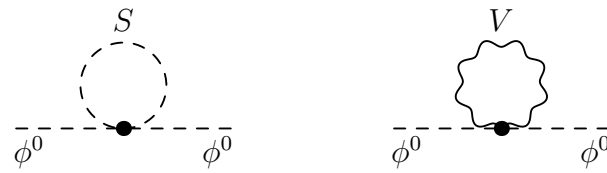


$$\begin{array}{ll} F_1 : & S_1 \\ F_2 : & S_2 \\ f\tilde{\chi}^0, f'\tilde{\chi}^+ & \phi^0\tilde{f}, \phi^+\tilde{f}' \end{array}$$



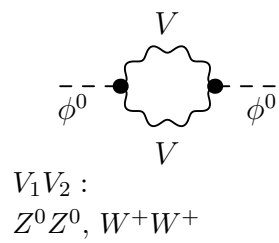
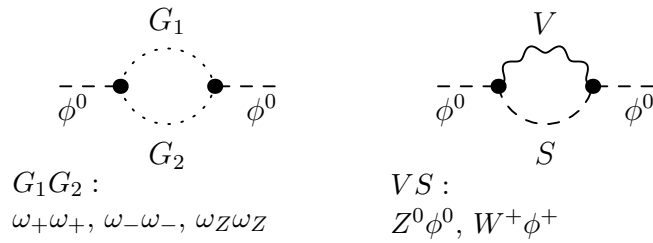
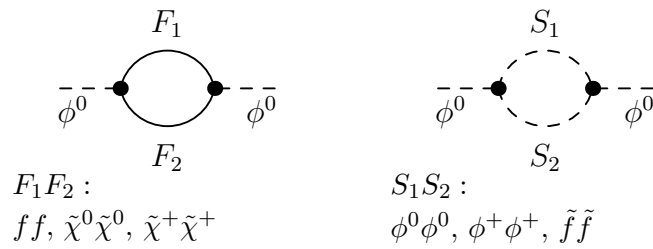
$$\begin{array}{l} VS : \\ \gamma\tilde{f}, Z^0\tilde{f}, W^+\tilde{f}', g\tilde{f} \end{array}$$

F.3 Selfenergies for $\phi^0 = (h^0, H^0, A^0, G^0)$

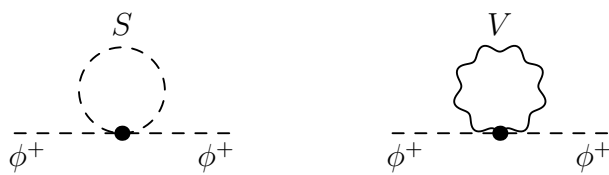


$S :$
 $\phi^0, \phi^+, \tilde{f}$

$V :$
 Z^0, W^+

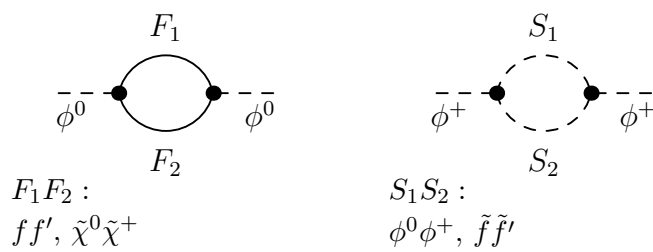


F.4 Selfenergies for $\phi^+ = (H^+, G^+)$



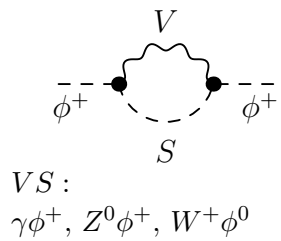
$S :$
 $\phi^0, \phi^+, \tilde{f}$

$V :$
 γ, Z^0, W^+



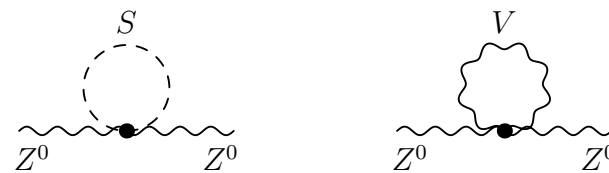
$F_1 F_2 :$
 $ff', \tilde{\chi}^0 \tilde{\chi}^+$

$S_1 S_2 :$
 $\phi^0 \phi^+, \tilde{f} \tilde{f}'$



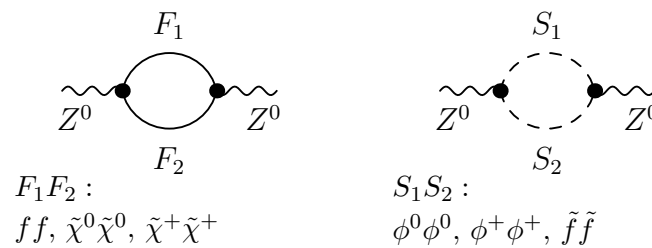
$VS :$
 $\gamma \phi^+, Z^0 \phi^+, W^+ \phi^0$

F.5 Selfenergies for Z^0



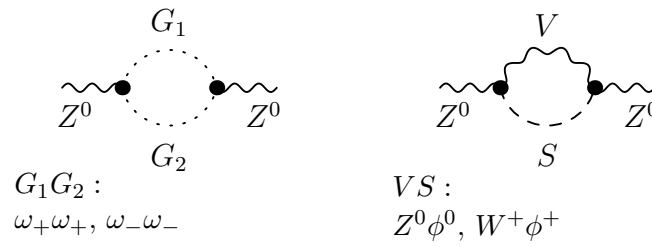
$S :$
 $\phi^0, \phi^+, \tilde{f}$

$V :$
 W^+



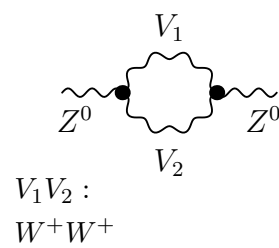
$F_1 F_2 :$
 $ff, \tilde{\chi}^0 \tilde{\chi}^0, \tilde{\chi}^+ \tilde{\chi}^+$

$S_1 S_2 :$
 $\phi^0 \phi^0, \phi^+ \phi^+, \tilde{f} \tilde{f}$



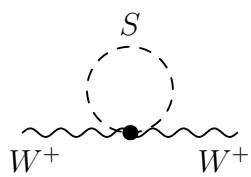
$G_1 G_2 :$
 $\omega_+ \omega_+, \omega_- \omega_-$

$VS :$
 $Z^0 \phi^0, W^+ \phi^+$

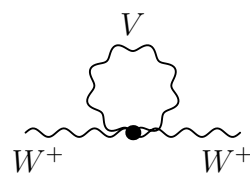


$V_1 V_2 :$
 $W^+ W^+$

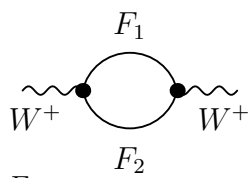
F.6 Selfenergies for W^+



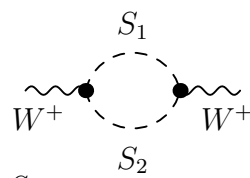
$S :$
 $\phi^0, \phi^+, \tilde{f}$



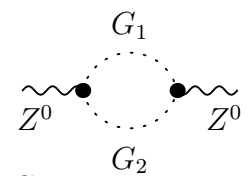
$V :$
 γ, Z^0, W^+



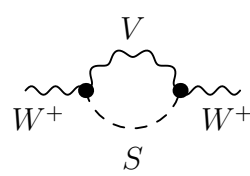
$F_1 F_2 :$
 $ff', \tilde{\chi}^0 \tilde{\chi}^+$



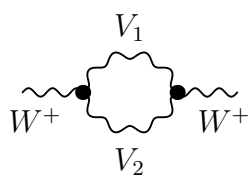
$S_1 S_2 :$
 $\phi^0 \phi^+, \tilde{f} \tilde{f}'$



$G_1 G_2 :$
 $\omega_+ \omega_+, \omega_- \omega_-, \omega_Z \omega_Z$

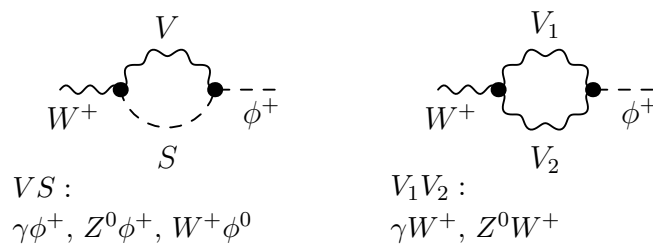
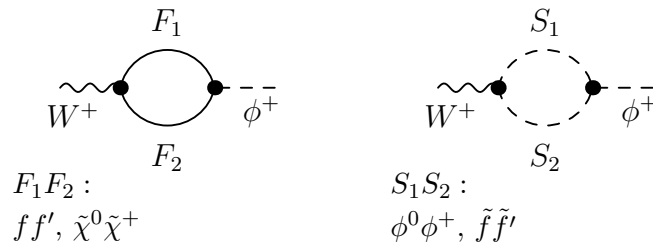
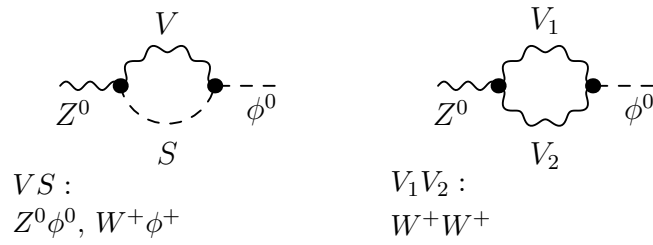
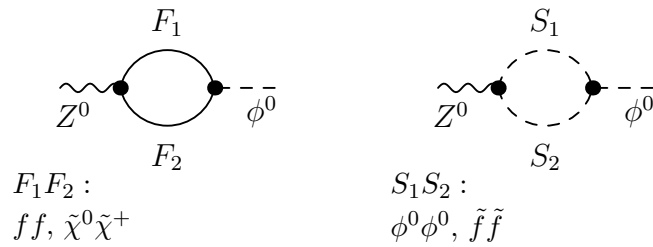


$V S :$
 $\gamma \phi^+, Z^0 \phi^+, W^+ \phi^0$



$V_1 V_2 :$
 $\gamma W^+, Z^0 W^+$

F.7 Mixed Selfenergies for $A^0, G^0, Z^0, H^+, G^+, W^+$



Bibliography

- [1] D.J. Chung, L.L. Everett, G.L. Kane, S.F. King, J. Lykken, and Lian-Tao Wang,
The Soft Supersymmetry-Breaking Lagrangian: Theory and Applications,
hep-ph/031278 v1.
- [2] L. Maiani, In *Gif-sur-yvette 1979, Proceedings, Summer School on Particle Physics*,
1-52.
- [3] L. E. Ibanez and G. G. Ross, Phys. Lett. B **110**, 215 (1982).
- [4] L. Alvarez-Gaume, M. Claudson and M. Wise, Nucl. Phys. B **207**, 96 (1982).
- [5] K. Inoue, A. Kakuto, H. Komatsu and S. Takeshita, Prog. Theor. Phys. **67**, 1889 (1982).
- [6] K. Inoue, A. Kakuto, H. Komatsu and S. Takeshita, [Erratum-ibid. **70**, 330 (1983)].
- [7] K. Inoue, A. Kakuto, H. Komatsu and S. Takeshita, Prog. Theor. Phys. **71**, 413 (1984).
- [8] W. Marciano, in Proceedings of the Eighth Workshop on Grand Unification, 16-18 April, 1987, Syracuse University, Syracuse, NY, ed. K. Wali (World Scientific, Singapore, 1988), pp. 185-189.
- [9] S. Dimopoulos, S. Raby and F. Wilczek, Phys. Rev. D **24**, 1681 (1981).
- [10] S. Dimopoulos and H. Georgi, Nucl. Phys. B **193**, 150 (1981).
- [11] N. Sakai, Z. Phys. C **11**, 153 (1981).
- [12] C. Giunti, C. W. Kim and U. W. Lee, Mod. Phys. Lett. A **6** (1991) 1745.
- [13] U. Amaldi, W. de Boer and H. Furstenau, Phys. Lett. B **260**, 447 (1991).
- [14] P. Langacker and M. x. Luo, Phys. Rev. D **44**, 817 (1991).
- [15] J. R. Ellis, S. Kelley and D. V. Nanopoulos, Phys. Lett. B **260**, 131 (1991).
- [16] H. Pagels and J. R. Primack, Phys. Rev. Lett. **48**, 223 (1982).
- [17] H. Goldberg, Phys. Rev. Lett. **50**, 1419 (1983).
- [18] L. E. Ibanez and G. G. Ross, Phys. Lett. B **131**, 335 (1983).
- [19] B. Pendleton and G. G. Ross, Phys. Lett. B **98**, 291 (1981).

- [20] L. E. Ibanez and G. G. Ross, Phys. Lett. B **105**, 439 (1981).
- [21] M. B. Einhorn and D. R. Jones, Nucl. Phys. B **196**, 475 (1982).
- [22] G. L. Kane, C. Kolda and J. Wells, Phys. Rev. Lett. **70**, 2686 (1993) [hep-ph/9210242].
- [23] J. R. Espinosa and M. Quiros, Phys. Lett. B **302**, 51 (1993) [hep-ph/9212305].
- [24] LEP Electroweak Working Group, LEPEWWG/2001-01.
- [25] A. G. Cohen, D. B. Kaplan and A. E. Nelson, Ann. Rev. Nucl. Part. Sci. **43**, 27 (1993) [hep-ph/9302210].
- [26] A. D. Dolgov, Phys. Rept. **222**, 309 (1992).
- [27] I. Affleck and M. Dine, Nucl. Phys. B **249**, 361 (1985).
- [28] S.P. Martin, *A Supersymmetry Primer*, hep-ph/9709356 v3.
- [29] Katharina Müller, *Einführung Supersymmetrie*, Universität Zürich, 2002.
- [30] H. E. Haber and G. L. Kane, Phys. Rept. **117** (1985) 75.
- [31] D. A. Ross and J. C. Taylor, Nucl. Phys. B **51** (1973) 125 [Erratum-ibid. B **58** (1973) 643]; A. Sirlin, Phys. Rev. D **22** (1980) 971.
- [32] J. A. Aguilar-Saavedra *et al.*, Eur. Phys. J. C **46** (2006) 43 [arXiv:hep-ph/0511344].
- [33] W. Siegel, Phys. Lett. B84 (1979) 193;
D.M. Capper. D.R.T. Jones and P. van Nieuwenhuizen, Nucl. Phys. B167 (1980) 479.
- [34] W. Siegel, Phys. Lett. B **84** (1979) 193
- [35] F. del Aguila and M. Perez-Victoria, Acta Phys. Polon. B **28** (1997) 2279 [arXiv:hep-ph/9710442].
- [36] T. Hahn and M. Perez-Victoria, Comput. Phys. Commun. **118** (1999) 153 [arXiv:hep-ph/9807565].
- [37] T. Blank, Dissertation (in german), TH Karlsruhe (2000).
- [38] Y. Yamada, Phys. Rev. D **64** (2001) 036008.
- [39] H. Eberl, M. Kincel, W. Majerotto and Y. Yamada, Nucl. Phys. B **625** (2002) 372 [arXiv:hep-ph/0111303].
- [40] W. Öller, H. Eberl and W. Majerotto, Phys. Rev. D **71** (2005) 115002 [arXiv:hep-ph/0504109].
- [41] A. Dabelstein, Z. Phys. C **67** (1995) 495 [arXiv:hep-ph/9409375]; Nucl. Phys. B **456** (1995) 25 [arXiv:hep-ph/9503443].

- [42] P. H. Chankowski, S. Pokorski and J. Rosiek, Phys. Lett. B **274** (1992) 191; Nucl. Phys. B **423** (1994) 437 [arXiv:hep-ph/9303309]; 497.
- [43] M. Böhm, H. Spiesberger and W. Hollik, Fortsch. Phys. **34** (1986) 687.
- [44] A. Denner, Fortschr. Phys. **41**(1993) 307
- [45] H. Burkhardt, F. Jegerlehner, G. Penso and C. Verzegnassi, Z. Phys. C **43** (1989) 497.
- [46] F. Jegerlehner, Nucl. Phys. Proc. Suppl. **131** (2004) 213 [arXiv:hep-ph/0312372].
- [47] M. Kuroda, arXiv:hep-ph/9902340.
- [48] Helmut Eberl, Dissertation, Technische Universität Wien, 1998.
- [49] T. Hahn, Comput. Phys. Commun. **140** (2001) 418 [arXiv:hep-ph/0012260].
- [50] M. Battaglia *et al.*, Eur. Phys. J. C **22** (2001) 535 [arXiv:hep-ph/0106204].
- [51] Supersymmetry Parameter Analysis (SPA) project, SPA website <http://spa.desy.de/spa/>
- [52] J. Kalinowski, Acta Phys. Polon. B **37** (2006) 1215 [arXiv:hep-ph/0512281].
- [53] W. Porod, Comput. Phys. Commun. **153** (2003) 275 [arXiv:hep-ph/0301101].
- [54] K. Kovarik, Dissertation, Comenius University, Bratislava, (2005).
- [55] K. Kovarik, C. Weber, H. Eberl and W. Majerotto, Phys. Rev. D **72** (2005) 053010 [arXiv:hep-ph/0506021].
- [56] W. Öller, Dissertation, TU Wien (2005).
- [57] P. Skands *et al.*, JHEP **0407** (2004) 036 [arXiv:hep-ph/0311123].
- [58] SLHALib - a library for SUSY Les Houches Accord I/O, website <http://www.feynarts.de/slha/>
- [59] M. Muhlleitner, A. Djouadi and Y. Mambrini, Comput. Phys. Commun. **168** (2005) 46 [arXiv:hep-ph/0311167].
- [60] John F. Gunion, Howard E. haber, Physical Review D Volume 37, Number 1 May 1988
- [61] G. Passarino and M. Veltman, Nucl. Phys. B160 (1979) 151.